Earth & Life Sciences
School of Natural Sciences

Ollscoil na Gaillimhe
University of Galway

# Mapping soil using neural network machine learning and remotely sensed geoscience data; a study in peat.


Dave O'Leary

BSc, MSc


*A thesis submitted for the degree of Doctor of Philosophy to the*

*University of Galway, Ireland*

Supervisor

Dr Eve Daly


Earth and Ocean Sciences

School of Natural Sciences

University of Galway


October 2022

HY-RES Hydro-geophysics and Remote Earth Sensing research group

# Table of Contents

# List of Figures

# List of Tables

# List of Equations

# Declaration

I, Dave O'Leary, declare that the work presented in this thesis is my own work and that is has not been used to obtain any other form of degree in this University or elsewhere. To the best of my knowledge and belief, the thesis contains no material previously published or written by another person except where due reference is made in the thesis itself.

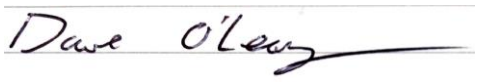

Dave O'Leary

# Acknowledgments

I would like to express my sincere gratitude to my supervisor Dr Eve Daly for all her assistance and guidance throughout my PhD and for her patience when it came to my writing style! My eternal thanks also go to Prof. Colin Brown for all the insightful conversations we've had and his enthusiastic interest in my project and career to date. Both Eve and Colin were involved with my undergraduate project also. It has been an amazing experience to have them both so deeply involved in my PhD work.

I would like to thank the 4 members of my GRC committee also, Dr Tiernan Henry, Prof. Mark Healy, Prof. Aaron Golden, and Prof. Peter Croot. Our yearly meetings were something to look forward to and it always felt more like a conversation than a review. I'd especially like to thank Prof. Mark Healy for his help throughout and for supporting my work through his WaterPEAT project, a place where a lot of the final ideas in this thesis stems from.

I'd specifically like to thank Dr Pat Tuohy (Teagasc) for all his support throughout my PhD. He supported my ideas, provided field sites and equipment for field work, and generally acted as a mentor to my progress.

The support I received from all members of the Department of Earth and Ocean Sciences, both staff and postgraduate, has been fantastic, from the inclusion in undergrad teaching to the chats over a few beers, I have felt more like a member of the department and a peer than a student. I think the fact that I returned to my undergraduate department to complete my PhD, says more than I could write about my respect for the people here.

I couldn't have completed this degree without funding and so I wish to acknowledge and thank the Irish Research Council for my funding under project number GOIPG-2018-233.

Finally, to my (now) fiancé Aileen, I don't know how she managed to put up with my ever-evolving feelings about undertaking a PhD, but she did, and I don't think I could have managed it without her. I can't count the number of ideas that came from just chatting the problem out with her, many of which feature in this final work. I give her full credit for coining the phrase "Big Data for Local Problems".

# Abstract

Several concepts exist in the discipline of data analysis that are often unknowingly used in geosciences. Specifically, the concepts related to Big Data, Data Assimilation, Digital Soil Mapping, and Exploratory Data Analysis. Recently the availability of large geo-spatial data sets, such as satellite remote sensing, has meant these concepts are appearing more and more in geoscience literature. However, any explanation or explicit understanding of these concepts is often missing. In this thesis, these concepts are highlighted and applied to several large geo-spatial datasets in the context of peatland identification and intra-peatland mapping of physical properties. Peatlands make up ~ 3 % of the land surface globally and account for ~ 10 – 30 % of all soil carbon, making these soils globally important in the carbon cycle. Drained and modified peatlands account for considerable emissions of carbon to the atmosphere. Peatland rehabilitation aims to return these peatlands to their natural state, making them carbon neutral, or even carbon negative in time. Advances in peatland identification and delineation are needed to update national and global peatland inventories and meet national reporting obligations. The geo-spatial datasets used in this thesis are optical satellite and airborne radiometric data. Modern machine learning neural network methods are used to firstly identify peat soil and update peatland boundaries, and secondly to visualise peatland physical property (landcover and soil moisture) variation within a site containing several discontinuous peatlands. The methods developed here follow the principles of data analysis and have applications outside the scope of this thesis.

# Chapter 1: Introduction

## 1.1 Key concepts

Most modern peatlands formed after the retreat of the last ice age (circa ~10,000 years ago) (Page and Baird, 2016). These are landscapes that have naturally accumulated layers of peat, a type of soil that consists of partially decomposed plant material. Peat usually forms under waterlogged, oxygen deprived conditions where the decomposition of the organic material is slowed. Peatlands are often described as wetlands, fens, or mires, with no global consensus as to the definition of each (Lourenco et al., 2022). Peatlands serve many ecosystem services (Figure 1.1.1) such as water regulation, flood retention and recreation potential (Page and Baird, 2016). Being mostly organic in composition, the storage of natural carbon (C) reserves is a valuable service they provide (Searchinger et al., 2022).

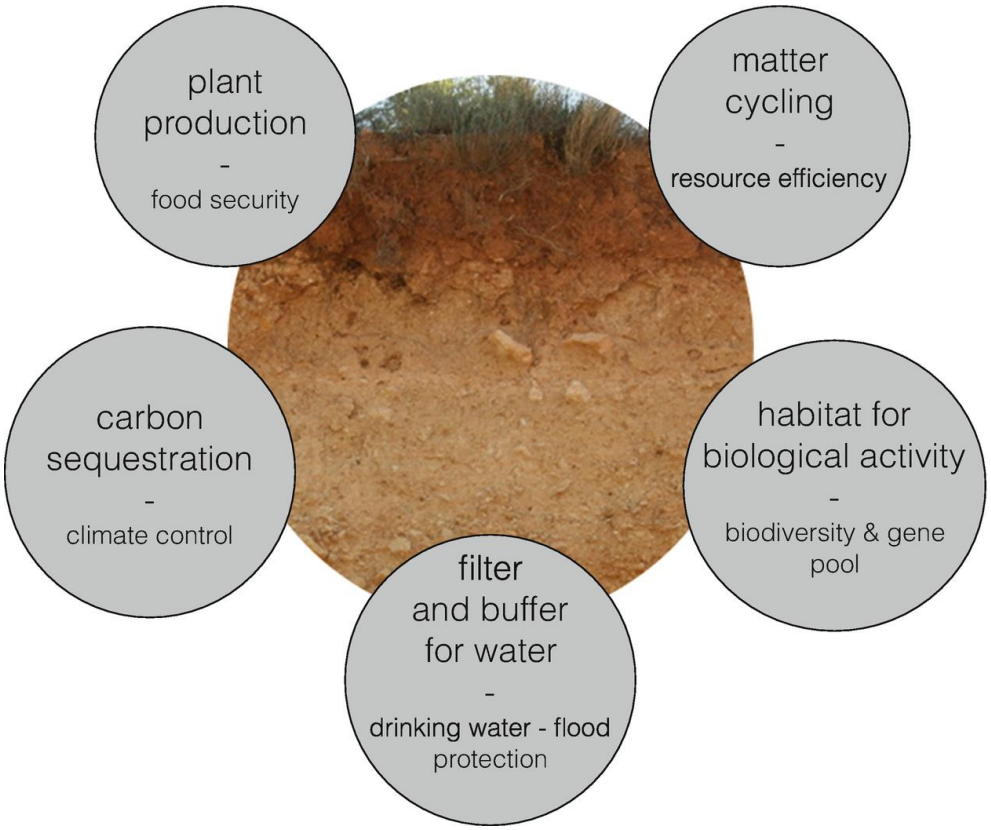


Figure 1.1.1: Peatland ecosystem services (Vogel et al., 2019)

Peatlands account for ~ 3% of the earths land surface (Xu et al., 2018), but hold between 5 – 30 % of the global soil C stock (Minasny et al., 2019; UNEP, 2022). This makes peatlands a very important component of any global effort to mitigate climate change. Humans have impacted peatlands globally via extraction and landcover modification (Kareksela et al., 2015). Recently, international consortiums (EU, 2020; Ramsar, 2018; UNEP, 2022; UNFCCC, 2011) have recognised the role peatlands play in the global carbon cycle and call for action to be taken to restore these ecosystems to their natural state. The creation of global initiatives, such as the Global Peatlands Initiative (GPI, 2016), aims to conduct policy leading research "*to improve the conservation, restoration and sustainable managements of peatlands*".

In order to meet these goals, methodologies employed to identify peat soils and analyse intra-peatland variability of ecological and hydrologically important indicators must be improved (Minasny et al., 2019). Traditional mapping techniques involved in-situ auger sampling at point locations (McBratney et al., 2003). This method is often coarse in scale and contain inaccuracies related to spatial boundaries and variation of physical properties (Zhang et al., 2017). Aerial photography has also been used to map peatland extent (Vitt et al., 2000), however this method requires experience and local knowledge on the part of the interpreter and may not identify a peatland under vegetation or agriculturally modified landcover.

Peatlands differ from other landcovers types in several ways. Peat has much lower bulk density then mineral soils (Kiely and Carton, 2010), and are usually saturated and have higher soil moisture content (Galvin, 1976). Recently, the advent of satellite remote sensing and airborne geophysical data acquisition campaigns, which are sensitive to such differences, has allowed for the advance of peatland mapping methodologies (Minasny et al., 2019) through the continual acquisition of large geo-spatial datasets at various spatial scales. There are four complimentary concepts that can be used to describe this advancement. These are (1) concept of Big Data (Gandomi and Haider, 2015), (2) Data Assimilation (DA) (Carrassi et al., 2018), (3) Digital Soil mapping (DSM) (McBratney et al., 2003) and (4) Exploratory Data Analysis (EDA) (Chatfield, 1986).

The concept of Big Data is subjective depending on the resources available. What might be considered "big" for one institute, may not for other due to, for example, computer resources available. However, the concept of Big Data can be summarised by the so called Three V's. That is Volume of data, the Variety of data and the Velocity, or rate of data generation (Gandomi and Haider, 2015).

DA aims to estimate the state of a system (atmosphere, weather, soil) by combining observations with mathematical models from various sources and is notably used in weather prediction (Carrassi et al., 2018). Observations refers to any measurement that can be taken of the system of interest. Models refer to any mathematical function that can be used to infer links between the measurement taken and a property of the system of interest. DA is the term that formalises the means of linking observations to models, ranging from traditional linear correlation to modern high order statistical machine learning and neural network prediction methods (Carrassi et al., 2018).

DSM represents the creation and population of spatial soil information systems by the use of field and laboratory observational methods coupled with spatial and non-spatial soil inference systems (Webster, 2007). This involves the use of geo-spatial data sources to provide spatial maps of predicted soil properties. In this way, DSM and DA are intrinsically linked. The key points of DSM are:

- To generate geo-referenced soil property information based on a link between spatial environmental data measurements and a theoretical or lab-based model (McBratney et al., 2003).
- Consists of a raster of pixels, where each pixel has a location in geographic space and a value related to the measured/predicted soil property.
- Can highlight the spatial distribution of soil property information and any associated errors.

EDA (Chatfield, 1986) is an initial analysis of data to discover patterns, highlight anomalies and general summary visualisations. Importantly this is a "data driven" approach, where user bias is removed if possible (Komorowski et al., 2016). The aims of EDA are to (1) maximise insight into a data source, (2) visualise potential relationships between data, (3) detect data that vary significantly from others, (4) develop an explanatory model of the data source, and (5) extract relevant data

from the overall data source. EDA naturally forms part of any data analysis, but it is rarely formally acknowledged.

Taken together, these form a concept introduced in this PhD thesis, Big Data for Local Problems, which takes the concepts highlighted and applies them to solve local, or field scale problems.

## 1.2 Project data and methods

The concepts of Big Data, DA, DSM, and EDA all assume the use of large volumes of data and robust, data driven analytical tools with which to make predictions from. Within the discipline of DSM, a number of key data sources can be considered.

### 1.2.1 Satellite data

Satellite remote sensing involves the continuous collection of electromagnetic (passive/optical) or microwave backscatter (active/radar) energy at a satellite orbiting the earth (Wang and Qu, 2009). This results in high temporal and spatial resolution satellite derived data which measures the surface to the top few cm's of the subsurface. Optical satellite data is surface reflections of electromagnetic energy generated by the sun and typically ranges from visible to shortwave infra-red wavelengths (Figure 1.2.1). Radar satellite data is reflected microwave energy (backscatter), initially emitted by the satellite. The measurement is the return strength of the microwave signal, typically measured as a relationship to the emitted signal and has the ability to penetrate several mm into the subsurface. Both have potential in peatland mapping (Czapiewski and Szumińska, 2022).

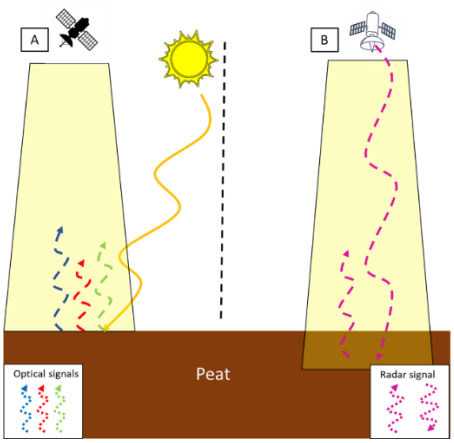


Figure 1.2.1: A) Diagram of optical satellite data acquisition. B) Diagram of radar satellite acquisition

Satellite data has been used to identify peatland spatial extent in several countries (Aitkenhead, 2017; Connolly et al., 2007) and in mapping of intra-peatland variation in physical properties such as vegetation cover (Bhatnagar et al., 2020) and soil moisture (Bechtold et al., 2018). However, satellite data is a measurement of the surface and does not penetrate deeper than ~ 10 cm.

The European Space Agency (ESA) operate several satellite-based missions (Sentinel, 2022), which provide these datasets for free to the public. In this thesis Sentinel 2 data (Sentinel-2) is utilised as a means to delineate landcover on the study site.

### 1.2.2 Airborne geophysical data

Airborne geophysical data provides a means to measure deep (several m's) subsurface properties such as soil texture, moisture, porosity, and permeability (Ameglio, 2018; Binley et al., 2015). Airborne geophysics can provide spatially consistent data over large geographical areas. Airborne Electromagnetics (Boaga et al., 2020) and Radiometrics (Beamish, 2014) are particularly prominent in peatland studies. Electromagnetics aims to measure the electrical conductivity of the subsurface and relate this to porosity, soil texture, or soil moisture (Binley et al., 2015). Radiometrics measures the naturally occurring radioactivity being emitted by geological materials (Martelet et al., 2006).

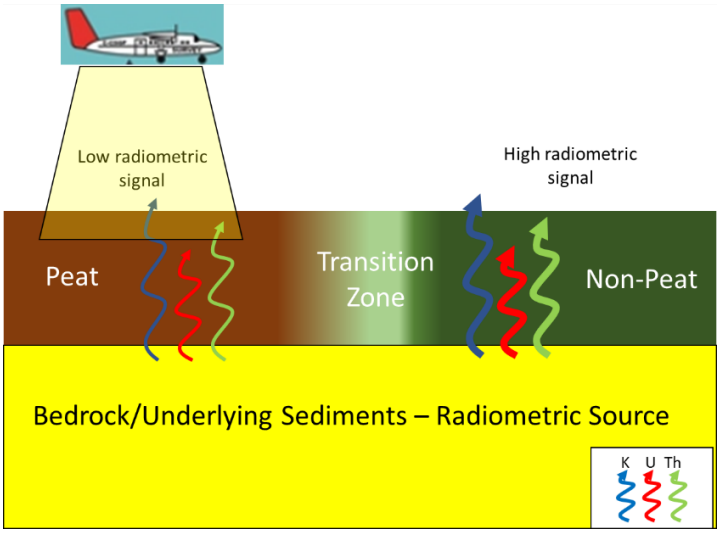


Figure 1.2.2: Diagram of airborne radiometric data acquisition (O'Leary et al., 2022)

In peatland studies, electromagnetic measurements have been used to estimate thickness (Siemon et al., 2020), however this may only be applicable to deeper peats, due to vertical resolution of airborne measurements (Boaga et al., 2020). Radiometric measurements have been used to determine the extent of peatlands (Beamish, 2014; O'Leary et al., 2022), as peat soil attenuates radiometric signal from geological bedrock, as opposed to non-peats, which may enhance it (Figure 1.2.2).

This thesis used airborne radiometric data acquired by a national mapping project in Ireland called “Tellus” (GSI, 2022d).

### 1.2.3 Combining data sources

Optical satellite and airborne radiometric data each provide a means to identify peatlands and measure intra-peatland landcover and physical property variation. Optical satellite data measures the landcover and radiometric data can measure subsurface properties. The ability to analyse these coincident data sources would provide the potential to measure surface to subsurface intra-peatland variability in a single integrated interpretation.

Tellus radiometric data are combined with the Sentinel 2 data in this thesis. These Big Data comprise the “observations” aspect within the concept of DA. The accessibility of such data highlights the huge resource that programs such as Sentinel and Tellus provide to researchers and the general public and adds to the range of applications for such datasets within the geosciences.

### 1.2.4 Machine learning

In order to link the observations to some physical property a model is required under the concepts of DA and DSM. In order to also keep within the principles of EDA, machine learning was chosen to analysis these observations and link to physical properties. Machine learning has been used in geoscience applications for several decades (Dramsch, 2020; Karpatne et al., 2019).

Machine learning is a specific computer model that updates itself (or learns) based on prediction performance (Valentine and Kalnins, 2016). This is in contrast to traditional numerical modelling, which rely on explicit rules to make predictions (Dramsch, 2020). Two specific forms of machine learning are used in this work, namely supervised and unsupervised.

In supervised machine learning a set of observations are “labelled”, that is they are explicitly linked to a specific value or property (Møller, 1993). The labelled data are then passed to a neural network, which determines a statistical relationship between the observations which link them to the label. New observations can then be passed to this “trained” network and it will output the “label” that best matches (Figure 1.2.3). In this way a supervised network can classify new observations. In order to stay within the principles of EDA in this thesis, a specific focus was placed on the choice of labelled training observations (See Chapter 3), as this has potential to affect the results of the supervised analysis.

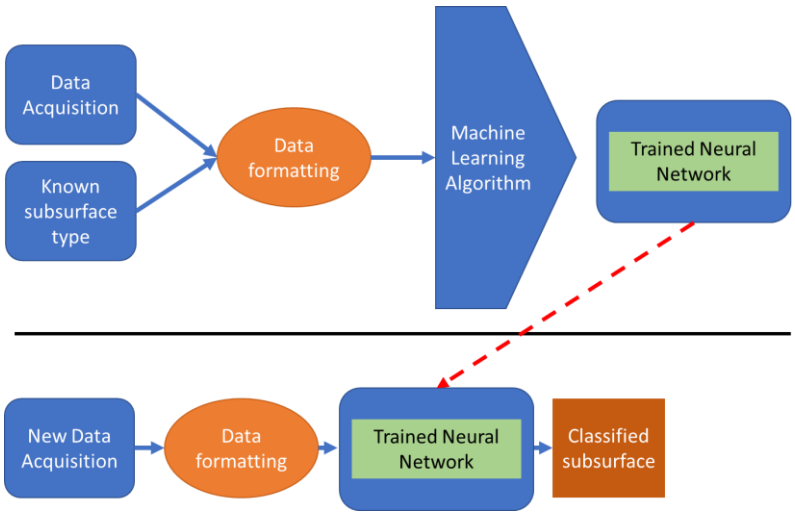


Figure 1.2.3: Workflow of supervised machine learning process

Unsupervised machine learning is a purely data driven approach and naturally conforms to the principles of EDA. Here, observations are grouped together into “clusters”

Figure 1.2.4) that are statistically similar to each other (Benabdellah et al., 2019). This analytical tool is useful when analysing multi-dimensional data, reducing the complexity of these data and providing a means to visualise the dataset.

One issue in clustering is that often the number of proposed clusters must be known or estimated before analysis (Delgado et al., 2017). This undermines the concept of EDA and so there is a need for a data driven method to determine the

appropriate number of clusters for any particular set of coincident geospatial observations (See Chapter 4).

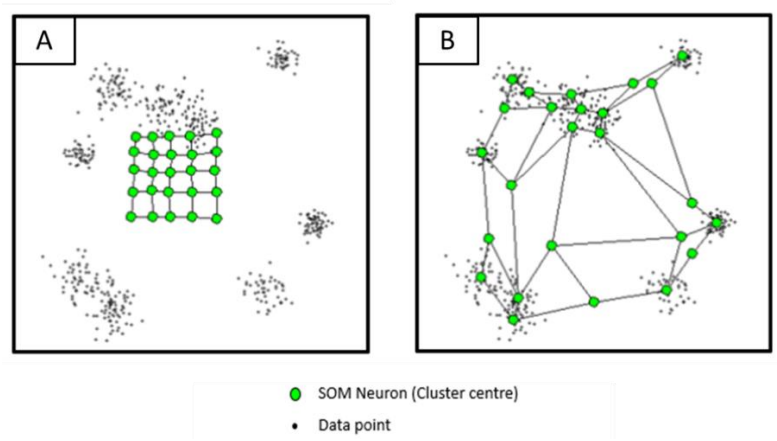


Figure 1.2.4: Simple example of Self Organising Maps (SOM) A) prior to clustering and B) after clustering a simple 2D example dataset. Ref: https://qph.fs.quoracdn.net/main-qimg-e2c94ae591fad6f4a8ba2deb6ef8e875.webp

## 1.3 Research objective and aims

The objective of this thesis is to advance the DSM method of identifying peat soils, updating peatland boundaries and visualising intra-peatland landcover and physical property variations using remotely sensed geoscience "big" data sources, incorporated DA and EDA principles. This is achieved via the following aims:

- Removal of user bias from prediction and model generation where possible, via minimal processing of data and use of neural network prediction methods.
- Develop a data driven method to determine the appropriate number of clusters for a geoscience dataset.
- Develop robust prediction procedure for identifying peat soils using airborne radiometric data using a neural network pattern recognition algorithm.
- Incorporate airborne radiometric data into prediction models of peatlands as a means of visualising subsurface physical property variation.
- Develop a framework to combine multiple coincident spatial data sources to visualise surface **and** subsurface physical property variation on a site.

## 1.4 Summary of chapters

Chapter 2 is a review of current challenges of peatland rehabilitation from policy, hydrology, water chemistry and monitoring. The focus of this chapter within this thesis is the introduction of emerging remote sensing techniques and the associated challenges with mapping and monitoring peatlands, however it also serves as an introduction to peatlands generally and global issues facing their rehabilitation.

Chapter 3 introduces a means to identify peat soils and update peatland boundaries using airborne radiometric data acquired over a large geographical area in the west of Ireland. It develops an innovative modern method of redefining peatlands boundaries and identifying new area of peatlands which may have been overlooked due to their size or a modification of landcover class, effectively masking them from more traditional techniques. The methodology outlined in this chapter has the potential to update national peatland maps based on a direct measurement of the subsurface. The method is applicable internationally, wherever these data exist.

Chapter 4 then analyses the intra-peatland variation of ecological and hydrological indicators of the study area outlined in Chapter 3. This chapter develops a method of determining the appropriate number of clusters, or groups, that a dataset can be divided into, which has applications beyond the scope of this thesis. Intra-peatland variation is visualised using a combination of optical satellite and airborne radiometric data sources in an unsupervised clustering method, to produce zoned maps and an integrated, surface to subsurface interpretation of the peatland with implications for meeting reporting obligations of peatland restoration under international treaties (e.g., European Habitats Directive)

Chapter 5 forms the overall discussion and conclusions from the methods presented in this thesis and highlights future work areas.

Several appendices are also included to present concepts and ideas not appropriate within the main body of this thesis. As this thesis is presented via publications, a breakdown of author contribution to each chapter is outlined in the appendices also.

# Chapter 2: **Management and rehabilitation of peatlands: the role of water chemistry, hydrology, policy, and emerging monitoring methods to ensure informed decision making**

S. Monteverde[1], M.G. Healy[1*], D. O'Leary[2], E. Daly[2], O. Callery[2]

[1] Civil Engineering and Ryan Institute, College of Science and Engineering, National University of Ireland, Galway, Galway, Ireland

[2] Earth and Ocean Sciences and Ryan Institute, College of Science and Engineering, National University of Ireland, Galway, Galway, Ireland

*Corresponding author. mark.healy@nuigalway.ie

## 2.1 Abstract

As the world's most abundant source of terrestrial carbon, peatlands provide numerous ecosystem services, including habitat biodiversity and freshwater quality. Land and water management practices in relation to peatlands, for either exploitation or rehabilitation, are complicated by several factors: spatial diversity in geochemistry; laborious survey methods that may be subject to confounding factors; regional and irregular climate variations; a lack of generalizability regarding appropriate strategies; and, in some countries, by non-implementation of water quality assessment policies for pollution control and land use. Such factors raise uncertainty in the effectiveness of restoration and rehabilitation strategies while modern peatland management looks to develop land use schemes that offer minimal risk to the environment. The aims of this paper were to (1) investigate the disparate factors influencing peatland management which confound appropriate interventions for enhanced water quality (2) examine how non-implementation of national policies for water pollution control may result in adverse environmental impacts, and (3) propose an innovative peatland management methodology for a detailed and robust land analysis with water quality being the primary consideration. The paper suggests that optical, radar, and radiometric remote sensing methods may be used to identify management zones within a peatland, that may require variable management strategies during restoration. Satellite

remote sensing and Earth observation methodologies are well documented; hence, the prospect and properties of a less documented airborne radiometric approach may present an opportunity for improved management of peatlands.

Keywords: Ecosystem services; peatlands management; restoration policy; geochemistry; water quality; remote sensing.

## 2.2 Introduction

Peatlands are considered to be environments sensitive to anthropogenic pressures since the initiated departure from their peak processing of resources for biofuel and agriculture. Although peat-covered landscapes extend across much of the globe, they account for only a small percentage of the Earth's land area (Xu et al., 2018). Prior treatment of peat soil, before the emergence of rehabilitation and restoration, and the conditions placed on it have since created the need for new knowledge on land and water management practices to help promote proper decision making for sustaining peatlands. Their protection is paramount, as they have been proven to act as a channel in the natural carbon cycle (Rixen et al., 2016) and serve as a vital asset towards carbon dioxide conveyance from air to earth material. Created by the build-up of partially decayed plant material and under wet conditions, development of these natural environments over the last 10,000 years has occurred at an average rate of 0.5 to 1 mm yr-1 (Renou-Wilson et al., 2011). Such a slow growth rate offers a major concern when trying to assess the effectiveness of peatland management; to determine not only the success of a conservation strategy but also to develop measures that may induce peat formation.

The goal of peatland restoration is to demonstrate efficiencies using the environmental protection schemes that are expected to restore wetland environments to their appropriate functioning capacity in nature (Kareksela et al., 2015). Rehabilitation efforts usually consist of an artificial manipulation on a natural peatland process to cause a change in either water level or vegetation; the success of which is usually difficult to claim if a peatland has suffered catastrophic damage (Tan et al., 2021). A common practice in rehabilitation involves raising the peatland water table through the construction of dams and drainage blocks at surface outlets (Buschmann et al., 2020). Construction measures effectively create a high soil water content and decrease oxygen availability for microorganisms, limiting and altering

the respiration process that occurs in peat-forming vegetation, enabling peat formation (Husen et al., 2014). When large-scale changes are made to peatlands (drainage, peatland afforestation, and turf harvesting), climate change and airborne and water pollution become a major consideration. The typical activities carried out on fens and raised bogs have invoked questions regarding the roles of peatlands and how they play into global equilibria. The often-scrutinized areas of peatland health consider how peat removal, draining, and drain blocking, which is believed to have a positive impact, can potentially introduce pollution into fresh water resources and alter the global greenhouse gas (GHG) budget (Abdalla et al., 2016). For example, raising water levels can create the anoxic environments that promote anaerobic respiration in the absence of oxygen (Zhu et al., 2018). This condition in the risen water table then has the potential to introduce gaseous methane, which is a much more powerful GHG than atmospheric carbon on a 100-year timescale (IPCC, 2021). Likewise, the anoxia engineered within a once-drained peatland can introduce reactive phosphorus (P) in the soil (van de Riet et al., 2013) and intensify the presence of ammonium ($NH4+$) in the uppermost layers of peat (Lundin et al., 2017). Ammonium behaviour is often well synchronized with the nitrification process, and the ways in which P movement corresponds to changes in water quality parameters usually indicate some effect of soil structure on geochemical properties (Morison et al., 2018). Phosphorus movement and mobilization are also strongly associated with peatland microbial activity and vegetation type and abundances (Luo et al., 2021).

Peatland activities on exhausted lands, whether practices consider environmental sustainability or energy and economic yield, have raised concern on land use and the pressures on water quality that they may present. Traditional approaches to monitoring diffuse pollution have relied primarily on walkover survey methods (Reaney et al., 2019), and in recent years there has been a focus on laboratory and desk-based research methods. The challenge with standard monitoring methods to date has been creating a reliable method to account for temporal and spatial changes in catchment-scale hydrology (Saarimaa et al., 2019; Shore et al., 2014). Modern remote sensing techniques seek to investigate the relationship between diffuse nutrient concentrations and loads on a catchment's hydrological controls (Shore et al., 2014).

Long-term alterations in the water table significantly influence peatland function, and peatland hydrological properties, such as soil-water retention characteristics, are crucial for raised bog self-maintenance (Liu et al., 2022). The rehabilitation work performed on peatlands, based on hydrology, is ineffectually documented and there is an increasing focus on the restoration of hydrological processes of degraded raised bogs, which involves blocking vast drainage networks and outlets (Menberu et al., 2016). In order for a raised bog to reach an optimal growth rate it must be annually waterlogged (Renou-Wilson et al., 2019). It is accepted that by inundating a peatland to an appropriate level, degradation becomes minimized through recreating the hydrological conditions of the healthy peatland's preferred state (Menberu et al., 2016). In any case, excessive runoff is almost always imminent, given the changes in a peatland's ability to store water at a specific time step. Where runoff occurs in degraded peatlands, there can often be a threat of contaminant transport through the bog, especially if fertilizers containing nitrogen (N) and P have been applied within the relevant catchment (Koskinen et al., 2017). Industrial peat extraction also increases the likelihood of pollution influx into neighbouring watersheds, ergo results in negative effects on downstream water resources. Constructed wetlands have been used as viable options to alleviate the negative impacts and have displayed good N and P retention capacity (Karjalainen et al., 2016). Frequent water table analysis has served as a good alternative when assessing water and contaminant retention ability of a restored site (Menberu et al., 2016); however, soil characterization of site-specific locations may provide a new proxy.

This review seeks to explore the unknown factors that may conceivably influence peatland management practices; particularly those that refer to the rain-fed bogs of the northern hemisphere. Most of the current successes of restoration on raised bog sites have lacked generalizability (Renou-Wilson et al., 2019); therefore, certain questions that pertain to raised bog activities have remained loosely answered. Questions such as: How does peatland drainage and use affect hydrology and water quality at field and catchment scale? Which peatland areas should be protected from drainage and intensive land use, and which areas can be used with limited environmental impacts? And finally, how can land and water management be combined in a sustainable way to limit the impacts of threats to water for human consumption and other environmental impacts?

Therefore, the aim of this review is to address the current policies that are active in the realm of wetland conservation and to assess novel techniques for developing peatland management methods. The techniques for identifying critical areas requiring improved management, in theory, can offer further understanding of the mechanisms that control nutrient pathways and retention across a watershed, allowing for knowledge to be gained in the role of nutrients for sustaining environmental structure and function.

## 2.3 Methodology

The manuscript is divided into three parts: the interaction between peatland chemistry and water quality parameters with water table changes, policies relating to the restoration of peatlands, and remote sensing methods for analysing and mapping the characteristics of peatlands that are important for hydrology. In a systematic review, information from published literature in the last 30 years was collated to answer the research questions: how does peatland management practices affect water quality and hydrology, and which are most effective? How has international policy affected management? How can emerging technologies be used to identify, characterise, and assist in the management of peatlands?

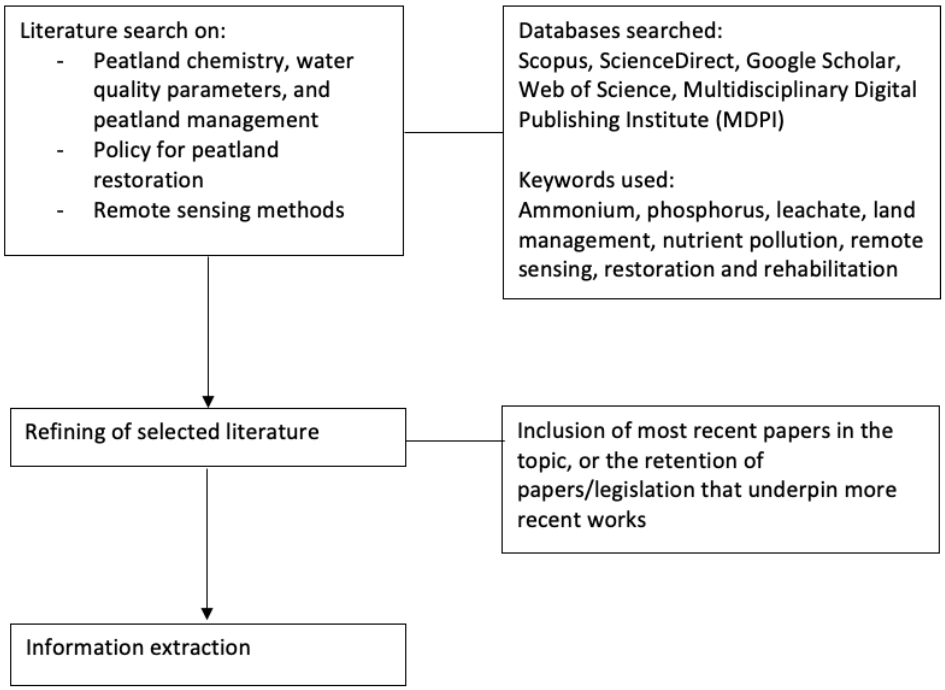


Figure 2.3.1: Methodology flowchart.

To answer these questions, a comprehensive systematic literature review on the following databases was performed: Scopus, ScienceDirect, Google Scholar, Web of Science, and the Multidisciplinary Digital Publishing Institute (MDPI). Keywords in the literature search included: ammonium, phosphorus, leachate, land management, nutrient pollution, remote sensing, and restoration and rehabilitation. Regional limitations were not applied in this paper, although only papers and policy documents published in the English language are included. A methodology flowchart is illustrated in Figure 2.3.1.

After the initial search results were compiled, the reference list was further reduced to include only original research papers or policy documents focusing on one of the three aspects of this paper. The reasons for exclusion of papers were if they lacked scientific rigor or if they were unrelated to the search criteria. In the case of research articles, and particularly in relation to the reporting of the impacts of management practices on water quality, only papers that reported long-term, robust scientific data before and after interventions, were included in this review. As a result of these criteria, 145 papers were selected of which over 50 % were published in the last five years. A schematic of the content of the following sections, which focus on the three areas identified above, is shown in Figure 2.3.2.

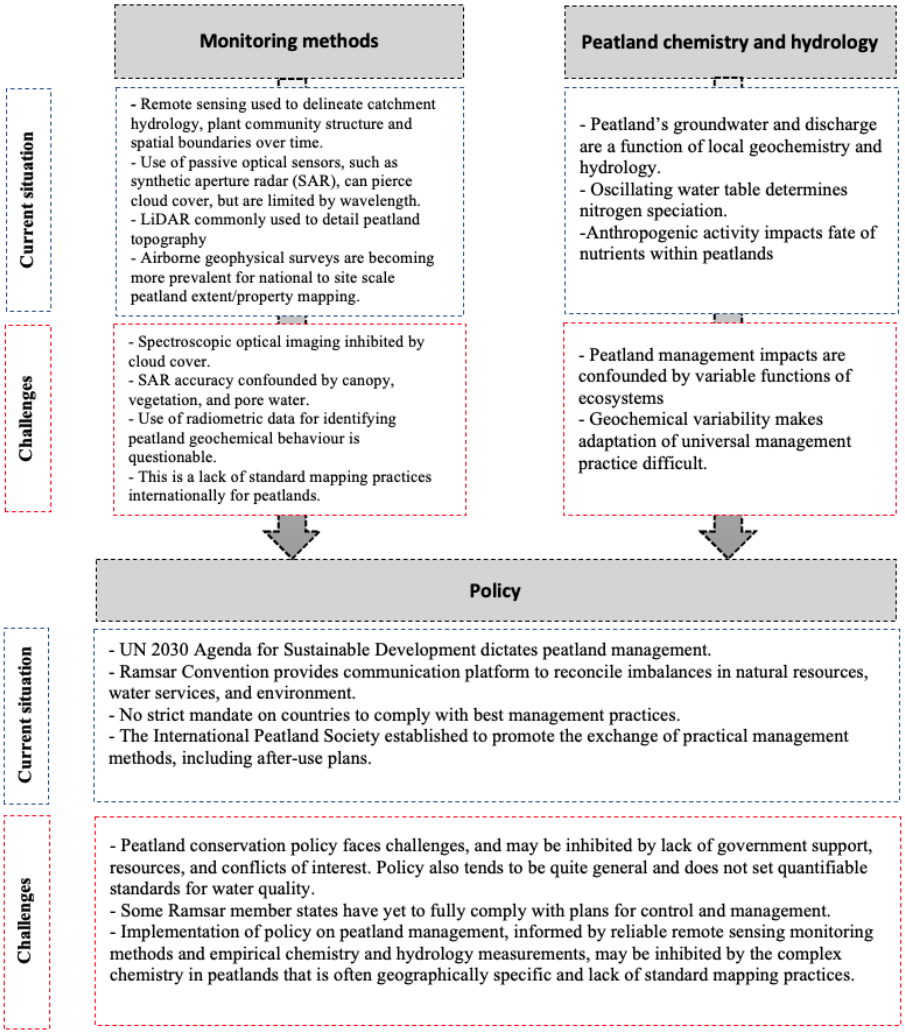


Figure 2.3.2: Current situation and future challenges of the three focus areas of this paper: monitoring methods, peatland chemistry and hydrology, and policy.

## 2.4 Interactions between peatland chemistry, water quality and water table

Peat formation is a perennial occurrence involving an incomplete decomposition of perished vegetation that is perpetuated while being subjected to waterlogged conditions. Essentially, poor drainage characteristics in the long-term result in peatland formation (Treat et al., 2019). When masses of peat-forming vegetation are fully saturated, an absence of oxygen inhibits the full decay of plant matter through an increase in vegetation productivity. When the peat is drained of its freshwater reserves, oxygen is reintroduced and the decay process restarts toward a complete reduction of plant remains (Overbeek et al., 2019).

Acidity and mineralized water variation are two of many parameters that differ across peatland types (Yang et al., 2021). The chemical content of a peatland's groundwater and its discharge express local geochemistry and hydrological developments, with raised bogs tending to be more acidic and fens more alkaline (Griffiths et al., 2019). However, peat accumulation rates are dependent on the supply and cycle of limiting nutrients, N and P (Morison et al., 2018). Microbial behaviour and anaerobic respiration cause a release of N and P from organic matter (OM) during decomposition (Andersen et al., 2013). Soil N forms a feedback mechanism with microbial biomasses in the peat as microbes utilize N and limiting P from soil and decomposition products, yet P cycling is more challenging to document as it is known to vary much less than N which can be associated by weight with peat depth and degree of composition (Morison et al., 2018; Tfaily et al., 2014). Barring any correlations with water table elevation and temperature, soil P is much more elusive as the primary limiting nutrient in freshwater resources (Griffiths et al., 2019). Measures of total phosphorus (TP), in nature, characterize a consequence of underlying fragmentation leaching from reduced parent material to cycle through soil bodies and pore water, and recent studies support the standing claim that a strong correlation exists between TP, water table elevation, and temperature (Griffiths et al., 2019; Munir et al., 2017; Živković et al., 2017).

Increased concentrations of orthophosphate ($PO_4^{3-}$) are usually anticipated at hollow and lawn locations (Macrae et al., 2013) due to an inherent nearness to surface pools and a variable water table height (Moore et al., 2013). With respect to peatland microform, Wood et al. (2016) quantified extractable $PO_4^{3-}$ and N cycling from five different peatlands and described them based on abundances in the topography. Using multiple linear regression, an upper limit of 18 $\mu g\ g^{-1}$ $PO_4^{3-}$ in hummocks and 48 $\mu g\ g^{-1}$ $PO_4^{3-}$ in hollows showed a distinct influence of water on concentrations; quantified spatial N cycling yielded fewer significant results. Sapek et al. (2009) assessed the response of inorganic nutrients to groundwater level fluctuations and found that natural drainage was accompanied by significant increases in both $PO_4^{3-}$ and $NH_4^+$ concentrations within high groundwater samples. Heightened subsurface temperatures during the dry season are significant simply because warmer soil suggests drier soil (Griffiths et al., 2019; Munir et al., 2017). Water table drawdown is often related to such soil temperature increases and the expectation is that the imposed circumstance should achieve greater productivity

in the decomposition of OM, due to the enhanced aeration (Tuukkanen et al., 2017). Although ambiguous with respect to the exact forms N and P, Griffiths et al. (2019) further identified total nitrogen (TN) and TP behaviour increasing with peat depth across several studied sites. Depending on peatland type (minerotrophic versus ombrotrophic) N-containing species may enter a fen peatland via ground water interaction and upwelling (Hill et al., 2016), and depending on the head level near the surface, oscillating oxic/anoxic environments at a groundwater interface can determine the speciation of N (Charlet et al., 2013; Tfaily et al., 2018).

Total P and its proportion of bioavailable PO43-, along with soil total inorganic N (TIN), constrain peat forming vegetation together with soil temperature and water table positioning (Munir et al., 2017). Active drainage and peat extraction alter pore water chemistry and reduce nutrient immobilization. With an already complex nature of water quality evolution, anthropogenic activity resulting in erosion and subsidence has impacted the fate of transients and the deposition of nutrients within peatlands (Tuukkanen et al., 2017).

## 2.5 Policies relating to the restoration of peatlands

### 2.5.1 The Ramsar Convention

The United Nations (UN) 2030 Agenda for Sustainable Development serves as the overarching motivation in peatland management for member states. Under Sustainable Development Goal six (SDG-6) for clean water and sanitation, protection of water-related ecosystems and addressing water pollution are most relevant in terms of peatland degradation (Lele, 2017). To promote engagement between partners on a national level, the Ramsar Convention, established nearly fifty years ago, now provides a platform of communication that is necessary for reconciling the imbalances between natural resources, water services, and the environment (Everard and McInnes, 2018; Tiéga, 2011). Over the last several decades, the attention brought on wetland ecosystem services, which includes peatlands and mires, has promoted measures that seek to benefit wildlife habitats for threatened species, as well as reduce net emissions in a global GHG budget (Huth et al., 2022). All relevant countries are encouraged to adopt conservation policies; however, there is no strict requirement or enforceable mandate placed on governments to ensure that they comply (Moomaw et al., 2018). As it currently stands, there is concern that intergovernmental efforts will not meet SDG-6 by 2030

(Ortigara et al., 2018). Policies attempt to meet the needs of all reliant communities, yet their full application can be inhibited by a lack of stakeholder support, resources, and conflicts of interest (Barchiesi et al., 2018).

The Ramsar convention defines environmental flow as a water adequacy in wetland discharge, stemming from properly functioning catchments that are capable of satisfying ecosystem services and benefits, while sustaining themselves in the environment (Barchiesi et al., 2018). A wetland's effects will propagate on to receiving water bodies and many of the endorsed treatments for ecosystems intend to limit degradation and biodiversity loss, while assisting water quality demands through the same preventions. A system for decision making within the Ramsar Convention assesses values based on ecosystem effects, such as water resource provision, maintenance of options, regulation of hazards and extreme events, and ecosystem processes (Kumar et al., 2017). Effective management would align the values of these services with the best options for policy instrumentation and help bridge the knowledge gaps in land use and environmental flow balance. It is a goal to inform management and reveal to stakeholders how ecosystems can be prioritized while maintaining a concern for socio-economic return.

The 2002 Guidelines for management planning of Ramsar sites and other wetlands (Ramsar, 2002) called for the implementation of a uniform approach to peatland restoration management. It had been viewed as impossible to measure the total extent of these land features in all of their complex chemical aspects; the focuses on wetland health considered point measurement data of key parameters such as nutrient concentrations (Ramsar, 2002). The agreement still stressed the importance of implementing guidelines and urged governments to evaluate policies and to advance strategies (Ramsar, 2002). Consistent recall of the notion on the *wise use of wetlands*, which emphasizes active management of these lands, has been upheld in the addendums of resolutions to date (Ramsar, 2015b), i.e., in resolutions XIII.17, XII.12, and VIII.17 (Everard and McInnes, 2018; Ramsar, 2006; Ramsar, 2015a).

Beyond the influence of Ramsar, regional mechanisms such as the European Union (EU) also act to motivate states into compliance with environmental flow policy (EC, 2000). A 2006 EU directive (EC, 2006) mandated that member states establish threshold values for groundwater substances, e.g., ammonium. Since

transposition of EU law is the responsibility of its members, threshold values vary from state to state (EC, 2006). In 2012, Ramsar member states adopted Resolution XI.8 Annex 2 (Rev. COP13) through which they agreed on the importance of incorporating aspects of nutrient quantification in peatland assessments (Ramsar, 2012).

### 2.5.2 Challenges facing implementation of policy

As of 2021, some Ramsar member states still had not fully adopted national plans for pollution control and management, or policies on wastewater management and water quality as they relate to environmental flow. Implementation of policy on peatland quality and environmental flows, at the international and national level, face challenges and it is evidenced that the existing strategies do not always address the quantitative issues of water quality, restoration, and management in detail (Reed et al., 2014). Regional bodies and international treaties communicate the intentions of the party with only general guidelines to approaches and therefore, it is difficult to determine acceptable standards for water quality, for instance, standards regarding nutrient load and leachate. Policy makers must decide to enact either accurate data measuring protocols or opt for cheaper and faster alternatives with less accurate results (Reed et al., 2014). Through analysis of the financial aspects to peatland management, Reed et al. (2014) emphasized that there are a number of ways by which peatland changes influence ecosystems service allocation. They suggested the use of a method whereby values are supplemented from other similar ecosystems when water quality data are lacking.

Another intergovernmental organisation with the intent of advancing scientific knowledge on peat, the International Peatland Society (IPS), was established to promote an exchange of practical management methods (Joosten and Clarke, 2002). In 2008, this particular organisation sought to facilitate responsible peatland management with steps to foster the creation of a global peatland strategy in the "wise use of peatlands" (Clarke and Rieley, 2010). The IPS stresses the importance of after-use plans, identifying the entities that will be accountable for the operation of specified after-use, implementation of the most current technical knowledge of peatland functions and services to inform the after-use management practice, and consistent survey analysis of programs in a timely manner to improve procedures

if the objectives are not realized (Clarke and Rieley, 2010; Gaudig and Tanneberger, 2019; Graf and Rochefort, 2016). Salomaa et al. (2018) describe criticisms and roadblocks to policy instruments at national levels due to disagreements regarding landowner rights and the requirements of conservation. Precise arrangement of after-use is likely to be settled by landowners or relevant stakeholders in consultation with a specific authority; arrangements typically incorporate an artificial rise in the peatland's water table (Clarke and Rieley, 2010). Mandatory policy is perceived as an effective instrument for attaining sustainability results, but the policies often lack acceptance.

### 2.5.3 Links between peatland management, policy, and water quality

Limited research fails to convey how peatland conservation measures are chosen at the national level and how they are effectively integrated during policy operation (Kamal et al., 2015; Salomaa et al., 2018). However, regardless of national policies and their acceptance, independent studies of peatland management and the effects of restoration are ongoing. Table 2.5.1 shows water quality changes of key nutrient species produced in peatland after-use strategies.

Table 2.5.1: Changes in mean concentrations (mg/L) of total nitrogen (TN), total phosphorus (TP), ortho-phosphorus (PO43-), ammonium (NH4+) and dissolved organic carbon (DOC) from several European catchments after various management interventions to restore them; measured annually in porewater studies (except for NH4+ concentrations in Beltman et al. (2014)), and biweekly in Stimson et al. (2017)).

| Management | Peatland type | Location | Mean annual rainfall (mm) | Concentration (mg $L^{-1}$) | | | | | | | | | | | |
|---|---|---|---|---|---|---|---|---|---|---|---|---|---|---|---|
| | | | | Before intervention | | | | | | After intervention | | | | | |
| | | | | TN | TP | $PO_4^{3-}$ | $NH_4^+$ | DOC | | TN | TP | $PO_4^{3-}$ | $NH_4^+$ | DOC | Reference |
| Rewetted / flooded[1] | Raised bog/fen | Sweden | 800 | 2.58 | 0.034 | 0.095 | 0.82 | | | 2.38 | 0.104 | 0.101 | 0.59 | | Lundin et al. (2017) |
| | Raised bog | Sweden | 800 | 1.58 | 0.016 | 0.009 | 0.82 | | | 1.51 | 0.021 | 0.012 | 0.97 | | Menberu et al. (2017) |
| | Minerotrophic fens, pine and spruce mires | Finland | 513-656 | 2.29 | 0.150 | | | | | 2.38 | 0.206 | | | | Beltman et al. (2014) |
| | Fen meadow | Ireland | | | | <0.05 | 0.17[3] | | | | | <0.15 | 0.19[3] | | |
| | Fen meadow | Ireland | | | | <0.05 | 0.13[3] | | | | | <0.10 | 0.44[3] | | |
| | Fen meadow | Netherlands[4] | | | | <0.05 | | | | | | <0.25 | | | |
| | Raised bog[5] | Wales | | | | | | ~90 | | | | | | 320 | Fenner et al. (2011) |
| | Forested peatland | Finland | 620 | ~2.6 | ~0.25 | ~0 | ~0 | ~50 | | ~12 | ~1 | ~0.7 | ~2.5 | ~250 | Koskinen et al. (2017) |
| | | | | | | | | | | | | | | | |
| Fertiliser application[2] | Blanket bog[6] | England | | | | ~1 | | | | | | 233 | | | Stimson et al. (2017) |
| | Cutaway peatland[7] | Ireland | 875 | | | 0.014 | | | | | | 3.01 | | | Renou-Wilson and Farrell (2007) |

[1]Porewater and groundwater nutrient measurements; [2] Nutrient measurements in runoff via peatland catchment drainage; [3] Ammonium ion concentrations measured approximately one week after restoration/flooding; [4] Utrecht catchment had a history of fertilization treatment (95 kg P $ha^{-1}$ $y^{-1}$ and 250 kg N $ha^{-1}$ $y^{-1}$); [5] Values reported are maxima for a control ("before intervention" in the categorization rubric of this table) and rewetted bog ("after fertilization"); [6] Data taken from the largest catchment in the Stimson et al. (2017) study; [7] P applied at 25 kg $ha^{-1}$ in 1999 and again in 2002. Sampling period from 1999-2004. "After intervention" value is the maximum recorded in 2000.

Considering the three management methods described the frequency of sample collection in the rewetted/flooded scenarios ranged from one week after treatment, in Beltman et al. (2014), to more seldom and annual sample collection regimes (Lundin et al., 2017; Menberu et al., 2017). Menberu et al. (2017) reported that water level fluctuation impacted pore water quality, especially in the time period immediately after management implementation. Lundin et al. (2017) investigated the effect of long-term inundation and contrarily demonstrated the success of rewetting; notably in decreasing ratios of $PO_4^{3-}$-P to TP and inorganic N to organic N, that began to stabilize with time. The temporal scale of each study accounted for hydroclimate variability by considering nutrient dynamics and biogeochemical behaviour over the years monitored (Gu et al., 2017). Discrepancy between the reported conclusions is a result of inherent variability. Drought duration prior to rewetting, intermittent water level fluxes, topography, and the magnitude of hydrologic instabilities can trigger or inhibit nutrient release (Blackwell et al., 2013; Brödlin et al., 2019; Gu et al., 2017); prolonged drought followed by heavy rainfall activated N loss and release in Wang et al. (2016). Even P mineralization can vary based on the spatial occurrence of microenvironment varieties within catchments, and depending on the chemistry of soils, increases of dissolved iron hydroxides through constant waterlogging (Gu et al., 2017; Jeanneau et al., 2014; Pant, 2020). Biogeochemical N turnover, however, differs from P transformations (Macek et al., 2020) through processes of: (1) plant and organic N mineralization to $NH_4^+$ (Hinckley et al., 2019) (2) anaerobic $NH_4^+$ oxidation under redox conditions; optimized growth of a functional group by soil exposure to the atmosphere (Faulwetter et al., 2009; Kim et al., 2017) (3) nitrification, the conversion of intermediate $NH_4^+$ to $NO_3^-$, governed by oxidation-reduction (Jiang et al., 2015) (4) $NO_3^-$ conversion to $NH_4^+$ occurring under anoxia and in environments with $NO_3^-$ limited bed material (Zhao et al., 2019), and (5) denitrification (Taghizadeh-Toosi et al., 2020).

In riparian wetlands, the mineralization of N follows the processes of its respective cycle (Reverey et al., 2016). Anoxia and the repressed redox environment in peatland rewetting can prevent nitrification, which in turn leads to a depletion of available $NO_3^-$ via the pending denitrification process (Hinckley et al., 2019). By this mechanism, nitrification cessation is a direct consequence of rewetting management and promotes the risk of introducing $NH_4^+$ in surface waters

(Nieminen et al., 2020). The peatland observed in Beltman et al. (2014) displayed a threefold increase in $NH_4^+$ following rewetting (Table 2.5.1). Although increases were detected, the data were derived from samples collected approximately one week after flooding and were likely the result of a rapid nutrient surge (Dinh et al., 2018; Sola et al., 2018). The high frequency of N evolution has implications for the management of N flux and is a crucial factor of consideration in peatland restoration (Kasak et al., 2021).

Peatlands can potentially act as critical source areas (CSAs), locations within a watershed where areas generating pollution overlap hydrologically sensitive areas (Ghebremichael et al., 2013), as they possess the capacity to chemically restructure accumulated nutrients (Gu et al., 2017). The attribution of land management practices and their critique are often masked by the details of catchments and the variable functions of ecosystems (Nieminen et al., 2020; Purre and Ilomets, 2018; Schulte et al., 2019). Prior to their most recent work on P speciation within peatlands, Negassa et al. (2019) addressed a deficiency in modern experimental data that links spatial variability of biogeochemical properties to peatland phenomena, under pristine and degraded conditions; specifically, regarding the influence of rewetting impacts on P evolution. In an added effort to rectify the notion, Negassa et al. (2019) conveyed the importance of considering soil P species and abundance with peatland class, temporal conditions associated with drainage and rewetting, and land use within catchments in order to better isolate biodiversity and anthropogenic nutrient impacts, caused via management. Most of a catchment's diffuse pollution originates from a small portion of the total area. CSAs are the locations from where major amounts of the total pollution disperse into the landscape (Hepp et al., 2022). Regarding agricultural practices, CSA concerns encompass N, P, and sediment (Giri et al., 2016). Primary CSA concerns involving wetlands have always included sediment and P, but there is very little information in the literature reporting influences of anthropogenic pressure on N cycling and N runoff (Giri et al., 2016). The spatial diversity of geochemical processes presents complication (Gu et al., 2017) and for survey analysis, it is important to establish efforts from informed peatland ecosystem and hydrologic relationships (Schulte et al., 2019).

## 2.6 Current and emerging survey methods of peatlands

In 2019, the UN Environment Assembly implemented policy (Resolution 16) calling on the UN Environmental Program (UNEP), in collaboration with the Ramsar Convention and member states, to establish a global inventory of peatlands; ergo, to record the wide use of specific interventions, mitigation, and planning for peatland maintenance and land use (UNEP, 2019). The UN Environment Assembly of the UNEP cites Ramsar Resolution XIII.13 as a main framework for interpretation and technical guidance (UNEP, 2019) on the value of satellite remote sensing and how techniques, along with geophysical survey methods, can inform restoration planning. Through remote sensing, it is recommended that practitioners determine peatland dimensions and site locations that could benefit from restoration works. The recommendations further state that if it is possible, the parameters of peat quality and the potential influences that it may have on the environment after restoration should be considered (Ramsar, 2018).

### 2.6.1 Current survey methods

Application of remote sensing technology to peatland profiling is not a recent concept (Worsfold et al., 1986). For roughly half a century, governmental agencies have been attempting to gain knowledge on the extent of peatland dimensions and Ramsar has consistently emphasized its SMART (specific, measurable, achievable, relevant and time-bound) objectives (Barchiesi et al., 2018; Scheltinga and Heydon, 2005), putting forth significant effort towards developing baseline inventories (Rebelo et al., 2008). When implemented, remote sensing can assist in the delineation of a catchment's hydrology, identify plant community structure, and highlight spatial boundaries (Harris and Bryant, 2009). Many remote sensing methodologies currently look to reduce the need for specific ground-based observations via a one-time calibration, while seeking increased accuracy in detecting land use and land cover changes. There is also the offered capability of monitoring sites under high temporal resolution, with some satellites being able to provide data on regular time intervals of one to sixteen days (Lees et al., 2018). This consistent reoccurrence allows for the monitoring of short term events, such as the seasonal oscillation of a peatland's surface height, flooding, drying, and peatland restoration over time (Tampuu et al., 2020).

### 2.6.2 Emerging survey methods

#### 2.6.2.1 Satellite remote sensing

Active remote sensing techniques emit their own energy source and passive systems detect radiation that is either reflected or emitted in response to a natural source, i.e., the sun. As methodologies continue to improve, active and passive techniques are often combined to reduce the influence of limitations characterized in a single set of inputs (Bourgeau-Chavez et al., 2018). Passive optical sensors, notably IKONOS, short-wave infrared, and UV-Vis near infrared, are capable of providing up-to-date information for the purpose of soil mapping and providing good resolution at multiple spatial scales (Escribano et al., 2017). However, the use of spectroscopic optical imaging for peatlands as a single metric presents limitations that are caused by cloud cover and an inability to detect small scale height variation across a landscape's surface, i.e., in the hummock and hollow microtopography (Anderson et al., 2010; Niculescu et al., 2016). Longer wavelength, active remote sensing methodologies such as synthetic aperture radar (SAR) can pierce cloud cover and capture three-dimensional topographic variation. The created microwave radiation and the backscatter detected by SAR sensors usually enable a capable methodology aimed at under-canopy observation, detecting inundation, and the classification of wet soils hidden by vegetation (Bourgeau-Chavez et al., 2018). However, a majority of these benefits are heavily dictated by the appropriate wavelengths (Millard and Richardson, 2018). For agricultural monitoring of land cover change, SAR can be ideal due to the scatter of longer wavelengths which are caused by easily discernible crop and large vegetation structures (Mandal et al., 2019). In ecosystems where plant cover is generally tall, SAR detection and volume scattering, as described in Bechtold et al. (2018) whereby electromagnetic radiation transmits between media, would be dependent on canopy structure and vegetation wetness (Millard and Richardson, 2018). When monitoring a peatland, water level variation is significant over very short distances and this is evidenced in the peatland microtopography (Millard and Richardson, 2018). In addition, volume scattering can occur as EM radiation infiltrates into surficial peat and this further extends to the properties of peat surfaces, texture, and roughness; therefore, not only is a backscatter rebound related to the canopy and vegetation, it is also affected by pore water content and the characteristics of the peat (Millard and Richardson, 2018). Since the

reproductive response observed in bog vegetation occurs over a multi-decadal time frame (Ratcliffe et al., 2018), an undisturbed peatland surface displays very limited temporal variation in contrast to an agricultural crop land (Millard and Richardson, 2018).

#### 2.6.2.2 Synthetic aperture radar (C-Band)

For the purpose of monitoring water table depth, Bechtold et al. (2018) explored the use of C-band backscatter data (information derived from a specific microwave range of frequencies) available through the European Space Agency's ENVISAT satellite. Concurrently, Millard and Richardson (2018) had made brief reference to a capacity for quality spatial resolution (eight meters aggregated to one-hundred meters for improved classifications) that could be obtained by C-band backscatter, especially in relation to peatlands. Bechtold et al. (2018) applied an advanced SAR technique and linked field observations of water table depth to the backscatter that may only be detected in the top one to two centimetres of peat soils, using vertical-vertical polarization. The results were considered useful for predicting some behaviour of water fluctuation beneath a peatland's groundwater interface, but due to limitations there was little consistency in the relationship between the study's measured water table heights and the backscatter response associated with threshold depths (Bechtold et al., 2018). Across the observed sites, it was suggested that a depth range of half a meter to one and a half meters below the surface presented a threshold where correlation between water level and backscatter was lost, and possibly explained by reduced capillary action (Bechtold et al., 2018). In spite of inconsistencies and ENVISAT SAR coarse spatial resolution of one kilometre, the predictions motivated by C-band SAR served as adequate indicators of water level dynamics above thresholds and the method was viewed as having high potential for future investigations (Bechtold et al., 2018).

#### 2.6.2.3 Combination of SAR and LiDAR data

In a 2016 report on wetland vegetation mapping, passive and active data from optical sensors and SAR were linked with airborne laser scanning via light detection and ranging (LiDAR) in the Danube Delta (Niculescu et al., 2016). Modern LiDAR is a tool that has been developing over the last decade and is capable of returning three-dimensional digital representations of surfaces based on laser cycling and wavelength (Giarola, 2018). In cases of remote sensing where surface heights are

generalized from field measurements and interpolation, the application of LiDAR offers a direct measure of vertical surface components and allows for vertical diversity with ten centimetre accuracy along a Z axis (Niculescu et al., 2016). Although the results of this study did not confirm the greatest accuracy when integrating all three sensor types together, Niculescu et al. (2016) revealed efficient abilities to discern ecological complexes through combinations of optical and airborne LiDAR data, and optical data paired with Satellite C-band RADARSAT SAR, for vegetation classes that exist within the area observed. To ascertain the health of a raised bog and the scope of a restoration procedure on its hydrological system, surveys have often relied on an ecotope typology, which is described by the smallest distinct living component within the scale of the landscape (Schouten et al., 2002). In a study similar to Niculescu et al. (2016), that involved vegetation distinctions on an ombrotrophic bog, airborne LiDAR data and IKONOS optical image bands (Anderson et al., 2010) were combined in a multispectral and spatial approach. Anderson et al. (2010) were able to demonstrate that airborne LiDAR data can detail peatland topography and allude to eco-hydrological distinctions. The study effectively enhanced the spatial characterization of a peatland's surface conditions and vegetation via the joining of airborne LiDAR data, with one-meter spatial resolution and a twenty-five-centimetre vertical accuracy to multispectral classifications of four-meter spatial resolution via IKONOS.

#### 2.6.2.4 Combination of modelling tools and LiDAR-based DEMs

Like degraded peatlands, contemporary agriculture tends to alter natural nutrient behaviour and introduces further complexity to the source-pathway-receptor scheme associated with nonpoint source pollution and hydrologically sensitive areas (Mockler et al., 2016). Novelties regarding freely available, remotely sensed information have advanced environmental modelling approaches and led to more exact descriptions of CSAs at the landscape and catchment scale (Djodjic et al., 2018). To capture and highlight agricultural nonpoint source pollution flows, studies often depend on the use of the Soil and Water Assessment Tool (SWAT) (Hua et al., 2019). This modelling tool is frequently paired with Airborne LiDAR based Digital Elevation Models (DEMs) in keeping with the current trend of using the highest resolution data available (Foulon et al., 2019). LiDAR-based DEMs are capable of achieving consistent spatial accuracy of between one and two meters (Lee et al., 2019), whereas other sources, e.g., Advanced Spaceborne Thermal

Emission and Reflection Radiometer, CartoDEM, and Shuttle Radar Topography, are less effective at providing high resolution imagery for small spatial applications (Goyal et al., 2018). This is especially important in peatland mapping where small vegetated structures, hummocks, and hollows dominate the topography (Kalacska et al., 2018). LiDAR continues to remain an effective component when incorporating land elevation criteria, even though the technique only captures a static representation of the ground surface and its vegetation (Millard and Richardson, 2018). However, peatland biomass responds at a slow enough rate (average rate of 0.5 to 1 mm $yr^{-1}$), even under optimal growing conditions (Renou-Wilson et al., 2011), which allows remote sensing survey regimes on the scale of years to be suitable when accounting for natural landcover change.

#### 2.6.2.5 Electromagnetic survey methods

Remote sensing and Earth Observation are terms usually associated with satellite borne methods; however, they can also refer to geophysical methods which are becoming more common for large-scale subsurface environmental investigations (Binley et al., 2015). Geophysical surveys enable vertical and lateral investigation into the subsurface to tens of meters and have been used for mapping peatlands in terms of spatial extent and intra-peat variability (Minasny et al., 2019), whereas satellite remote sensing typically returns information from the top few centimetres of a surface. Broadly speaking, geophysical surveys can be broken into airborne and ground surveys, where the former benefits from larger survey areas and the latter from an increased resolution. The Electromagnetic (EM) method uses low frequency EM waves to map variation in the electrical conductivity of subsurface structures and relates to physical properties such as saturation, porosity, permeability, and mineral content (Carcione et al., 2003). To peatland hydrogeological investigations, EM data offer the means to characterize a subsurface where passive and satellite methods may only provide surficial information (Boaga, 2017).

Airborne EM methods consisting of both frequency-domain and time-domain approaches, measure the apparent electrical conductivity of the ground to depths ranging from a few to a few hundred meters, depending on the instrument selected and the ground conductivity (Paine, 2003). Apparent conductivity serves as a descriptor for integrated soil properties such as bulk density, salinity, and moisture

content (Paine, 2003). Boaga (2017) highlighted the development of the ground-based frequency domain electromagnetic (FDEM) method and its use in hydrogeophysics. FDEM has been shown to be a powerful tool for characterizing soil properties through the use of a multifrequency system that collects information from the soil at many simultaneous depths (Boaga, 2017). The approach offers high spatial resolution and a depth of investigation from centimetres to several decametres, depending on the instrumentation and the properties of the ground.

Silvestri et al. (2019a) employed the time domain EM (TDEM) survey method and the study served as the premier undertaking in the use of airborne electromagnetics (AEM) for regional scale peat depth analysis. The TDEM survey results were combined with artificial neural network (ANN) methodology to estimate peat thickness from 14 field samples where peat thickness was known. This network was then employed to estimate peat thickness and volume over a larger survey area. TDEM can be appropriate for peatland characterization due to its heightened sensitivity to shallow variations in subsurface properties (Silvestri et al., 2019b). The amount of field observations performed was regarded as a primary limiter to the studies, as peat characterization could not be performed extensively (Silvestri et al., 2019a). In Silvestri et al. (2019b), the AEM methodology was used to construct an accurate three-dimensional representation of a peatland, accounting for peat thickness across the entire ecosystem. Aside from the logistical adversities, e.g., flight line spacing and cost, both studies highlighted limitations of the TDEM method. Limitations included difficulty with imaging the base of peat due to low electrical conductivity contrasts between organic matter and bedrock, an inability to detect thin layers of both peat and clay, and a low number of field samples for ground truthing (Silvestri et al., 2019a; Silvestri et al., 2019b). However, it was noted that in the presence of high electrical contrasts, this method would have an increased ability to detect peat thickness and may be more applicable in other situations.

#### 2.6.2.6 Ground penetrating radar

Ground-based geophysical methods, such as ground penetrating radar (GPR) again, use low frequency EM waves with slightly higher energies than those detected by EM methods to identify peatland stratigraphy and thickness (Zajícová and Chuman, 2019). GPR is capable of detecting changes in the EC of water

occupying void space; however, it cannot detect hydrological connections without some form of supplemental inputs, e.g., a tracer solution (Holden, 2004). Characterization by EC, via electrical resistivity surveys, has also been explored in peatland assessments (Clément et al., 2020). The concept fuelling this particular avenue of research lies in the chargeability of peat. Peatland conductance, or resistivity, in the partially decomposed organic matter could allow for mapping by electrical properties (Márquez Molina et al., 2014). By this measure, nutrient species and independent ions cannot be directly quantified but relationships with chargeability can be drawn as this has been performed in agricultural assessments of TN and mineral N (Fahmi et al., 2019). However, similar to the application of GPR, when considering airborne EM and the physical diagnostic of EC, if peat substrate materials are highly conductive or if conductance is highly variable over short distances (Parsekian, 2018) the signal interference potential in the substrate could mask the desired detection. The methods mentioned thus far, and similar methods of induced polarization and EM induction, are all variations of an EC metric (McLachlan et al., 2017).

#### 2.6.2.7 Radiometric surveys

Lastly, gamma ray spectrometry, or radiometric survey, relies on the decay of potassium ($^{40}$K), uranium ($^{238}$U), and thorium ($^{232}$Th) radionuclides which are characteristic elements of bedrock materials; and, unlike the previous methodologies, signal detection takes the form of a passive reading due to the radioactive decay of the associated elements that make up the top sixty centimetres of the subsurface, approximately (Beamish, 2013). The incoherent scattering produced during radioactive decay (Beamish, 2013) can undergo attenuation or, put another way, a loss of flux occurs as a portion of gamma scatter interacts with an absorber medium, i.e., water. Soil can be described as a three-phase system with solid, liquid and gas being referred to as the parent material. Porewater and air are the phases and aspects of the parent material that affect the radiometric attenuation in the soil. Depending on the level of saturation, soil water content lends to a functioning increase in the attenuation of the gamma signal. Beamish (2013) highlighted the theoretical depth of investigation in the majority of near-surface earth materials to be approximately sixty centimetres, depending on saturation. As peat is made up of organic material it acts solely as an attenuator as opposed to a source of the radioactive signal. The relatively low dry bulk density

combined with high porosity and typically high saturation give peat its unique significance within the realm of radiometric surveys. Beamish (2013) demonstrated that intra-peat variability could be noted within an airborne radiometric survey from Northern Ireland. This variability was linked to either varying peat depth or peat saturation with ground truthing required to verify any results. The effect of saturation is clearly demonstrated when focused on peat.

The ability to precisely distinguish boundaries has led to radiometric associations in the general mapping of peatlands. In Northwest Germany, Siemon et al. (2020) most recently used radiometric detection with helicopter-borne FDEM for mapping peat volume within a bog. The German study sought to quantify thickness and extent, but it was noted that the radiometric data could not be used solely. Due to the nature of the radioactive decay and the parent material, and the attenuators, e.g., degree of water saturation in the peat, the precise nature of the radioactive decay cannot be known through simple qualitative analysis (Siemon et al., 2020). It is considered a must to combine radiometric input with some other method for developing novel methodologies.

As Siemon et al. (2020) have paired radiometric data with AEM, Gatis et al. (2019) have combined the data with airborne LiDAR. In the latter example, a digital surface model produced from the LiDAR, with one-meter resolution, was aggregated to contain cell sizes of ten meters in order to better accommodate radiometric counts. The soil attenuation information and the detected microrelief produced a spatial interpretation that accounted for peat depth and offered a modelled scale that is considered to be effective enough for land management decisions (Gatis et al., 2019). Airborne geophysical survey by radiometric detection and its integration have also been previously used in conjunction with peat depth and soil organic carbon (SOC) data to spatially interpolate SOC throughout a peatland (Keaney et al., 2012).

## 2.7 Conclusion

Discrepancies between state-level attitudes and international initiatives have historically dampened the efforts of an accepted global policy; one that is aimed at safeguarding environmental flow derived from peatland ecosystems. Regardless of destructive activities, national intricacies, and the posteriority of sustainable

development goals placing peatlands in states of distress, there is uncertainty regarding the effectiveness of rehabilitation and restoration.

To assess the benefits of management activities and to weigh those benefits against their potentially hazardous impacts, there must be an informed methodology that can provide suitable hydrological and geochemical characterization at a site scale. Such a methodology should serve a twofold purpose: offering data that may infer the health of a peatland ecosystem and data that can act as input for water quality and NPS pollution models.

General applications of remote sensing give true results covering many soil processes; however, their use for identifying peatland geochemical behaviour is questionable. High variation in subsurface water levels that occurs over short distances within a peatland has long been a challenge for groundwater predictions, and this water level flux is suspected to have a dramatic influence on the composition and chemical activity of stored water.

Exploration into the synergistic use of optical, radar, and radiometric resolution will expand as a metric for assessing the relevant phenomena, whether they be natural or anthropogenic. These combined techniques can provide detail from within the shallow subsurface and may counteract the current limitations associated with existing electromagnetic methods.

# Chapter 3: **Digital soil mapping of peatland using airborne radiometric data and supervised machine learning – implication for the assessment of carbon stock.**

Dave O'Leary [a], Colin Brown [a], Eve Daly [a]*

[a] Hy-Res Research Group, Earth and Ocean Sciences and Ryan Institute, College of Science and Engineering, National University of Ireland, Galway, Galway, Ireland, H91 TK33

*Corresponding author: eve.daly@universityofgalway.ie

## 3.1 Abstract:

Peatlands account for approx. 4.23 million km$^2$ of the land surface of Earth and between 5% and 20% of the global soil carbon stock, however much uncertainty exists. The release of carbon from modified peatlands is significant and affects the global carbon balance. The importance of conservation and rehabilitation of peatlands is clear. Global estimates currently use national scale mapping strategies that vary depending on available resources and national interest. The most up-to-date methods rely on satellite remote sensing data, which detect peat based on a multiband spectral signature, or reflected radar backscatter. However, satellite data may not be capable of detecting peat under landcover such as pasture or forest. Airborne geophysical surveys provide relevant subsurface information to update or redefine peatland extent maps at a national scale. Radiometric surveys, which measure the naturally occurring geologically sourced potassium, uranium, and thorium, offer the largest potential. Modelling of gamma ray attenuation shows that peat has a distinctive attenuation signature, due to its low bulk density, when considering all recorded radiometric data. This study exploits this signature by combining airborne radiometric data in a machine learning framework and training an artificial neural network to detect those data which have been acquired over previously mapped peatlands. A ~ 95% predictability is achieved. The trained neural network can be then used to predict the extent of all peatlands within a region, including forested and agriculturally modified peatlands, and an updated peatland map can be produced. This methodology has implications for global

carbon stock assessment and rehabilitation projects where similar datasets exist or are planned, by updating the extent and boundary positions of current peatlands and uncovering previously unknown peatlands under forestry or grasslands.

Keywords: Peatland restoration, Neural Networks, Airborne Geophysics.

## 3.2 Introduction

Peatlands provide a range of ecosystem services such as water regulation, biodiversity, and climate regulation (Grand-Clement et al., 2013; Kareksela et al., 2015). They occur globally (Figure 3.3.1) in the humid tropics (e.g., Southeast Asia) and cool temperate regions (e.g., northern Europe) (Dargie et al., 2017; Tanneberger et al., 2017; Xu et al., 2018). Peatlands are estimated to account for approximately 4.23 million km2 (or 2.84%) of the global land area (Xu et al., 2018) and contain between 5% – 20% of the global soil carbon (C) stock (Treat et al., 2019). The release of C from drained peatlands is significant and affects the global C balance (Evans et al., 2021; Kareksela et al., 2015; Qiu et al., 2020; Yu et al., 2011). The importance of conservation and restoration of peatlands in reducing greenhouse gas emissions can be seen with the creation of the Global Peatlands Initiative (GPI, 2016), recent reports (Searchinger et al., 2022) and the ambitious 55% reduction in emissions outlined in the European Union (EU) 2030 climate and energy framework (EU, 2020). However, there are considerable uncertainties at all scales (local to global) on peatland extent and volume (Xu et al., 2018) and new tools are required to update existing peatland databases (Minasny et al., 2019; Monteverde et al., 2022).

At the global scale, peatland maps are created by combining the Harmonized World Soil Database (HSWD) with regional and nationally available soil maps (Xu et al., 2018; Yu et al., 2010) A review paper (Minasny et al., 2019) outlines 12 national scale peat mapping attempts (Brazil, Indonesia, Scotland, Ireland, Canada etc), ranging from traditional methods to modern digital soil mapping techniques (McBratney et al., 2003; Zhang et al., 2017). The inconsistent techniques, and the uncertainties for each technique, used in national scale soil mapping projects translates to global uncertainty of peatland extent (Xu et al., 2018). Countries with access to remotely sensed satellite and geophysical data can provide more accurate national peatland maps, and the inclusion of these data should be encouraged (Minasny et al., 2019). Additionally increases in peatland map resolutions are

needed to include previously unmapped peat in national inventories (Connolly and Holden, 2009).

Optical satellite data are often used as part of national mapping projects (Aitkenhead, 2017). Their high spatial resolutions (10-30 m) measure the surface reflectance for several bands of visible and near-visible electromagnetic energy. Often, individual optical images are combined into land cover maps, an example is CORINE 2018 produced at a scale of 25 hectares (ha) (CORINE, 2018) to detect peatlands (Aune-Lundberg and Strand, 2021; Wijedasa et al., 2012). Synthetic Aperture Radar (SAR) satellite data measures the strength of a returning radar signal and are sensitive to moisture to depths of ~10 cm and spatial resolutions of ~10 m (Wang and Qu, 2009). These data have been used successfully to delineate peatlands (Merchant et al., 2017; Novresiandi and Nagasawa, 2017). SAR data are unaffected by cloud coverage, however they are sensitive to local meteorological conditions such as rainfall (Hird et al., 2017), which affects soil moisture, making global mapping difficult without significant ground calibration. Optical and SAR remote sensing techniques sample the landcover and the very near surface respectively and so may not detect peat soils modified by agriculture or forestry (Gatis et al., 2019), which are significant contributors to C stock assessment (Donlan et al., 2016; Wilson et al., 2016).

National scale geophysical surveys appear to provide the most accurate estimates of peatland area, with the electromagnetic (Boaga et al., 2020; Siemon et al., 2020) and radiometric (Airo et al., 2014; Berglund and Berglund, 2010) methods showing prominence. The radiometric technique, the focus of this article, measures the naturally occurring radiation present in geological material (Minty, 1997), most usually Potassium ($^{40}$K), Uranium ($^{238}$U) and Thorium ($^{232}$Th). These elements decay directly, or via daughter elements, at discrete energy levels (Minty, 1997), and are recorded as gamma ray counts per second (cps). A 4th Total Count measurement of all radioactive sources is also recorded from the full energy spectrum. Different geological material is made up of different combinations of elements, so the level of the initial radioactive source may vary depending on the underlying geology present. Surveys can be conducted by aircraft, allowing for large areas to be consistently surveyed. Traditionally these data were used for bedrock and sediment mapping (Martelet et al., 2006), but several local, regional and review studies have investigated the potential of radiometric data when considering

peatland mapping (Ameglio, 2018; Beamish, 2014; Reinhardt and Herrmann, 2019; Siemon et al., 2020).

Radiometric data give a direct measurement of the subsurface. Gamma rays emitted from geological material must pass through any overburden present. This overburden acts as an attenuator (Beamish, 2013). Mineral soils may act as an additional source of radiation due to their parent material (Rawlins et al., 2007). Peat soils, however, have unique attenuation properties due to low bulk density, high porosity and pore saturation, and little radioactive parent material to contribute to the signal. Very low radiometric signal may, therefore, be indicative of peatlands within the landscape (Beamish, 2014). Previous studies have chosen the boundary between peat and non-peat soils within radiometric data arbitrarily (Beamish, 2015), based on average observed values of potassium (Berglund and Berglund, 2010) and in combination with other airborne datasets (Siemon et al., 2020). A method of edge detection, Horizontal Gradient Magnitude, used in potential field studies can act to remove this subjectivity (Beamish, 2016). However, the increased use of machine learning for mapping applications may be more suited to an objective identification of peatland extent (Hird et al., 2017; Minasny et al., 2019; Zhang et al., 2017). No radiometric studies on peatland area mapping to date have included machine learning methods, such as those described in this paper.

The aim of this paper is to develop a technique to investigate the potential of airborne radiometric data to complement and improve regional and local scale mapping efforts to delineate the extent of peatlands. To achieve this, modelling the attenuation of three normally recorded elements was performed to highlight potential statistical differences between these data acquired over peat and non-peat soils. Such differences may then be exploited by a supervised machine learning algorithm. An existing national peatland database (Republic of Ireland) was selected to provide training areas for this algorithm. Ireland has between 11,000 km2 and 16,500 km2 of peatlands (Connolly and Holden, 2009; Xu et al., 2018), the range highlighting the uncertainty in the various mapping techniques used. Three national databases are available which outline peatland area. These are the CORINE 2018 (CLC18) landcover (CORINE, 2018), the 1:250k Irish Soil Information System (ISIS) (Creamer, 2014b) and the 1:50k Quaternary Geology Map (QGM) (GSI, 2022b)

databases. Their validity is confirmed below using Loss on Ignition (LOI) (Heiri et al., 2001) analysis from a national soil sampling campaign.

An updated peatland area map was then produced using datasets acquired during a national airborne survey called Tellus. These methods may be used to update national and international extent of peatlands, facilitating C emissions estimates, and informing restoration projects.

## 3.3 Materials and Methods

### 3.3.1 Airborne Radiometric Data

The Tellus survey is an airborne geophysical survey commissioned by the Geological Survey of Ireland (GSI, 2022d). It began in 2012 and to date approximately 80% of the land area of the country has been covered. The survey acquires coincident Electromagnetic, Radiometric and Magnetic data. The radiometric data are of interest in this study.

The survey is acquired in acquisition "Blocks" which cover large geographic regions. Each block has a similar acquisition geometry; however, some equipment differences exist between acquisition blocks. Survey lines are flown at 345°, with a line spacing of 200 m. Radiometric data are acquired with a 1Hz frequency, which approximates to a 60m inline spacing. The nominal survey altitude is 60 m, however occasionally this is exceeded due to terrain or flight restrictions/requirements. Data from all blocks undergo similar processing performed by the contractor (SGL, 2017) in line with international guidelines (IAEA, 2003).

This study uses data from Block A2 of the Tellus airborne survey (Figure 3.3.1). These data were acquired between June and October 2016 and consist of 115 flight lines and 43,141 line kilometres. This block covers most of mid-west of Ireland, approx. 7,900 $km^2$, and consists of 652,950 individual data locations. These data were acquired in Irish Transverse Mercator (ITM, EPSG 2157) and all datasets used in this study have been re-projected to this reference system. Alongside geographic coordinate, elevation, and altitude specific data, 4 radiometric datasets were used in this study. These are the Potassium (K), Uranium (U), Thorium (Th) and Total Count (TC) data. These data were provided in concentration units, with an approximate depth of investigation of 40 – 60 cm (Beamish, 2013). In this study, a sensitivity factor (SGL, 2017) for each element was used to transform these data

back to counts per second (cps), which is required when considering radiometric attenuation equations (Equation 3.4.1 & Equation 3.4.2).

Finally, each data channel was interpolated using minimum curvature to a 50 m x 50 m grid. QGISv3.16 was used for visualisation and GIS analysis (Figure 3.3.1).

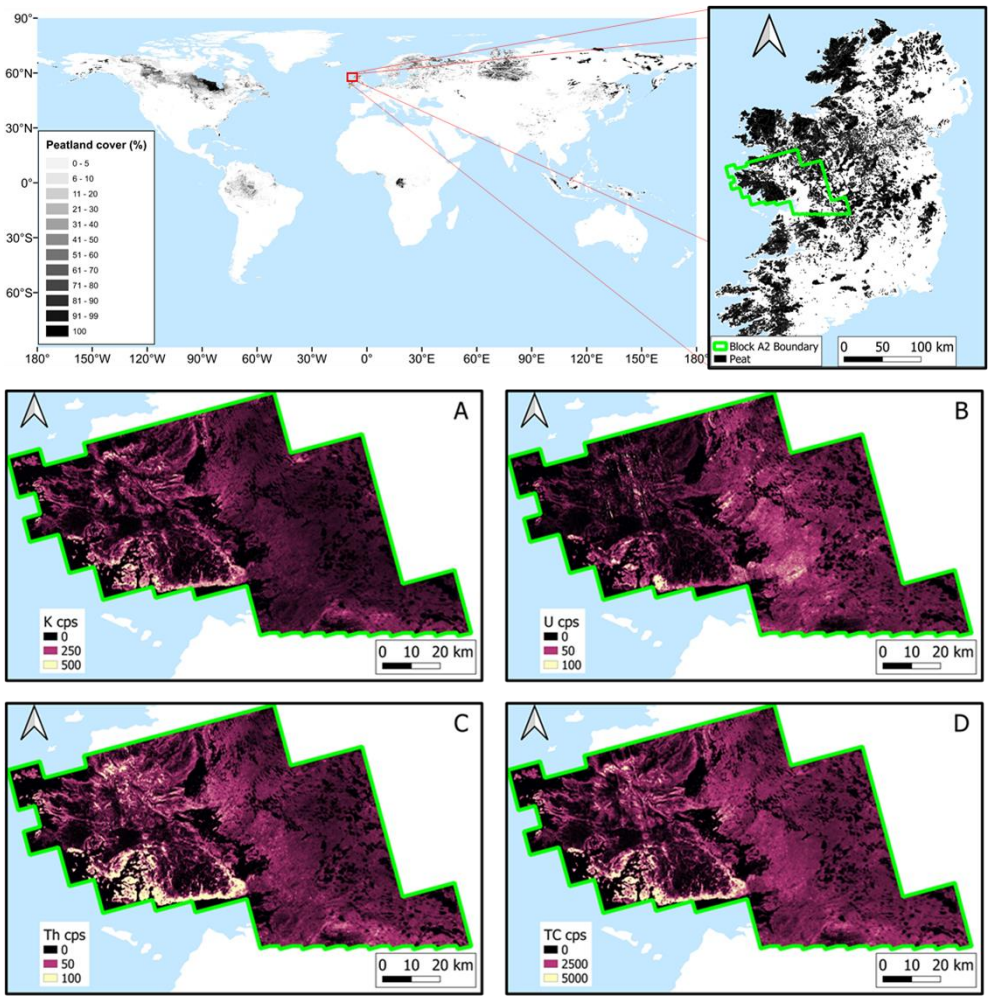


Figure 3.3.1: PEATMAP Global peatland area estimation (Xu et al., 2018), creative common (Top Left), PEATMAP of Ireland, with study location boundary of Tellus Block A2, green boundary (Top Right). Tellus Block A2 Radiometric data (Bottom). A) Potassium cps. B) Uranium cps. C) Thorium cps. D) Total Counts cps

### 3.3.2 Topsoil Survey

The Tellus topsoil survey provides a shallow (0.2 m) and deep (0.5 m) topsoil geochemical analysis, with one survey site per 4 km2. Since 2011 approximately 50% of the country has been covered.

Loss on ignition (LOI), used as a measure of the organic content of the sample (Heiri et al., 2001), was extracted from this dataset for both shallow and deep samples within the Tellus airborne A2 block, which contains 1,849 sample locations. A high LOI (> 50%) is indicative of peat soils, or soils with high organic content in Ireland (Creamer and O'Sullivan, 2018). An average LOI was calculated from the shallow and deep samples in order to provide a single representative LOI for a sample location. There are insufficient LOI data to incorporate in the machine learning approach described in Section 3.3.4.

### 3.3.3 National Peat databases

The CLC18 landcover classification is the most recent release from the European Environmental Agency (EEA). This is a European landcover classification program, which has produced standardised landcover classifications, derived from satellite remote sensing data products by national teams, at several reference years from 1990 until 2018. The dataset consists of 44 landcover classifications (Kosztra et al., 2017) with peat extent mapped using the classification of “Peat bogs” and “Moors and Heathlands”. This database has a minimum mapping unit (MMU) of 25 ha (0.25 $km^2$), a minimum linear feature resolution of 100 m and a reported thematic accuracy of 85% (CORINE, 2018).

The QGM is a national map produced by the Geological Survey of Ireland at a 1:50k (1 cm = 500 m) scale. It aims to map the thickest unit in the top 1 m of the subsurface (GSI, 2022a). This is achieved primarily via traditional mapping techniques, boreholes, and ground geophysical surveys. No overall accuracy is reported for this database, however traditional mapping techniques often have most uncertainty at boundaries of mapped units (Zhang et al., 2017). Ongoing surveys aim to increase overall confidence (GSI, 2022c). This database consists of 83 classifications of sediment types. Peat is classified as “Blanket Peat”, “Cut over raised Peat”, “Fen Peat” and “Raised Peat (intact)”

The ISIS database is a probabilistic soil association map produced by the Environmental Protection Agency (EPA) and national agriculture and food authority (Teagasc) at 1:250k (1 cm = 2,500 m) scale. It was produced in a machine learning framework using legacy soil maps, environmental co-variates and validation datasets (Creamer, 2015b; Creamer and O'Sullivan, 2018). The classification system divides the soils of Ireland into 11 Great Groups following World Reference Base

(WRB) principles. Peat is classified under "1xx" relating to the Great Group classification of 1 for peats in Ireland. The accuracy of this database to predict soil types has reported values about 30 – 40%.

These databases can be used to remove areas from the study site that are not relevant and to identify training areas for use in the machine learning algorithm (Table 3.3.1). All databases were clipped to the Tellus Block A2 boundary. Polygons related to water bodies, urban centres and other non-relevant landcover or subsurface types were merged from all three national databases to produce a maximum extent mask layer of exclusion zones. Radiometric data acquired in these exclusion zones are removed.

Table 3.3.1: Landcover classes removed from Tellus A2 Block Area

| **Landcover classes removed:** | | |
|---|---|---|
| Airports | Urban (all) | Intertidal flats |
| Beaches, Dunes, Sands | Dump/Mineral Extraction sites | Water (Lakes/Rivers) |
| Coastal Lagoons | Industrial areas | Sea |

Each national database was then simplified into "Peat", based on the relevant database definition, or "non-Peat" areas, by merging the remaining polygons, which provide the training areas. Comparison with LOI definition of peat showed that all three national databases were suitable for use in defining training areas (QGM: 86.4%, CLC18: 86.2%, ISIS: 83.1% agreement), however the QGM was selected as it best matches the expected penetration depth of radiometric data (Beamish, 2013). A more detailed justification for selection of the QGM can be found in Appendix 1. Figure 3.3.2 highlights the full workflow.

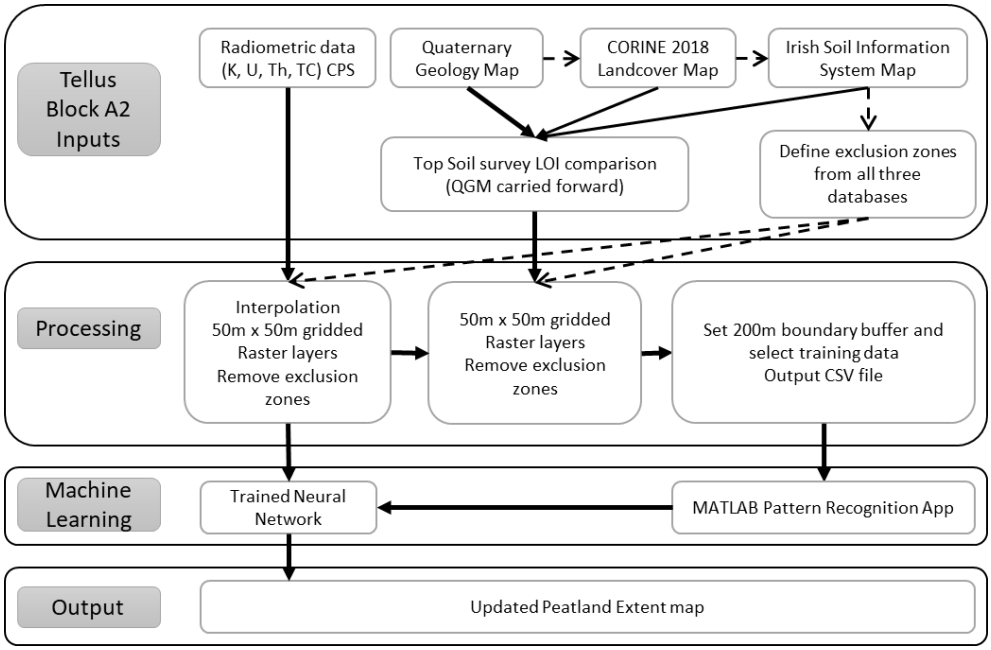


Figure 3.3.2: Workflow Diagram

### 3.3.4 Machine Learning Supervised Classification

Classification is the process of grouping together data which share common properties into a set of classes (Delgado et al., 2017). Machine Learning (ML) algorithms are suited to this task, especially where the underlying relationship in the data set is poorly understood (Valentine and Kalnins, 2016) and rely on pattern recognition and statistical relationships as opposed to a pre-determined mathematical model (Dramsch, 2020). In supervised classification, a subset of data is associated with an a priori set of "classes". A statistical relationship is found between the input data and the associated class (Dramsch, 2020; Shen, 2018). This relationship can be exploited to predict the classification of new data. Therefore, the input data need to be a good representation of the relationships of interest.

In this study, supervised machine learning classification was used. Machine learning can exploit the statistical differences between the radiometric data layers, where traditional geophysical (i.e., inversion) or numerical (i.e., regression) techniques may not due to the complexity of radiometric data (Reinhardt and Herrmann, 2019). The QGM database provided the a priori (target) for supervised classification.

In order to ensure the input data selected to “train” the artificial neural network (ANN) were acquired over the subsurface type of interest, a 200m buffer zone was defined along either side of all peat boundaries in the QGM and no training data were selected from within the buffer zone. “Peat” classed radiometric data were selected from the remaining peat areas of the QGM outside this buffer zone. This was done to reduce the uncertainty of the QGM areas chosen as training sites, as the most uncertainty in traditional mapping techniques exists at boundaries of mapped unit (Zhang et al., 2017). This also removes any potential overlap between these classes due to the radiometric acquisition footprint, approx. 180 m radius (Minty, 1997). No other filtering of the data was performed.

A total of 168,414 radiometric data points were extracted from within the remaining “peat” area. The same number of datapoints were extracted randomly from within the “non-peat” areas. These datapoints contain 4 data predictors, K, U, Th, and TCs (cps), and a classification of non-peat (value = 2) or peat (value = 1). Normalisation was applied to bring each radiometric dataset to a common scale (between 0 and 1). These labelled data form the training data within the machine learning framework.

The main assumption in the machine learning training, and subsequent application, is each datapoint is representative of radioactivity from a 50 m x 50 m square produced during interpolation of the airborne radiometric data. The 90% contribution footprint of radiometric data acquired at 60 m altitude is an approx. 180 m radius circle (Minty, 1997). As the aircraft is moving and recording every 1 sec, in reality this area becomes an ellipse. However, the greatest contribution to the signal is from directly below the aircraft and so the interpolation is considered standard in radiometric studies.

This work utilises the MATLAB™ Pattern Recognition Application, which uses a scaled conjugate gradient backpropagation network (Møller, 1993) with the default of 10 hidden layers for machine learning classification sufficient to capture the complexity of the relationships between the input data and the classification. The input data were the normalised four radiometric datasets, which removed any scale differences between the data. The target classes were defined as “non-Peat” or "Peat”. The input dataset was randomly divided into training (70%), validation (15%) and testing (15%), a standard procedure when training an artificial neural

network (ANN). A confusion matrix (Ting, 2010) for all the input data is then used to access the success of machine learning training.

## 3.4 Theory/Calculations

Radiometric data are often presented as a map, which is representative of each element's concentration within an approximate depth of the subsurface, similar to Figure 3.3.1. This depth has previously been explored via modelling of gamma ray attenuation in subsurface materials (Beamish, 2013) and quantification of a depth of penetration for various overburden types, with "wet peat" being 60 cm and mineral soils between 40-60 cm. This represents the depth in each material within which 90% of the radiometric signal is originating.

The general assumption is that bedrock is the radioactive parent material present in mineral soils (Beamish, 2015; Priori et al., 2014; Rawlins et al., 2007), which contributes to the radiometric signal acquired at the aircraft. However, peats are considered to be a non-radioactive overburden, with the exception of reported uranium enrichment (Vodyanitskii et al., 2019) in certain cases.

### 3.4.1 Radiometric Attenuation

The measured gamma ray flux (Im) can be considered as a gamma source with an intensity (Io), measured in photon rate per second of emission, which has been reduced after passing through some material. In crustal materials (rocks), gamma ray sources are radionuclides present since the formation of the planet and are dependent on the material's geochemistry (Minty, 1997). Attenuation of this gamma emission is exponential and related to a linear attenuation coefficient (μ) of the material through which the gamma ray passes, and the thickness (x) of the material (Davisson and Evans, 1952).

The linear attenuation coefficient can be described as the mass attenuation coefficient (μm) multiplied by the density (ρ) of the material. The mass attenuation coefficient is related to the number of electrons present in a material. The full equation for gamma ray flux measurement is given by the following:

$$I_m = I_o \, exp(-(\mu_m \times \rho)x)$$

Equation 3.4.1: Equation of gamma ray flux

A more appropriate equation was proposed (Endrestøl, 1980) and further explored by Beamish (2013) which resulted in a three-phase system which accounts for the three phases of geological material, solid (s), water (w) and air (a). An additional step is added here to account for the passage of the gamma rays through the air to the detector at aircraft altitude. This results in a 4-phase system of one-dimensional (1D) attenuation from an underlying source to a detector at aircraft altitudes (Equation 3.4.2).

$$I_m = I_O \exp\left(-\begin{pmatrix}[(\mu_s \times \rho_s) \times (1 - \emptyset) \times x] + [(\mu_w \times \rho_w) \times (S\emptyset) \times x] \\ +\left[(\mu_a \times \rho_a) \times \left(\emptyset(1 - S)\right) \times x\right] + [\mu_{al} \times h\,]\end{pmatrix}\right.$$

Equation 3.4.2: 4 phase gamma ray attenuation equation

Where:

Ø = Porosity (Volume of void spaces) expressed as a decimal percentage
S = Saturation (Volume of liquid within void spaces) expressed as a decimal percentage
μs/w/a = Mass attenuation coefficient of solid/water/air (Minty, 1997) for an energy range.
ρs/w/a = Bulk density of solid (variable), water (1) or air (0.001293) expressed in g/cm3
x = thickness of layer expressed in cm.
μal = Linear attenuation coefficient of air per metre (as provided by the survey contractor, (SGL, 2017))
h = production altitude (60 m)

For each aircraft observation point, there are 3 independent data (K, U and Th) and 5 unknown parameters (Equation 3.4.2), so it is an underdetermined system of equations. This means that the same data can be modelled with many combinations of the parameters of the non-radioactive medium. It is not possible to estimate, e.g., the thickness of peat, without additional ground-based constraints on the other parameters, especially for areas where peat thickness > 60 cm will substantially reduce the signal to noise ratio.

This equation (Equation 3.4.2) can be used to produce a simple 1D model of gamma ray attenuation of some initial source intensity (cps) passing through a non-radioactive medium, with the attenuation being controlled by the physical properties of that medium. These are media density (g/cm$^3$), porosity (%), saturation (%), and layer thickness (cm). All three recorded elements (K, U and Th) can be modelled using specific attenuation coefficients for each (Minty, 1997). TC

data cannot be modelled as they represent an integration of the full energy spectrum detected and no one attenuation coefficient can be used.

### 3.4.2 Modelling Peat vs Non-Peat Attenuation effect

Modelling was performed using Equation 3.4.2 to produce a theoretical radiometric dataset of K, U and Th responses from one million models of random combinations of typical subsurface physical properties for peat and non-peat in Ireland (Table 3.4.1) (Galvin, 1976; Kiely and Carton, 2010).

Table 3.4.1: Physical Properties used in modelling radiometric attenuation. Initial intensity refers to the counts per second intensity directly underlying the attenuating material. Bulk Density refers to the material density of the overburden. Porosity refers to the volume of void spaces. Saturation refers to the filled void spaces. Thickness refers to the constant vertical thickness of the overburden

| **Physical Property** | **Peat** | **Non-Peat** |
|---|---|---|
| Initial Intensity (cps) | K, U, Th = 500 ± 50 cps | |
| Bulk Density (g/cm$^3$) | 0.01 – 0.25 | 1.1 - 1.65 |
| Porosity (%) | 90 – 99 | 30 – 70 |
| Saturation (%) | 80 – 100 | 10 – 70 |
| Thickness (cm) | 50 | 50 |

The initial intensities were allowed to vary randomly within defined limits (Table 3.4.1) to replicate the probabilistic nature of radioactive decay in a given time window (Minty, 1997). Thickness has the most influence on radiometric attenuation (Beamish, 2013), but is not an intrinsic physical property of the overburden. In order to observe radiometric attenuation due only to property differences, the thickness remained constant (50 cm) for all models. Each model is a 1D representation of vertical gamma ray attenuation of 3 elements (K, U, Th) from source to aircraft, passing through a three-phase overburden of constant thickness, variable physical property values, and a 60 m air column.

The final element in modelling radiometric data is the addition of random noise. This represents noise in real radiometric data that is not corrected during processing, such as small aircraft motion. Noise estimates were taken from Tellus Block A2 data. Noise calculated using Beamish (2013) resulted in levels of $K_n$ = ±6.76 cps, $U_n$ = ±2.42 cps, $Th_n$ = ±2.32 cps. Noise was independently and randomly assigned within these limits to each model dataset.

This yields two million datapoints with a modelled K, U, Th response and classification of peat or non-peat. All responses were normalised to fall between a minimum of 0 and a maximum of 1, a standard part of any machine learning workflow (Valentine and Kalnins, 2016). A histogram analysis is used to visualise the responses for each element/modelled overburden combination and a correlation analysis is used to examine the relationships between the responses within each modelling scenario.

## 3.5 Results and Discussion

### 3.5.1 Modelling radiometric attenuation in peats and non-peats

The purpose of the modelling exercise was to conceptualise the statistical differences, existing between radiometric responses acquired over non-radioactive peat compared to those acquired over non-peat overburden, which would be exploited by an ANN. A histogram was used to display the two million modelled responses (Figure 3.5.1), where rows show modelling scenarios and columns show the three different element responses. The top row shows the response from all 2 million models. The middle row shows the 1 million responses when modelled using peat physical properties and the bottom row shows the responses when modelled using non-peat physical properties.

The top row highlights an important observation. The U and Th responses exhibit a slight bi-modal distribution, when compared to K responses. The middle and bottom rows reveal that the peaks in the top row line up with the peat modelled responses, indicating that the attenuation responses in a peat, compared to a non-peat model, are becoming notably different at higher gamma ray energies. Th responses from peat models are less attenuated compared to K responses, whereas non-peat models display similar attenuation across all three elements (Figure 3.5.1).

The reason for this can be determined from Equation 3.4.2 and the range of physical parameters used to define a peat and a non-peat (Table 3.4.1). The very low bulk density (< 0.25 g/cm3) and very high saturation and porosity values attributed to peat (Galvin, 1976) mean that the attenuation of gamma rays in peat models is controlled mostly by the given porosity and saturation. This coupled with

a stronger attenuation coefficient for K compared to U and Th means that as gamma energy increases, attenuation decreases for peat models.

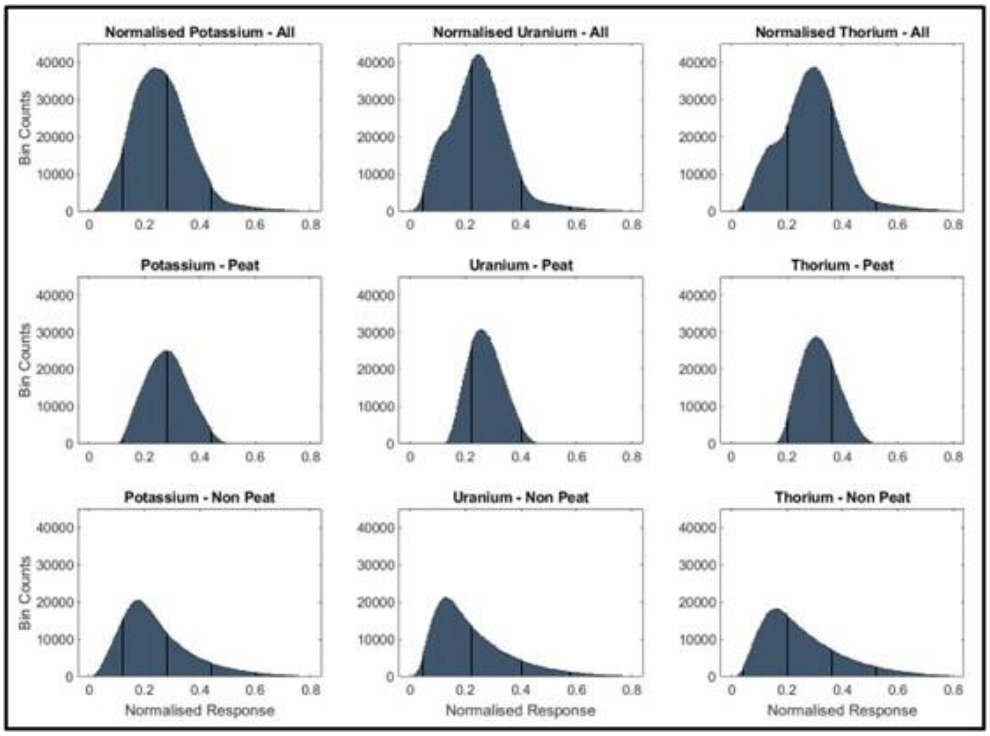


Figure 3.5.1: Histogram analysis of modelled radiometric data, showing distribution and response difference for each radiometric element and modelling scenario

Non-peat models, by comparison, have a larger bulk density (1.1 – 1.65 g/cm3) and a larger potential range for porosity and saturation (Table 3.4.1) (Kiely and Carton, 2010). Therefore, the attenuation of a non-peat model is controlled by the combination of physical parameters, including a more significant impact from the bulk density of the solid component of the model. This results in more consistent attenuation regardless of gamma ray energy.

An interesting observation of this analysis is that, given a non-radioactive overburden and a constant depth, non-peat models have an increased and more consistent attenuation across the three elements when compared to peat models. This appears to be counter-intuitive to published literature which highlight peatlands as strong attenuation areas within radiometric surveys (Beamish, 2014; Siemon et al., 2020). However, the models presented here do not consider the effect of parent material in non-peat soils, which will effectively mask any underlying radiometric source signal (Rawlins et al., 2007; Reinhardt and Herrmann,

2019). The lack of parent materials in peats result in areas of low radiometric signal in radiometric surveys in addition to the attenuation strength of a peat soil. This observation highlights another “radiometric difference” between peat and non-peat soils, in that peat soils act as an attenuating medium, whereas non-peat soils act as both a source and attenuator of radiometric signal.

The distributions of each of the histograms are determined by the range of physical parameters used in each model (Table 3.4.1). As this range is unknown for any real-world survey, recorded distributions may not match this modelled scenario. However, the differences between the data may be of use. In order to show this, a correlation analysis was performed separately for peat and non-peat modelled datasets to show how one modelled dataset changes with respect to another within each modelling scenario.

Radiometric responses modelled with peat physical properties are less correlated compared to responses modelled using non-peat properties. The combination of two things results in this lower correlation: (1) the sensitivity of the radiometric responses in peat to the relevant attenuation coefficients and (2) the introduction of randomness in the form of initial intensity and noise, which naturally decreases correlation between datasets. Here, however, the randomness is applied equally to both peat and non-peat modelled radiometric responses. The greater sensitivity to attenuation coefficients in peat modelled responses results in the random noise having an increased effect compared to non-peat modelled responses.

It is noted that the level and randomness of the initial source intensity are estimates, and there is no empirical evidence for their choices, however normalisation removes the importance of their relative strengths. The noise levels used are orders of magnitude lower than the chosen initial signal. Decreasing the initial signal level decreases the correlation and the removal of randomness results in near perfect correlation in both modelling scenarios.

### 3.5.2 Machine Learning Training

A confusion matrix is used to describe training success (Figure 3.5.2). This matrix shows how successful the ANN is at classifying the training data (described in Section 3.3.4) using the labels provided (Ting, 2010). The “target” is the

classification pre-assigned to each data point, the "predicted" refers to the classification assigned by the ANN post training.

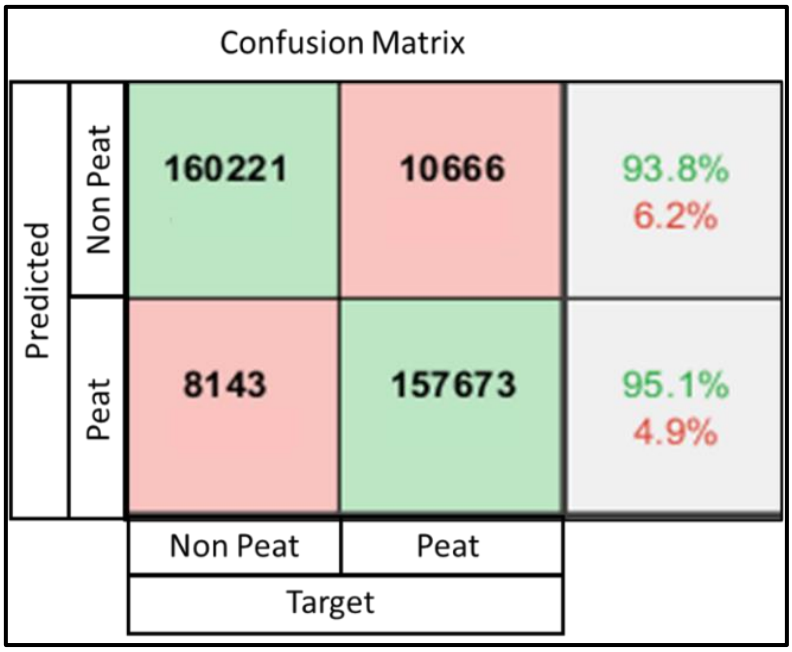


Figure 3.5.2: Confusion matrix showing the training success. Coloured squares show number of data points either re-classified or un-changed. Grey squares represent percentage of matching classification i.e., 95.1% of the data predicted to be "peat" was originally classified "peat" in the QGM and remain un-changed. 4.9% have been re-classified as "peat" by the neural network from "non-peat" in the QGM.

The overall training success indicated that 94.4% of all training data were classified the same as the QGM (with the buffer zone) by the neural network with 5.6% being re-classified by the neural network. It is likely that some mis-classified QGM areas were still present, despite the caution of the 200m buffer zone, as shown by this re-classification. An analysis with a buffer zone of 300 m either side of the QGM boundaries resulted in a marginal improvement in the classification accuracy to ~ 96%. ANN has therefore identified a statistical model to differentiate between radiometric data acquired over peat and non-peat overburden and can now be applied to the full Tellus A2 block dataset.

### 3.5.3 Updating the Peatland Map

All datapoints from the Tellus Airborne A2 block were normalised with the same parameters as the training data and passed to the trained ANN, which outputs a classification of peat or non-peat (Figure 3.5.3-A).

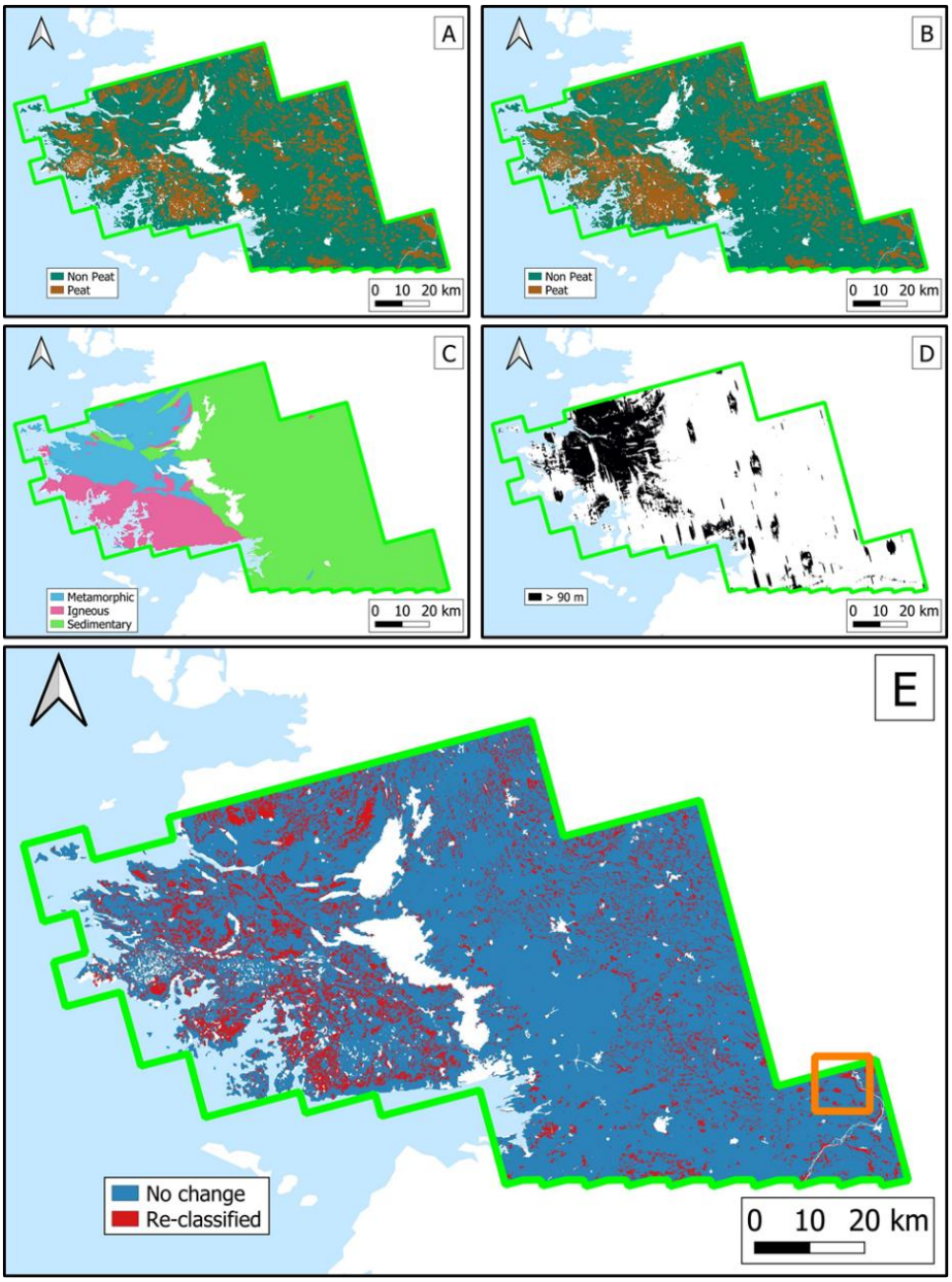


Figure 3.5.3: Radiometric based peat map. A) ANN Classified peatland area. B) QGM database peatland area. C) Simplified Geology map. D) Tellus Survey >90m clearance from ground E) Red = areas that the ANN is different to the QGM. Blue = the classification is the same as the QGM. Orange boundary is study site detailed in Section 4.3.1. A, B, D and E Maps have exclusion zones removed

This updated peatland map can be compared to the QGM database (Figure 3.5.3-B). Both peatland extent maps show good agreement, as expected as the ANN was trained using the QGM. By calculating a difference (Figure 3.5.3-E), areas that were reclassified by the ANN can be seen. This difference map shows that the results are not significantly influenced by the underlying geology (Figure 3.5.3-C) or

topography related high fly zones (Figure 3.5.3-D), both important considerations in radiometric studies (Beamish, 2015; Minty, 1997).

Underlying geology may influence the initial source intensity as well as contribute to the parent material of the soil, both having an effect on the recorded radiometric signal (Beamish, 2015; Rawlins et al., 2007). Complex topography can decrease the quality of radiometric data due to rapid changes in aircraft altitude to maintain terrain clearance (Figure 3.5.3-D). There may also be non-vertical gamma rays originating from valley sides (Minty, 1997; Reinhardt and Herrmann, 2019).

The ANN classification result contains interesting features when compared to the other databases. The resolution of the three national databases is controlled by mapping units and accuracy measurements. The ANN result is based on individual 50 m x 50 m squares, which represent the resolution of this database. However, any isolated classified square is therefore more likely to be a product of noise than a correct classification and may require the use of a spatial filter. However coherent groups of similar classification are likely to be true classifications. The argument for increased resolution is furthered by the fact that each 50 m x 50 m area has been derived from a direct measurement of the subsurface. This is compared to a surface (1 cm – 2 cm depth) measurement present in the CLC18 database, and only sparse subsurface measurements present in QGM and ISIS databases. These traditionally derived maps resolutions may also be affected by local issues, such as access to land to validate soil type, which will not affect the results of an airborne survey presented here.

While the effect of geology is partially accounted for via regional spatial sampling within machine learning training, the decrease in spatial resolution of radiometric data due to complex topography and high fly zones is unavoidable, as the area from which gamma rays originate expands greatly with increased clearance above the surface (Reinhardt and Herrmann, 2019). Although a linear correction is applied to correct the data to production altitude (SGL, 2017), the effect of complex topography cannot be accounted for. Therefore, while there is still a valid statistical relationship present in the recorded radiometric data in mountainous regions, the area from which the gamma rays originate is not well constrained. Therefore, any result from mountainous regions, such as the western portion of the study area (Figure 3.5.3-E) would require extensive ground truthing

and combination with other peatland area datasets (Connolly et al., 2007) to assess accuracy.

### 3.5.4 Predicting Peatland Extent in Flat Terrain

In contrast to mountainous regions, relatively flat terrain exhibits no such complexity. The remaining discussion will highlight an example of the proposed method's ability to update the extents and spatial distribution of peatlands centred on a former industrial extraction site.

The chosen site is located at the eastern side of the Tellus A2 block (Figure 3.5.3-E). It is known locally as Garryduff bog and until recently was harvested for material to generate electricity at a nearby power plant. This site was chosen for this study as it provides a representation of a typical industrial peatland site in the northern hemisphere and surrounded by grassland and some forestry.

All three simplified national peatland databases are shown (Figure 3.5.4-B/C/D) highlighting the differences in peatland extent and spatial distribution. Each database can be visually compared to the aerial image, which outlines the Garryduff bog (Figure 3.5.4-A). The QGM and ISIS databases show peat extent outside the Garryduff boundary and show a connection between other peatland areas. The CLC18 shows increase in peatland extent.

The direct measurement has another implication for the ANN classification, namely that it may "see through" landcover. In particular, the radiometric data may detect peatlands under anthropogenically modified land use, such as grass or forest. This is evident in the study area (Figure 3.5.4-E) as the ANN classification has detected two distinct areas of peatland in the south-western quadrant of the study area (black dashed box). These are partially detected on the QGM and ISIS databases, and not detected on the CLC18 database. The CLC18 database identified these areas as "Mixed Forest" and "Pasture" (west to east). The QGM identifies these areas as "cut over raised peat" and "Till derived from limestone" respectively.

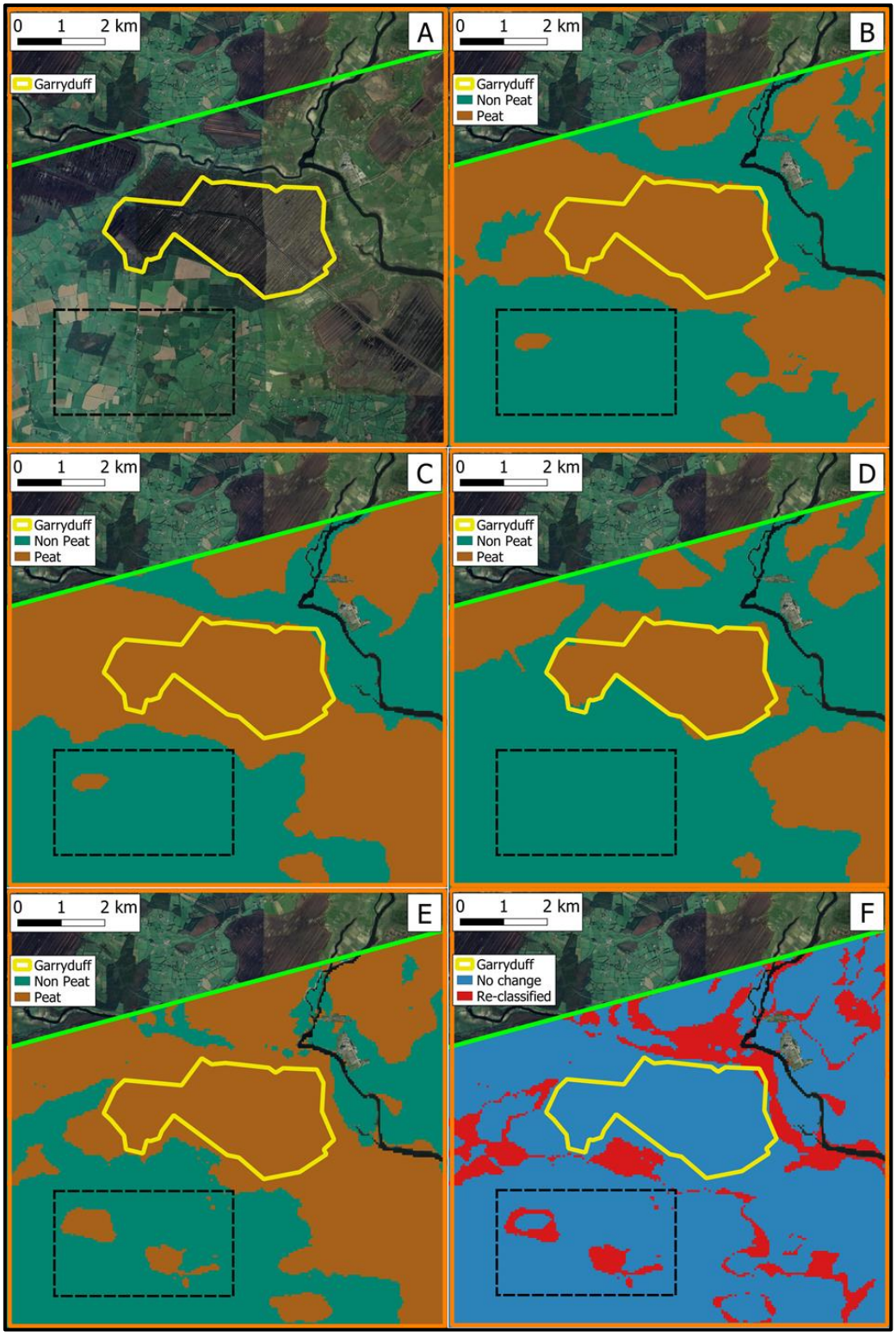


Figure 3.5.4: A) Google image of study area. Yellow boundary defined from commercial surveys on site. Black Dashed area highlighting two sites identified as peat by ANN classification, seen as dark green (forest) and light green (grass). B) Simplified QGM database of study area. C) Simplified ISIS database of study area. D) Simplified CLC18 database of study area. E) ANN classification of study area. F) Difference between B and E.

The ISIS identifies these as “peat” and “fine-coarse loamy drifts with limestone”. The ANN classification shows that these areas are larger than previously identified. It is noted that these areas were not included in training data (Section 3.5.2) for the ANN due to the buffer zone, but are still identified as peat by the ANN. See Appendix 2 for zoomed images for each of these sites.

This result is also relevant for currently known peatlands, such as the Garryduff site. The ANN classification has extended the boundaries beyond this industrial peatland (red boundary) into the surrounding areas. The difference (Figure 3.5.4-F) shows areas of the site that have been reclassified by the ANN classification, compared to the QGM, which highlights the increases in resolution provided by this method.

The radiometric signal has been shown to be affected by vegetation cover (Reinhardt and Herrmann, 2019), which can act as both an attenuator or a source of radiation. Within this study site, ANN classified areas are not strictly following visible vegetation boundaries (Figure 3.5.4-E), such as forests. This leads to the conclusion that the presence of vegetation (e.g., grass and forest) may not affect the classification of the underlying subsurface. As results from radiometric attenuation modelling have shown, peat has a distinctive attenuation signature in radiometric acquired data when considering all recorded radiometric datasets, which may be independent of vegetation cover.

## 3.6 Conclusions

The methods presented can be used for international peatland mapping projects where similar datasets exist and may provide important updates to peatland inventories by identifying areas of previous unrecognised peat and updating boundary locations for established peatland sites. This has implications for global carbon stock assessment, rehabilitation projects and land management decisions. The method is reliant on good quality airborne radiometric data and some a priori knowledge of peatland extent in order to provide appropriate training areas. These areas should be spatially distributed across the full study site in order to capture any effects of changing geology to the radiometric data. As the method relies on statistical relationships between all recorded radiometric datasets, it is more suited to large areas and large datasets. Smaller areas may not exhibit such statistical relationships as clearly, as the range of attenuation properties may be

limited. Once a large area has been classified, however, the results can be used as a product for more focused localised studies or incorporated into other peatland mapping projects.

# Chapter 4: **Observations of intra-peatland variability using multiple spatially coincident remotely sensed data sources and machine learning**

Dave O'Leary [a], Colin Brown [a], Mark G. Healy [b], Shane Regan [c], Eve Daly [a*]

[a] Hy-Res Research Group, Earth and Ocean Sciences and Ryan Institute, College of Science and Engineering, University of Galway, Galway, Ireland, H91 TK33

[b] Civil Engineering and Ryan Institute, College of Science and Engineering, University of Galway, Galway, Ireland, H91 TK33

[c] Science and Biodiversity Unit, National Parks and Wildlife Service, Dublin, Ireland

*Corresponding author. eve.daly@universityofgalway.ie

## 4.1 Abstract:

Peatlands are important sites of ecosystem services, particularly as soil carbon stores, and are recognised in many international climate strategies. However, drained peatlands, which have been modified for industrial extraction or agriculture, are responsible for carbon emission. Peatland restoration aims to return these degraded sites to a natural state. Multiple means of remotely monitoring the success of peat restoration are available, ranging from space-based satellite measurements (optical and radar) to airborne geophysical measurements (electro-magnetic and radiometric). This paper integrates multi-band, spatially coincident, remotely sensed data into a single framework, resulting in a comprehensive interpretation of intra-peatland variation of key restoration indicators. It uses a semi-automatic, data driven approach with unsupervised neural network machine learning clustering. A Multi-Cluster Average Standard Deviation metric is introduced which can determine the appropriate number of clusters for any dataset. The method was applied to a site in Ireland, representative of degraded peatlands, where optical satellite and airborne radiometric geophysical measurements were combined. The method was successful at determining the appropriate number of clusters for single and combined datasets, and the resulting cluster signatures provided visually compelling representations of

the intra-peatland variation. This resulted in a comprehensive interpretation of intra-peatland variation of several key peatland restoration indicators, namely surface vegetation levels and soil moisture to ~ 60 cm of the peat surface. The study provides a framework for high spatial and temporal resolution monitoring of peatland restoration using future drone-based platforms.

Keywords: self-organising maps; unsupervised classification; peatland restoration.

## 4.2 Introduction

Peatlands are recognised as significant ecosystems for biodiversity, water system services and carbon (C) stores (UNEP, 2022). The United Nations Framework Convention on Climate Change (UNFCCC) highlighted peatlands as a priority via the introduction of the Wetlands Drainage and Rewetting (WDR) activity under Article 3.4 of the Kyoto Protocol (UNFCCC, 2011). Peatlands account for 5 – 30% of soil C stock (Minasny et al., 2019; UNEP, 2022) while covering only ~3% of the earths land surface (Xu et al., 2018). Drained/degraded peatlands, used for industrial extraction, forestry, or agriculture (pasture), are responsible for emissions which are affecting the global C balance (Evans et al., 2021; Qiu et al., 2020; UNEP, 2022).

The goal of peatland restoration is to return modified peatlands to their natural state, usually via changes to water table depth and vegetation (Monteverde et al., 2022), with water table management being a key environmental control on C exchange between the soil and atmosphere (Wilson et al., 2022). Peatlands which have been historically drained and undergone restoration appear to be non-uniform in recovery, creating “locally novel ecosystems” (Kreyling et al., 2021). Spatial changes in depth to the water table will have consequences for several ecosystem functions such as plant community composition, water runoff and nutrient cycling (Kasischke et al., 2009). This implies that restoration plans require local measurement of properties within a peatland before and after restoration in order to measure success (Heger et al., 2022; Renou-Wilson et al., 2019). The two main requirements to determine the effectiveness of a peatland restoration are ecological and hydrological monitoring (Mackin, 2017). Ecological monitoring represents mapping spatially and ecologically distinct features for the measurement of landscape structure and change. Hydrological monitoring is focused on environmental factors such as water table depth, flow, and

hydrochemistry. Both require monitoring prior to, during and after restoration into the future.

There are several established and emerging remote sensing techniques that can be used to measure peatland properties (Minasny et al., 2019) and they have advantages over more traditional methods (e.g., large areas, consistent spatial sampling). These can include satellite remote sensing (Bhatnagar et al., 2020), airborne geophysical surveys (Boaga et al., 2020), drone-based surveys (Dronova et al., 2021), and ground geophysics (Altdorff et al., 2016). Optical satellite and airborne radiometric data are analysed in this paper.

Satellite remote sensing methods (optical and radar) are prominent in the peatland mapping literature (Czapiewski and Szumińska, 2022). For example, the Sentinel program (Sentinel, 2022) is a series of earth observation missions performed by the European Space Agency and European Commission initiative, Copernicus. This program provides free access to optical (Sentinel-2) and radar (Sentinel-1) data at spatial resolution of ~ 10 – 30 m and a temporal resolution of between 3 and 10 days, depending on the satellite mission. These have become popular as they provide consistent spatial and temporal resolution and are sensitive to physical properties related to peatland identification and monitoring (Minasny et al., 2019) as they are sensitive to landcover (optical) and the near surface (radar) to a depth of ~ 10 cm.

Optical sensors on satellites record multiple bands of electromagnetic energy as reflectance values, ranging from the visible to shortwave infra-red. These values can be used to identify landcover type via “spectral signatures” and seasonal changes in landcover via changes to these signatures (Aune-Lundberg and Strand, 2021; CORINE, 2018). However, optical data are degraded or non-existent in the presence of cloud cover/shadow, which reduces the temporal resolution in temperate regions (Connolly, 2019). Often, indices (mathematical combinations of data bands that produce a single number which is sensitive to particular physical properties of interest) are used (Czapiewski and Szumińska, 2022; Wang and Qu, 2009). Of these, Normalised Difference Vegetation Index (NDVI), Enhanced Vegetation Index (EVI) and Normalised Difference Water Index (NDWI) are popular (Frampton et al., 2013). Within a peatland these and other indices can yield

information on landcover types such as bare peat and vegetation (Bhatnagar et al., 2020) at a resolution of ~ 10 – 30 m.

Airborne geophysical surveys are suited to peatland mapping (Airo et al., 2014; Berglund and Berglund, 2010; Boaga et al., 2020), as they cover large areas quickly and consistently (Ameglio, 2018; Binley et al., 2015) and are sensitive to subsurface physical properties such as density, porosity, and water content. National airborne geophysical surveys which include electromagnetic and gamma-ray spectrometry (radiometric) data can be used in regional and local scale peatland studies (Beamish and Young, 2009; Berglund and Berglund, 2010; Siemon et al., 2020).

As peat is a non-radioactive material, several studies have attempted to link radiometric data to peat thickness estimation (Gatis et al., 2019; Keaney et al., 2013; Siemon et al., 2020). However, attenuation models (Beamish, 2013) show that 90% of radiometric signal is attenuated in ~ 60 cm of typical peat, therefore limiting peat thickness estimation but may have potential for mapping peatland extent (O'Leary et al., 2022) and subsurface physical properties within this depth range. Soil moisture variation in this layer may be responsible for radiometric signal variation as water is a strong attenuator (Beamish, 2013; Endrestøl, 1980). It is likely that a complex combination of thickness and soil moisture are the biggest drivers of radiometric signal variation within a peatland (Reinhardt and Herrmann, 2019); however, vegetation may also have an attenuation effect (Minasny et al., 2019; Minty, 1997).

Peatlands are complex ecological and hydrological environments (Price et al., 2003). The influence of such complexity within a peatland requires simultaneous analysis of multiple data sources over a site in order to extract meaningful and comprehensive information about peatland processes (Kreyling et al., 2021; Räsänen et al., 2022). Machine learning, which is becoming prevalent in geoscience (Dramsch, 2020), has the ability to exploit non-linear statistical relationships between data bands to aid in data visualisation and model building. Un-supervised machine learning can achieve this, using the concept of exploratory data analysis (EDA; (Chatfield, 1986). EDA aims to (1) maximise insight into a data source, (2) visualise potential relationships between data vectors, (3) detect data vectors that vary significantly from others, (4) develop an explanatory model of the data source, and (5) extract relevant data bands from the overall data source.

Clustering (synonymous with the term classification) is the grouping together of multi-band data vectors (Kaufman, 2005), where the grouped input data vectors are statistically similar to each other. Many clustering techniques have been developed such as centroid, hierarchical, density and spectral clustering, each with their own advantages and disadvantages (Benabdellah et al., 2019; Delgado et al., 2017). See Table 4.2.1 for a list of descriptors used in this paper.

Table 4.2.1: Definitions of data descriptors in text

| Name: | Definition: |
|---|---|
| Data Source | A single source of spatially and temporally coincident data (e.g., Sentinel-2 data from a single date, radiometric data) |
| Data Band | A single stream of data from within a data source (e.g., Sentinel-2, Band 8 or radiometric, K cps) |
| Data Vector | All data that are located on a single spatial coordinate from described data bands and data sources (e.g., Sentinel-2, 13 bands become a data vector of 13 numbers at spatial location x, y) |
| Data Space | The virtual multi-dimensional space with as many axes as there are data bands being analysed |
| Cluster | A single identifier for a subset of input data vectors (e.g., Cluster 1 contains x number of input data vectors) |
| Cluster Signature | A single data vector that can describe all data vectors associated with a particular cluster |

The aim of this paper is to develop a data driven, objective, and semi-automatic technique to determine the range of appropriate number of clusters, using an unsupervised classification of spatially coincident data bands from multiple data sources. This has implications across many domains of research. The technique is demonstrated in this paper using 4 bands of airborne radiometric and 13 bands of optical satellite data over previously delineated peatlands (O'Leary et al., 2022). These datasets, which should ideally be spatially and temporally coincident, are related to spatial physical property variation (landcover and soil moisture), which are important indicators of restoration success (Mackin, 2017). The methods presented provide a framework to perform an initial investigation prior to a peatland restoration program and a means to monitor success of such a program into the future (Mackin, 2017). They have implications for integrated

interpretations of datasets from multiple sensors, including those in future high-resolution drone-based applications.

## 4.3 Materials and Methods

### 4.3.1 Clustering

#### 4.3.1.1 Self-Organising Maps

Traditional centroid-based clustering methods, such as K-Means (Gersho, 1982), rely on minimising the distance between data vectors and a finite number of cluster signatures in the dataspace. Self-Organising Maps (Kohonen, 2013) rely on competitive learning within a neural network to assign any data vector to a particular cluster (Valentine and Kalnins, 2016). This is a form of unsupervised classification (Kiang, 2001) and is considered suitable where the goal is to visualise multi-dimensional data (Benabdellah et al., 2019) by exploiting non-linear statistical relationships between datasets that traditional (linear) methods (correlation, regression, etc.) cannot capture.

In order to cluster the data within the Self-Organising Maps algorithm (Kohonen, 2013), a number of cluster signatures must be "initialised". These contain the same number of bands as the data vectors and are initially assigned random values in the data space. A data vector is compared to each cluster signature, via a data space distance metric, and the "winning" cluster is assigned. The winning cluster signature is updated to be more numerically similar to the data vector it represents. This process takes place for all input data vectors iteratively until each is assigned to a cluster. Each cluster signature is then said to represent a set of input data vectors that are numerically similar to it.

Determining the appropriate number of clusters for a dataset is difficult (Benabdellah et al., 2019; Delgado et al., 2017) often requiring subjective, a priori, or expert knowledge of the clustering algorithm. Clusters are chosen based on an expected or known number (Marsh and Brown, 2009). Frequently, clustering validation tools are used (Benabdellah et al., 2019) to determine if the number of clusters is statistically significant. These calculate several internal statistics such as the Calinsku-Harabasz index (Caliński and Harabasz, 1974), Connectivity index (Xing et al., 2005), or the Davies-Bouldin index (Davies and Bouldin, 1979).

#### 4.3.1.2 Appropriate number of clusters

The simple and novel approach presented here expects that the appropriate number of clusters for a set of input data vectors is any which returns similar cluster signatures after multiple clustering attempts. To achieve this, the clustering process is performed multiple times (e.g., 100 loops) for an increasing number of clusters, starting with 1 and increasing to X (e.g., 20) cluster signatures (Figure 4.3.1).

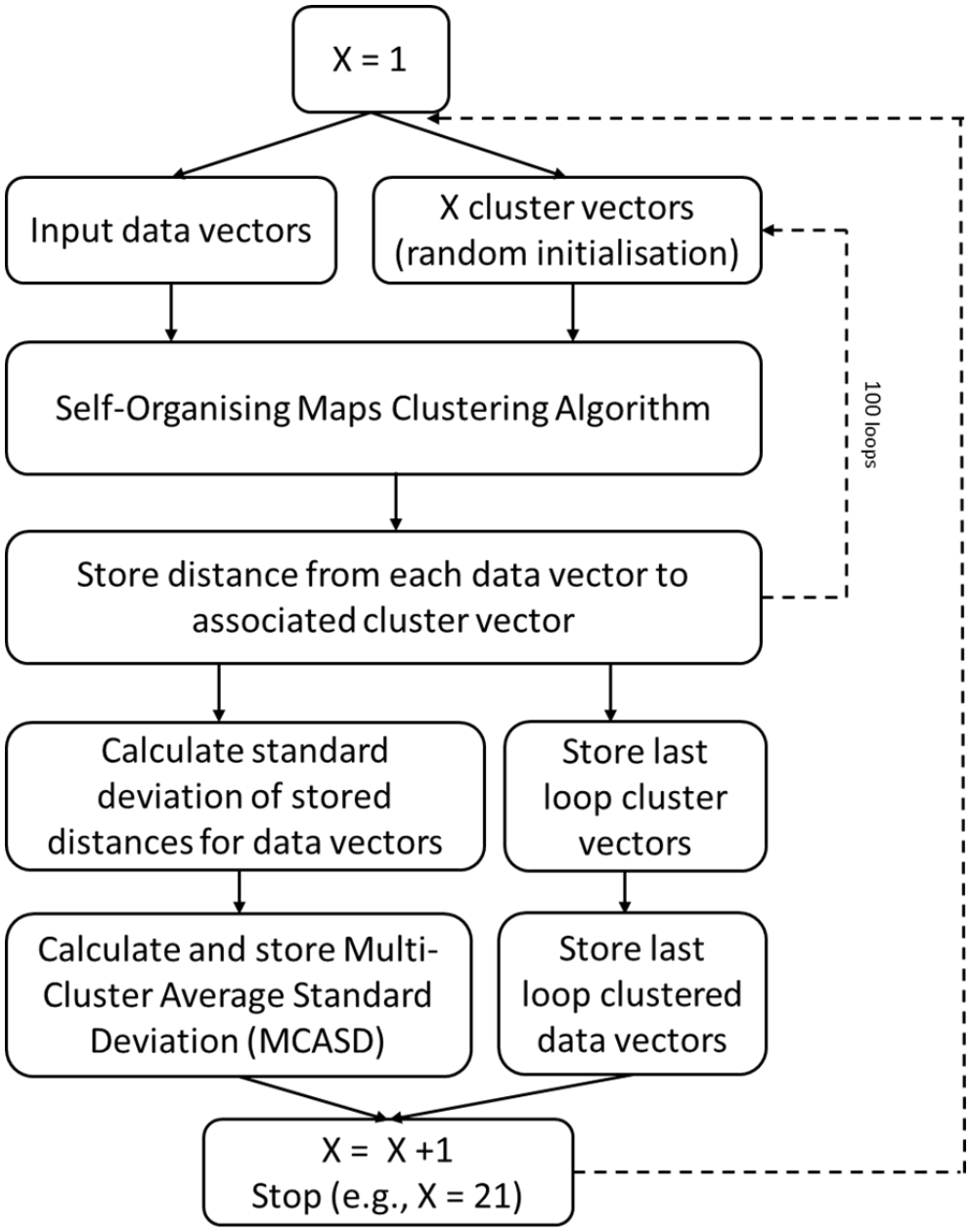


Figure 4.3.1: Multi-Cluster Standard Deviation (MCASD) flowchart

For each clustering loop the distance, in the data space, between the cluster signature and each associated data vector is calculated and saved. Then, the standard deviation of distance is calculated for each data vector once all loops are complete. Finally, an average of the standard deviations is calculated, resulting in the Multi-Cluster Average Standard Deviation (MCASD) metric. The aim of a MCASD analysis is to facilitate the choice of highest number of clusters, and therefore the highest spatial resolution, without compromising the stability of the solution, which is determined from multiple clustering loops. A low value of MCASD is a consequence of repeatable cluster signatures, despite random initialisation (Delgado et al., 2017), and is an indication that the associated number of clusters is appropriate to describe the range of input data vectors. A maximum of 100 loops and 20 clusters proved adequate to determine which number of clusters is appropriate for the data in this study.

#### 4.3.1.3 MCASD in practice

To demonstrate the MCASD method on spatial data, a data source with a known number of clusters was used as input data vectors. This synthetic data source has previously been used in an example of the application of Self-Organising Maps to geospatial data (Marsh and Brown, 2009). It can be considered analogous to a geo-spatial dataset as it shows a varying background with a non-distinct border and anomalous structures, where each pixel has an assigned geographic coordinate. A graph of the MCASD metric against number of cluster signatures (Figure 4.3.2-A) shows that 1 – 4 clusters are appropriate to visualise this data source.

The data source is a greyscale image of rice grains which are randomly orientated within a variable background intensity (Figure 4.3.2-B). The image consists of 65,536 data vectors organised as a single data band with a brightness value ranging between 1 – 256. This image can be broken into four groups, (1) bright background, (2) dark background, (3) rice on light background, and (4) rice on dark background. Figure 4.3.2-C shows the output of the first cluster loop when the number of clusters is 4 and shows the expected classifications with some minor misclassification present.

This clustering method does not take coordinates of the pixel into account, but instead groups data based on similarity between the various data layers (in this

case a brightness value). Each data vector is then given a number (1 – 4 for example) representing which cluster it belongs to. The data vectors are then reprojected back to their respective location in the image and coloured based on this number. The resulting spatial distribution is related to geographical locations where data are similar.

The spatial distribution would change with the number of clusters used, however the purpose of MCASD analysis is to provide confidence that the number of clusters chosen, and that the spatial distribution of the clusters is relevant and appropriate.

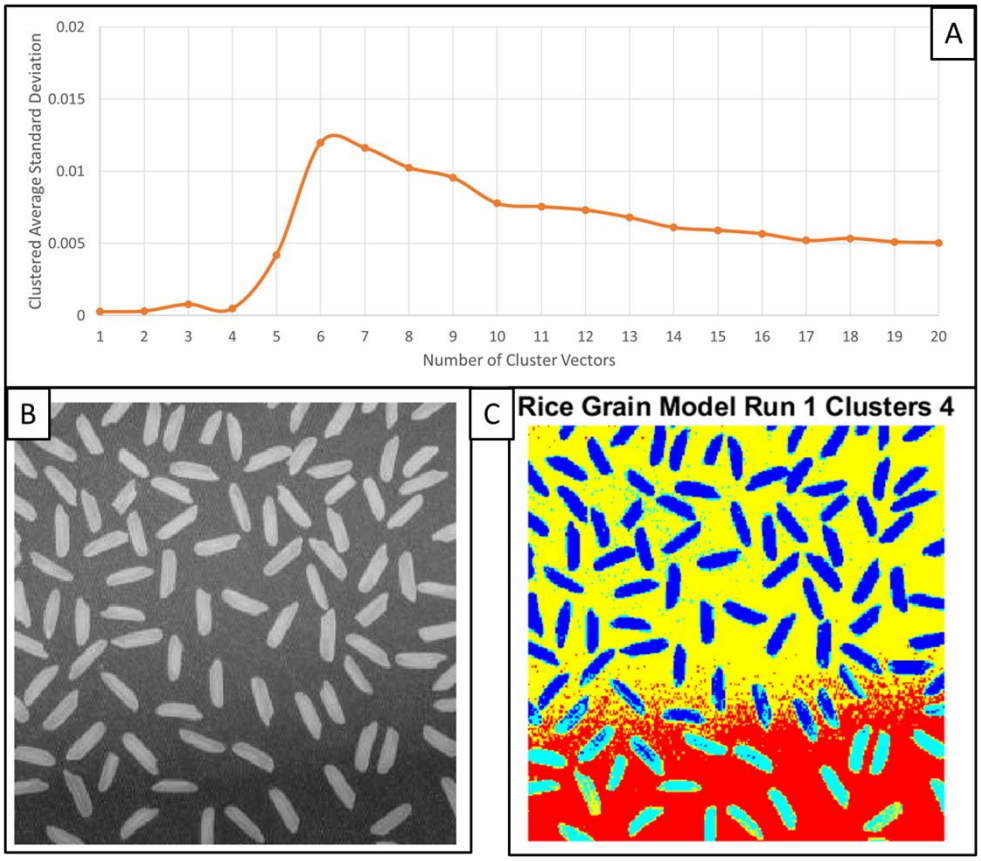


Figure 4.3.2: A) MCASD graph for maximum of 20 experimental cluster signatures. B) Original Grey scale image C) Clustered output coloured by cluster number

### 4.3.2 Site

A site in central Ireland was chosen because (1) it is typical of those industrial peatlands in the northern hemisphere being targeted for restoration (Bord na Móna, 2021), (2) there are ground-based datasets to constrain the interpretations

in this paper, and (3) spatially coincident Sentinel-2 (S2) and radiometric datasets are available.

Garryduff peatland (Lat: 53.25° N, Long: 8.08° W) is a former raised bog, and has been an extraction site from 1968 until 2019 (Bord na Móna, 2021) (Figure 4.3.3-A). The site is described as ~50% bare peat, with active drainage channels, standing water and emerging wetland vegetation making up the rest. Peat thickness on site is generally greater than ~ 50 cm (Bord na Móna, 2021). The site was actively pumped to maintain an artificially deep water table.

The peatland boundaries (Figure 4.3.3-B) were defined using radiometric data (O'Leary et al., 2022) and a supervised machine learning methodology. This resulted in a 50 x 50 m resolution raster, delineating pixels which have been defined as either Peat or non-Peat. O'Leary et al. (2022) demonstrate that the technique improves delineation of peat boundary and peat under modified landcover compared to recognised national databases (CORINE, 2018). Therefore, only the 16,633 pixels (~ 4,200 ha) that fall within areas defined as peat (Figure 4.3.3-B) are carried forward for further analysis.

The underlying bedrock is recorded to be limestone and shale (GSI, 2022a) and the quaternary sediment is a mixture of “cut over raised peats”, “alluvium” (close to the rivers) and “till derived from limestone” (GSI, 2022b). Landcover classification (Figure 4.3.3-C) from the European Space Agency (CORINE, 2018) shows a mixture of peat bog, grassland and forestry but provides no information on soil type. The CORINE 2018 landcover map has a resolution of 25 ha (CORINE, 2018), and has been converted to a raster with 50 x 50 m resolution for visualisations within this study.

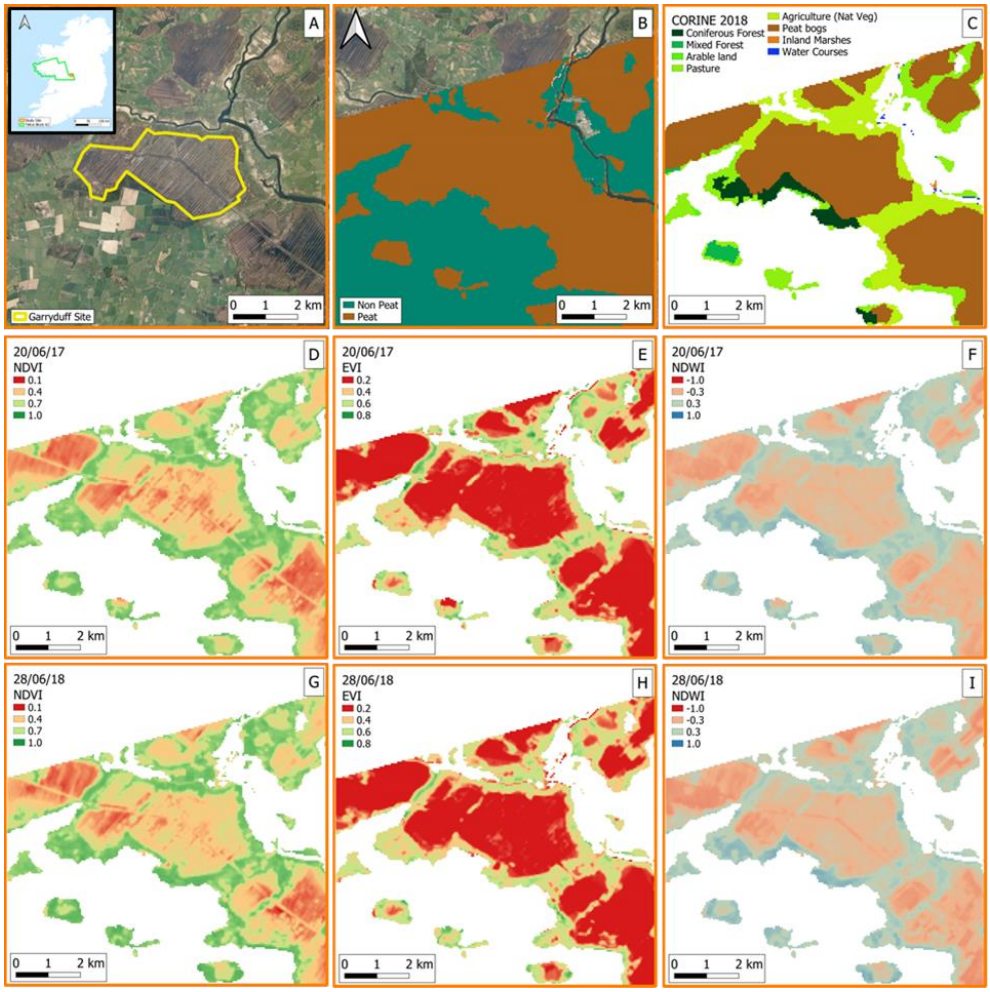


Figure 4.3.3: A) Aerial image with industrial peatland boundary with inset showing Tellus Radiometric Block A2 and study location within Ireland. B) Peat vs non-Peat extent for the study site edited from O'Leary et al. (2022) highlighting the spatial extent of data used in this study. C) CORINE 2018 landcover classification. D) - I) S2 images of NDVI, EVI, and NDWI for days in summer 2017 and 2018. North Arrow in B is relevant for all images.

### 4.3.3 Optical satellite data

S2 satellites were only launched in June 2015 and no cloud-free images from the study site were acquired during June 2016, when the radiometric data source was acquired, highlighting the issue of cloud cover inherent in the use of all optical satellite data in temperate latitudes such as Ireland (Connolly, 2019). As an alternative to a temporally coincident dataset, two Level 1-C S2 images, acquired on 20/06/2017 and 28/06/2018, were downloaded from the Copernicus Hub (https://scihub.copernicus.eu). These dates were chosen as they were (1) cloud-free over the study site and (2) were acquired at a similar time of the year as the radiometric data source in this study (see section 4.3.4). The temporally and

seasonally closest cloud-free S2 image was acquired in June 2017. In order to verify that this image is representative of the landcover variation at the time of radiometric data acquisition, a second image, acquired in June 2018 was also analysed to establish that landcover did not significantly change from one year to the next.

DOS1 atmospheric correction (Chavez, 1996) was applied to the all data bands in QGISv3.16 using the SCPv7.10.5 plugin (Congedo, 2021). The data were re-projected to a common reference system (EPSG: 2157 – Irish Transverse Mercator) and resampled to 50 x 50 m resolution, required to match "pixel to pixel" to other datasets used in this study. The standard indices (Bhatnagar et al., 2020), highlighted in Section 1, were calculated to visualise and compare the two S2 data sources (Figure 4.3.3-D to I).

### 4.3.4 Airborne geophysical data

The Tellus survey (GSI, 2022d) is a national airborne geophysical acquisition survey that acquires spatially consistent data covering Ireland. It collects three coincident geophysical datasets, electromagnetic, magnetic, and radiometric. The data are acquired in acquisition blocks with similar acquisition parameters. Survey lines are flown at 345° and a line spacing of 200 m and ground clearance of 60 m. However, this is occasionally exceeded due to terrain or flight restrictions.

Radiometric data were collected at 1Hz, which equates to ~ 60m sample spacing along flight lines. Data processing is performed by the contractor and follows international guidelines (IAEA, 2003). The radiometric data in this study were selected from the Tellus Block A2 (Figure 4.3.3-A). A total of 6,445 datapoints were acquired over the Garryduff site as a set of 25 flight lines (~ 387 line km's) on 3$^{rd}$ June 2016. The data bands were downloaded as elemental concentrations for Potassium (K), Uranium (U) and Thorium (Th) and converted to counts per second (cps) via sensitivity values, which are contractor provided values to convert recorded gamma ray counts per second to an elemental concentration (SGL, 2017). The Total Count (TC) data band is provided in cps. Each data band was then interpolated using minimum curvature to a 50 x 50 m grid and QGISv3.16 was used for visualisation and GIS analysis (Figure 4.3.4-A to D). All data were reprojected to the common reference system. The interpolation, along with the inherent low signal environment that peatlands present (Beamish, 2014), are the cause of

negative values in the radiometric signal. While not physically possible, they are not removed from this analysis as the neural network methods rely on statistical relationships between the data bands, not their absolute values.

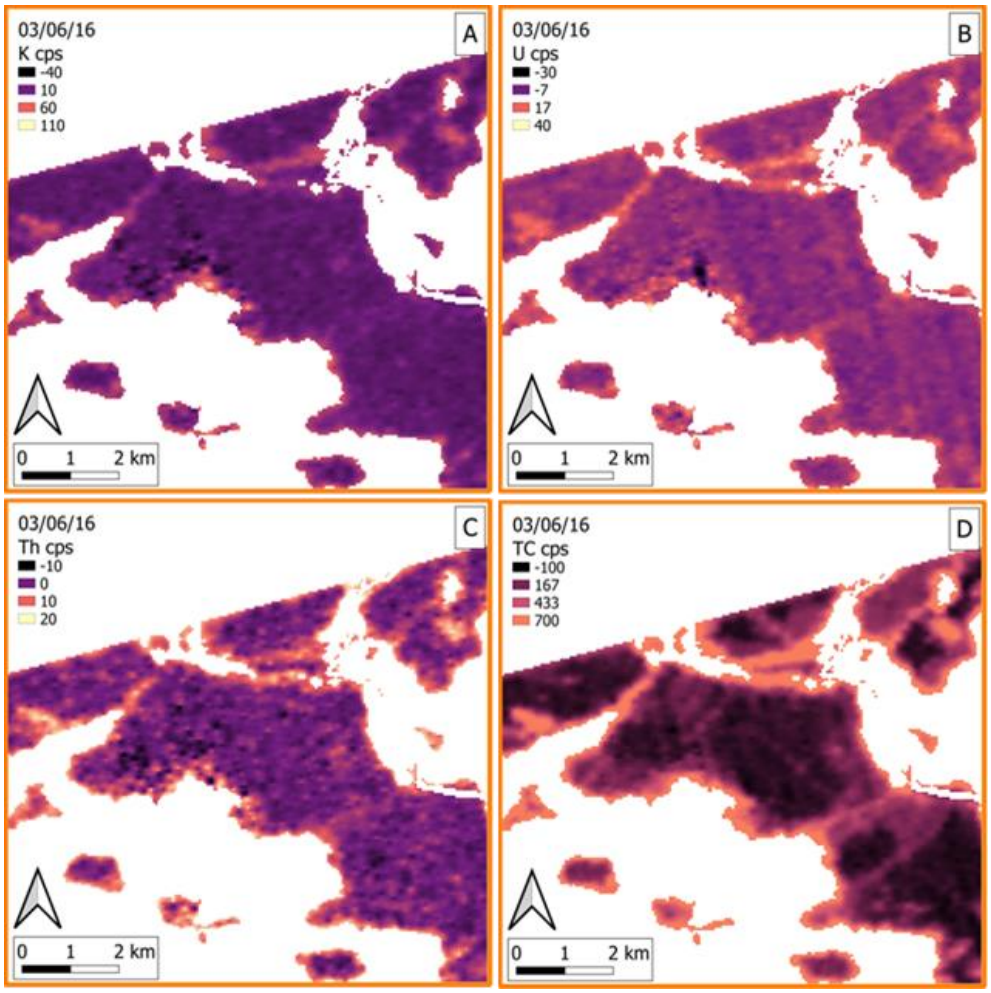


Figure 4.3.4: A) Tellus Radiometric K cps. B) Tellus Radiometric U cps. C) Tellus Radiometric Th cps. D) Tellus Radiometric TC counts per second (cps)

### 4.3.5 Data organisation and traditional analysis

S2 images (13 optical bands), and the radiometric (4 cps bands) data sources were analysed separately using the MCASD method. Each S2 image was also combined with the radiometric data source and analysed as an integrated, 17 band, data source. Data bands were placed into columns and normalised (with each column scaled between 0 and 1), to remove scaling bias between bands. Once MCASD analysis was complete, the results were presented as a MCASD graph,

similar to Figure 4.3.2-A, a raster map showing the spatial distribution of the clusters and a unique cluster signature graph, similar to a "spectral signature graph" (Huete, 2004) used in S2 classification applications.

Linear correlation analysis was performed between S2 indices (Figure 4.3.3-D to I) and radiometric data bands (Figure 4.3.4-A to D) to justify the selection of S2 data source and the use of non-linear machine learning over traditional data analytical methods. This analysis was also performed between four radiometric data bands and peat thickness data (Bord na Móna, 2021) (See Appendix 3) from within the Garryduff site boundary to aid discussion on intra-peatland variation of radiometric signal.

One possible means to identify intra-peatland variation of radiometric signal is through the use of Horizontal Gradient Magnitude (HGM) analysis (Beamish, 2016), which highlights areas of changing radiometric signal. This analysis was applied to the TC band of the radiometric data source as a comparison to the machine learning method presented here.

## 4.4 Results

### 4.4.1 Linear Correlation analysis

Correlation was performed between four radiometric data bands and a peat thickness data source (Bord na Móna, 2021), where there were 3,554 coincident data vectors. This returned correlation coefficients of: K cps: -0.04, U cps: 0.19, Th cps: -0.06 and TC cps: 0.25. These correlation results indicated a weak link between radiometric band variability and peat thickness variability within the Garryduff site boundary (See section 6.3)

Correlation was also performed between the four radiometric data bands and the S2 indices (Figure 4.3.3-D to I). These results indicated a moderate correlation between the radiometric data bands and the relevant indices, with the correlation being marginally higher for 2017 S2 data source (Table 4.4.1).

Table 4.4.1: Correlation coefficients between radiometric data bands and calculated S2 indices

| | NDVI 2017 | EVI 2017 | NDWI 2017 | NDVI 2018 | EVI 2018 | NDWI 2018 |
|---|---|---|---|---|---|---|
| K cps | 0.53 | 0.57 | 0.54 | 0.51 | 0.57 | 0.52 |
| U cps | 0.46 | 0.50 | 0.45 | 0.43 | 0.49 | 0.43 |
| Th cps | 0.53 | 0.56 | 0.52 | 0.50 | 0.56 | 0.51 |
| TC cps | 0.71 | 0.75 | 0.71 | 0.68 | 0.74 | 0.89 |

### 4.4.2 MCASD on S2 data sources

The top row (Figure 4.4.1) from MCASD analysis shows that four clusters are appropriate when clustering S2 data from 20/06/17 and that three clusters are appropriate for S2 data from 28/06/18. The middle row shows the unique signature (Huete, 2004) for each cluster signature. Both data sources had similar cluster signatures in terms of amplitude of band values. The bottom row shows the spatial distribution for the associated clustered result for each S2 data source. The main difference between the MCASD results is that the rededge1 (B5) amplitude is significantly larger in S2 data from 2018, compared to 2017. From the spatial distribution and cluster signature plots, it appears that Cluster 3 (2018) is comparable to Clusters 3 and 4 (2017).

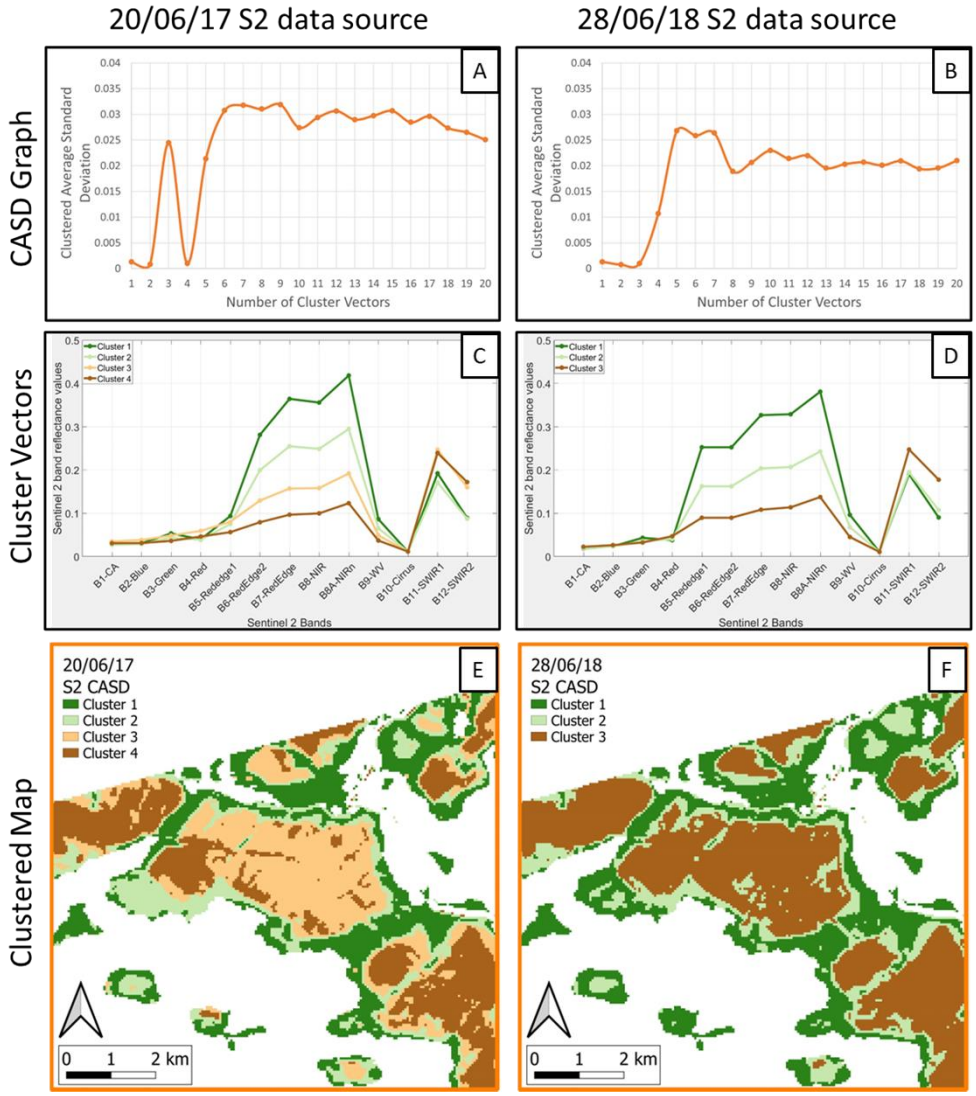


Figure 4.4.1: MCASD analysis for two (2017 and 2018) S2 data sources. A-B) MCASD graph for maximum of 20 experimental cluster signatures. C-D) Cluster signatures for S2 bands. E-F) Spatial distribution of each clustering solution.

### 4.4.3 MCASD on radiometric data

The MCASD graph (Figure 4.4.2-A) shows that 2 – 5 clusters may be used to group these radiometric data bands. The 5-cluster result is then shown via the unique cluster signature plot (Figure 4.4.2-B) and the spatial distribution map (Figure 4.4.2-C).

The cluster signature plot of normalised radiometric values shows that radiometric signal is relatively high for all four bands in Cluster 1 and low in Cluster 5. The spatial distribution of these clusters shows that Cluster 1 is generally found around the edges and Cluster 5 is located in the interior of the peatland areas.

There is potential for spatial variability in the sub-peat radiometric source intensity to be a factor in intra-peatland signal variation (Beamish, 2014). However, the study site is underlain by a single geological unity (GSI, 2022a) and so it is assumed that the sub-peat source of gamma rays is spatially constant.

Horizontal Gradient Magnitude analysis was applied to the TC band of radiometric data source (Figure 4.4.2-D). Areas of high values (red) indicate a changing radiometric signal in this band and areas of low values (blue) indicate areas of stable signal (Beamish, 2016). The edges of the peatland show the highest value, as the data pass from non-peat to peat soils (O'Leary et al., 2022) and intra-peatland variation of radiometric signal is also highlighted.

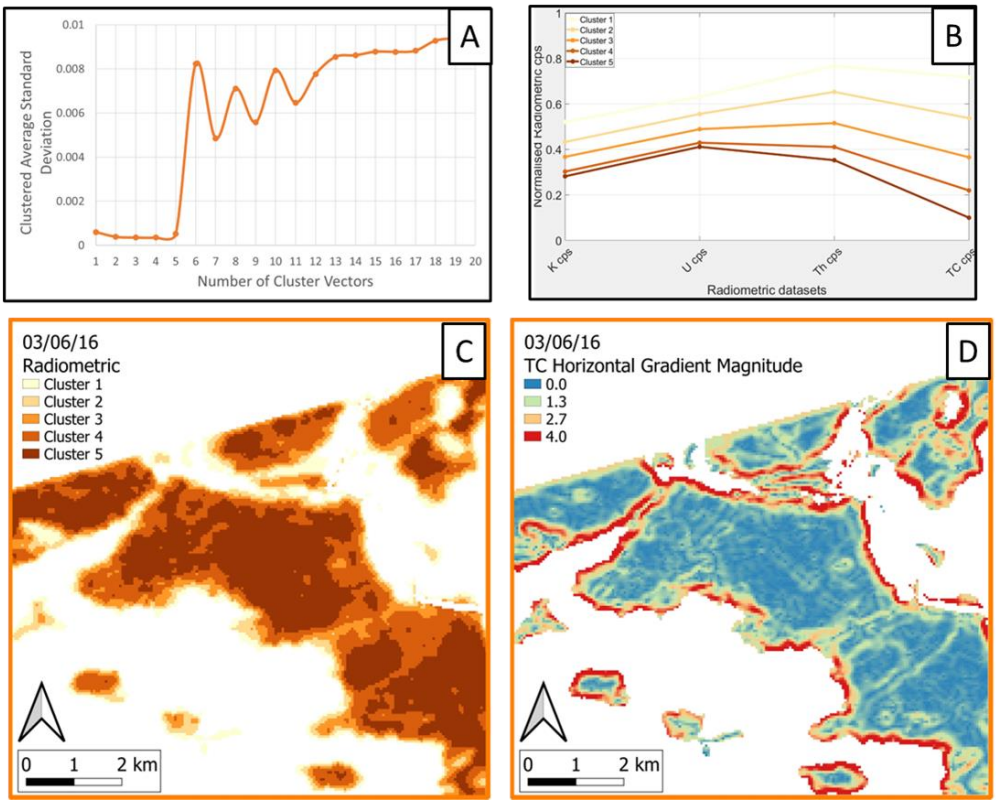


Figure 4.4.2: MCASD analysis for radiometric data source. A) MCASD graph for maximum of 20 experimental cluster signatures. B) Normalised cluster signatures for radiometric data bands. C) Spatial distribution of the 5-cluster solution. D) Horizontal Gradient Magnitude Analysis of TC data band (Beamish, 2016) (Blue = low horizontal gradient, Red = High horizontal gradient).

### 4.4.4 MCASD on combined S2 and radiometric data

S2 data bands were combined with radiometric data bands to provide a single integrated data source originating from the landcover and the subsurface to a maximum depth of ~ 60 cm. The 2017 S2 data bands, combined with radiometric data bands, are shown (Figure 4.4.3). The results, when combined with 2018 S2 data bands, are very similar (See Appendix 4).

The MCASD analysis determines that three clusters can be used to appropriately group these data bands (Figure 4.4.3-A). The spatial distribution of these clusters (Figure 4.4.3-B) shows that Cluster 1 is generally located at the edges and Cluster 3 is generally located towards the centre of defined peatlands.

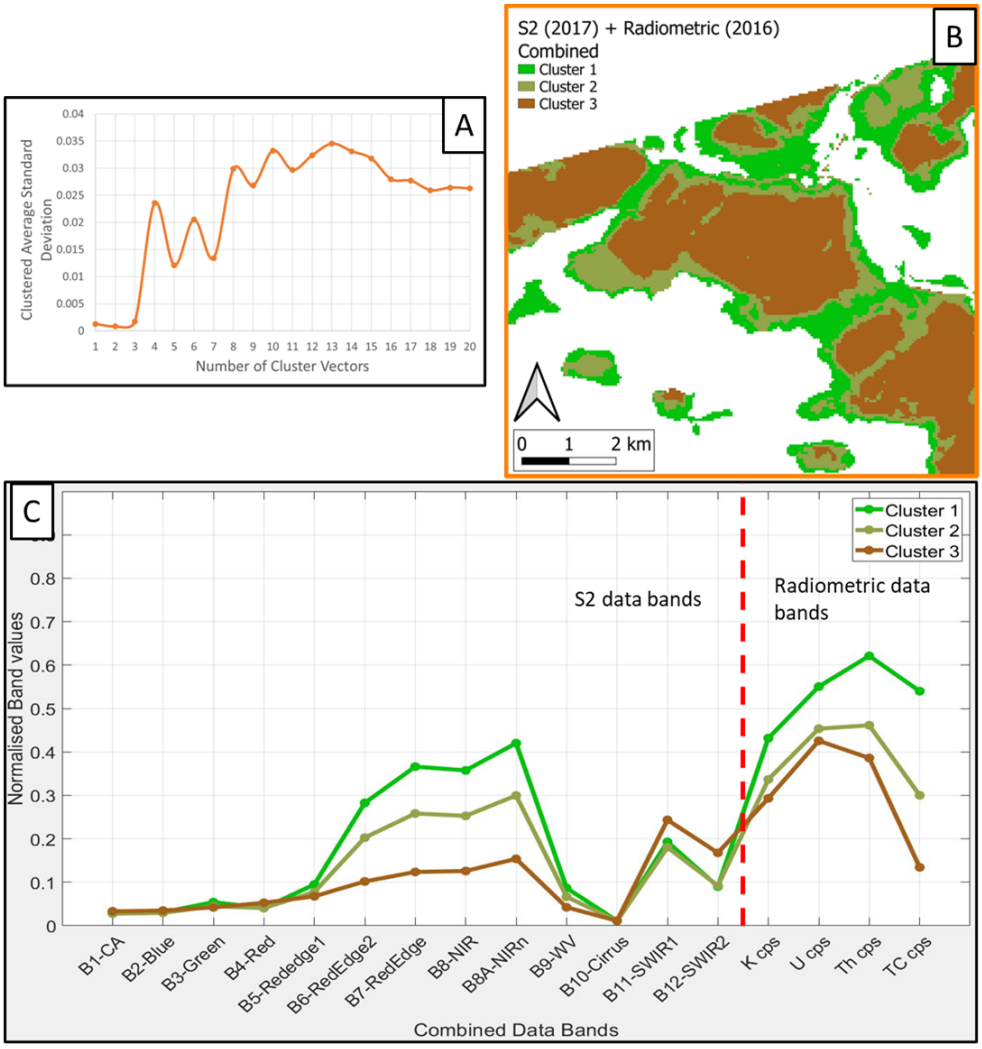


Figure 4.4.3: MCASD analysis for combined S2 and radiometric data source. A) MCASD graph for maximum of 20 experimental cluster signatures. B) Spatial distribution of the 3-

cluster solution C) Cluster signatures for all data bands (S2 bands are absolute values and radiometric bands are normalised values for ease of visualisation)

The cluster signatures (Figure 4.4.3-C) for S2 bands are shown in absolute values and radiometric bands are shown in normalised values as the absolute dynamic ranges of S2 and radiometric data sources are significantly different. Cluster 1 shows elevated values of S2 green (B3) and S2 red edge to near infra-red (B5 - B8A) and high radiometric band values. Cluster 2 has mid-range values of both B5 - B8A and radiometric bands. Cluster 3 is defined by low B5-B8A bands, high S2 short wave infra-red (B11 – B12) and low radiometric band values.

## 4.5 Discussion

### 4.5.1 Intra-peatland landcover mapping from S2 data

The S2 optical satellite data provided a means to analyse the intra-peatland landcover variation as a function of time, a proxy ecological indicator for vegetation (Bhatnagar et al., 2020). All 13 bands of the S2 data source were included in the analysis. The majority of the literature uses limited data bands to calculate indices, representative of the landcover type of interest (Arekhi et al., 2019; Hird et al., 2017; Maduako et al., 2017). Bhatnagar et al. (2020) used a combination of 10 bands alongside several indices in a machine learning prediction framework. However, to the authors' knowledge, no studies have yet combined the aims of exploratory data analysis (Chatfield, 1986) and unsupervised neural network clustering with full spectrum S2 data.

Indices have been traditionally derived due to physical relationships between relevant data bands and landcover of interest (Gao et al., 2000; Liu and Huete, 1995) and tend to be universally applicable and not necessarily site specific (Frampton et al., 2013). By including all 13 S2 data bands in this analysis, the results were not biased by any subjective choice of indices and were focused on the site under investigation. The standard indices calculated here showed the S2 data from 2017 and 2018 to be similar (Figure 4.3.3-D to I); however, none of them included B5, the red edge component, which showed significant discriminatory power (Figure 4.5.1) that might otherwise have been missed.

The choice of the appropriate number of clusters has been determined by MCASD analysis. The spike noted when MCASD was performed for three clusters in the 2017 S2 data source (Figure 4.4.2-A) indicated that three was not an

appropriate number of clusters for this data source. The MCASD analysis prevents the use of the three-cluster result in any further analysis.

The spatial distribution of both S2 MCASD analysis are shown with visual comparison from CORINE 2018 landcover (Figure 4.5.1-C) and are similar to the spatial distribution of calculated indices (Figure 4.3.3-D to I). This indicates that the MCASD analysis provided a means to visualise all 13 bands of these complex data sources in a comparable way to recognised methods.

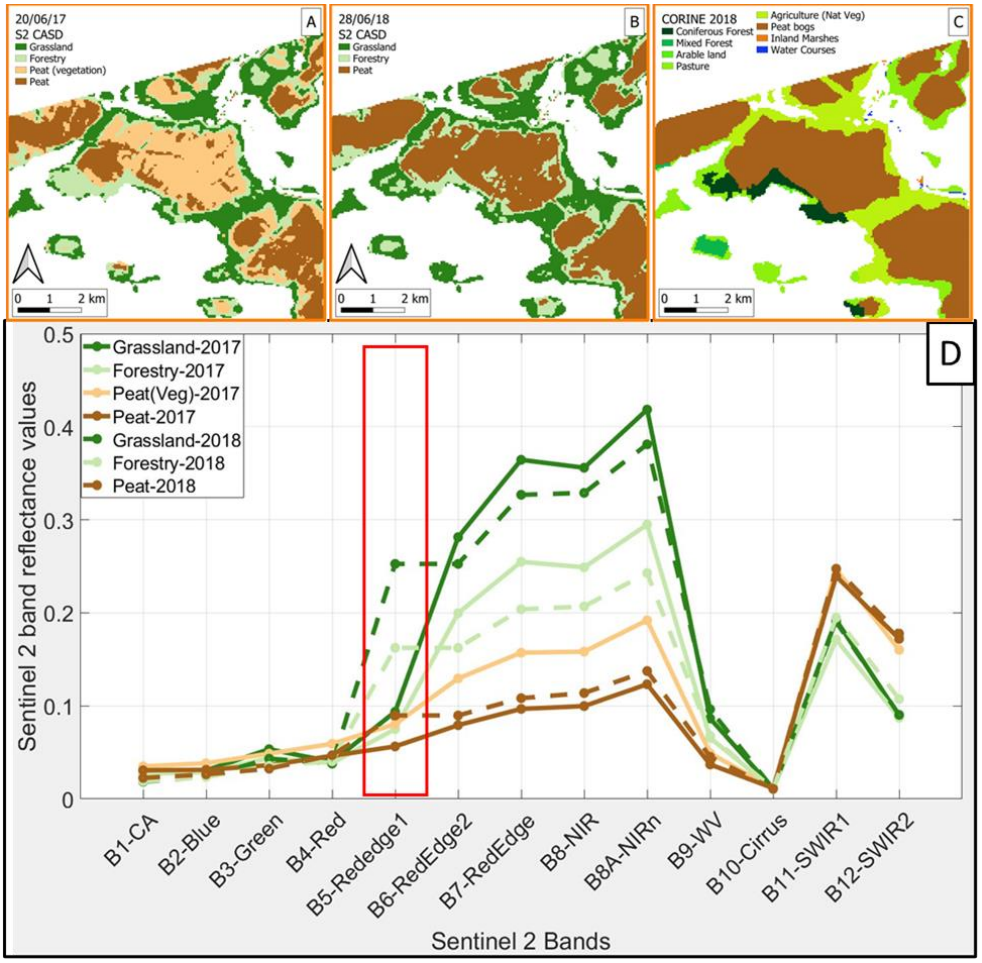


Figure 4.5.1: A) Spatial distribution of 2017 S2 MCASD analysis. B) Spatial distribution of 2018 S2 MCASD analysis. C) CORINE 2018 landcover classification. D) Cluster vector signature plot (Solid lines = S2 2017 4 cluster result, Dashed lines = S2 2018 3 cluster result). Red box highlights B5-rededge. Grassland = CORINE 2018 “arable land”, “Pasture”, “Agriculture (Nat Veg)” classes. Forestry = CORINE 2018 “Coniferous Forest”, “Mixed Forest” classes. Peat and Peat (Veg) = CORINE 2018 “Peat bogs” class.

The cluster vector signatures for both S2 MCASD results were overlain on a single plot (Figure 4.5.1-D). The absolute values for the cluster signatures were very similar. The main difference is the S2 rededge1 (B5) data band were significantly different between the two cluster signature results (Figure 4.5.1-D).

The reason for the difference between the two data sources may be explained by differing environmental conditions. A heatwave was recorded in Ireland in 2018 (Met Eireann, 2018), resulting in an increase in drought conditions. The red edge part of the electromagnetic spectrum is sensitive to plant chlorophyll content and increased red edge reflectance can indicate vegetation stress. (Filella and Penuelas, 1994). Here, this stress was highlighted in the increased B5 reflectance values noted in 2018 S2 results and generally lower values in B6-B8A, when compared to 2017 S2 results. This environmental difference might also explain the difference in appropriate cluster numbers (Figure 4.4.1-A/B) between the two S2 data sources. The heatwave in 2018 may have caused less green vegetation (predominantly shrubs and birch trees (Bord na Móna, 2021)) in the area classified as “peat bogs” (Figure 4.3.3-C), therefore changing the reflectance values and the MCASD results in this area.

Using two instances of S2 data sources served several purposes. Firstly, it allowed for a comparative analysis, alongside the correlation results (Table 4.4.1) to validate the use of S2 2017 data source when combined with a radiometric data source from the previous year. Secondly, it highlights the need for objective analysis when choosing the appropriate number of clusters for a data source. Thirdly, it highlighted the potential of the framework developed here to show temporal (gradual or sudden (Watson et al., 2014)) changes to peatland landcover, similar to that described in Bhatnagar et al. (2020), as the same analysis could be applied to seasonally averaged S2 data to show gradual change, or to individual instances of S2 data to show sudden change.

### 4.5.2 Subsurface Intra-peatland variation of radiometric signal

Several studies have attempted to link the TC band in radiometric data to peat thickness. Gatis et al. (2019) combined this band with high resolution topography indices and Keaney et al. (2013) implemented a combined interpolation of this band with in-situ peat thickness measurements. Both studies reported mixed results and a decrease in confidence with increased peat thickness. Correlation

analysis between radiometric data bands and peat thickness (section 4.4.1) indicated that the radiometric data bands were not sensitive to peat thickness variation at this site. This is likely due to peat thickness being consistently greater than ~ 60 cm (Bord na Móna, 2021).

Water has a ~ 10% greater attenuation strength compared to geological material (Beamish, 2014; Endrestøl, 1980). Peat has very low bulk density (Kiely and Carton, 2010) and very high porosity (Galvin, 1976). The low bulk density further reduces the attenuation strength of the solid component of a peat soil (O'Leary et al., 2022), while high porosity provides pore space for high volumetric water content in the soil.

Vegetation may also have an attenuating effect on gamma rays (Minasny et al., 2019; Minty, 1997), This is an ongoing area in the relatively new discipline of radiometric mapping of soils (Beamish, 2015; Rawlins et al., 2007). However, the effect was not noted in these results as clusters identified as having vegetation from CORINE 2018 landcover (Figure 4.3.3-C) also had a high radiometric value, indicating less attenuation.

One means to analyse radiometric signal variation is the Horizontal Gradient Magnitude (Beamish, 2016) which highlights areas of changing radiometric signal (Figure 4.4.2-D). This method, however, only uses a single data band (TC) and does not provide a means to spatially link areas of similar radiometric signal. In this study, the use of MCASD analysis included all radiometric data bands acquired over this site and determined they can be gathered into a maximum of five clusters (Figure 4.4.2-A), highlighting the spatial distribution of these clusters in the landscape.

The spatial distribution of these clusters (Figure 4.4.2-C) are qualitatively comparable to CORINE landcover (Figure 4.3.3-C). Clusters 4 and 5 appear to follow the “peat bogs” classification. And Clusters 1, 2 and 3 appear to follow the vegetation classifications. However, the radiometric results are sensitive to subsurface physical properties. These results may indicate areas of similar soil moisture across the site, with Cluster 1 being least and Cluster 5 being most saturated. The use of airborne radiometric data was to provide a means to analyse the intra-peatland subsurface variation of soil moisture (Beamish, 2013; Endrestøl, 1980), a hydrological indicator in the context of peatland restoration monitoring.

### 4.5.3 Integrated landcover and subsurface interpretation

Traditional correlation is a linear link between data sources, however the complexity inherent in peatland (Price et al., 2003) results in the need for a non-linear algorithm, such as neural networks, to exploit any link. The combination of optical and radar satellite data has yielded increased confidence in water table depth prediction (Räsänen et al., 2022). However, satellite data sources only measure the very near surface (Minasny et al., 2019) and must infer subsurface information. Radiometrics is a direct measurement of the subsurface and was combined with 2017 S2 in an unsupervised neural network.

The combined result (Figure 4.4.3) represents an interpretation from land surface to subsurface depth of ~ 60 cm. The spatial distribution of the combined MCASD analysis closely followed the CORINE 2018 (Figure 4.5.1-C) landcover, however there was increased resolution within the "peat bogs" landcover class. The cluster signature plot (Figure 4.4.3-C) shows that the areas of strong vegetation response (B5 – B8A) in the S2 data bands are linked with the highest radiometric values, indicating less attenuation of radiometric signal in these areas. Areas of low vegetation response are linked to areas of strong radiometric attenuation, but the data do not rule out the possibility that near-surface (i.e., below ~2 mm) water might also be contributing to a low radiometric response.

S2 data also act as a proxy for soil moisture in the top few mm of the surface, specifically via the SWIR (B11 and B12) (Tian and Philpot, 2015), with increased soil moisture generally resulting in decreased reflectance in these bands. When compared to Clusters 1 & 2, a relative increase in B11 and 12 reflectance in Cluster 3 (Figure 4.4.3-C), indicates a relative decrease in surface (~ 2 mm) moisture. However, this cluster also shows a relative decrease in radiometric response, indicating an increase in the subsurface (~ 60 cm) moisture. This validates a combined data source MCASD analysis to provide a full vegetation to surface to subsurface analysis and further highlights the advantage to including all 13 S2 data bands.

Based on the understanding of S2 and radiometric responses, the peatlands area is now classified into three clusters (Figure 4.4.3). Cluster 1, which represents grass lands around the edge of the peatlands, likely with thin, dry peat and overlain by with mineral soils. Cluster 2, which represents forested and/or grassland areas

with wet soil, highlighted by a reduced radiometric response indicating either wetter or thicker peat material is present. And Cluster 3, which represents open peatlands areas, with limited vegetation, relatively low surface soil moisture, and relatively high subsurface soil moisture.

### 4.5.4 Implications for and beyond peatland monitoring

The combined MCASD analysis has provided a data driven, semi-automatic method to analyse multiple data sources. In the context of peatlands, once a peatland extent has been identified, this framework may provide a tool to monitor peatland restoration (Mackin, 2017) by providing a set of baseline conditions prior to restoration, as well as temporal monitoring during and after restoration (Bhatnagar et al., 2020). Other temporally and spatially coincident data sources may also be integrated to this framework.

Sentinel 1 radar backscatter data may provide soil moisture information to ~ 10 cm depth (Bauer-Marschallinger et al., 2019; Bechtold et al., 2018). However, currently the noise in this source of data results in a spatial resolution which is not ideal for plot scale studies. Airborne electromagnetic measurements may be able to estimate peat thickness (Boaga et al., 2020; Siemon et al., 2020), however often vertical resolution is an issue, especially in areas with thin peats.

This study highlights the difficulties of acquiring satellite-based optical data in temperate areas with persistent cloud cover (Connolly, 2019). One way around this would be to acquire coincident optical and radiometric data bands using airborne or drone platforms (Dronova et al., 2021; Mustaffa et al., 2020; von Hebel et al., 2021). This could provide a temporally and spatially coincident data source, which is repeatable throughout the lifecycle of a restoration project.

Restoration of peatlands aims to return these sites to near natural conditions including reintroduction of peatland habitats (Renou-Wilson et al., 2019) and maintaining a water table at ~ 10 cm depth (Evans et al., 2021). Repeat MCASD analysis of optical (landcover) and radiometric (soil moisture) measurements (as well as other relevant datasets), may provide a useful tool in monitoring vegetation and water table levels over time, both indicators of restoration success (Mackin, 2017).

The methods presented in this article have application beyond the scope of peatland restoration and may be useful in any environment that requires a multi-sensor approach to analysis such as soil mapping (Brogi et al., 2019) and precision agriculture (von Hebel et al., 2021).

## 4.6 Conclusions

This paper has developed a new metric, Multi-Cluster Average Standard Deviation (MCASD), to facilitate the choice of the most appropriate number of clusters in an unsupervised classification of data from multiple sources. It demonstrates how stable clusters with the highest spatial resolution can be generated with, for example, Self-Organising Maps. The method was demonstrated using different combinations of satellite optical and airborne radiometric data over a peatland but has implications for many research domains such as seabed mapping, precision agriculture and any discipline utilising multi-dimensional geospatial data.

The use of machine learning neural networks in this study allowed for an objective analysis of intra-peatland variability of all data bands from S2 optical data. Self-Organising Maps produces a “spectral signature” for each cluster highlighting differences in spectral bands. This “full spectrum” approach does not rely on only specific spectral bands of S2 data, as with indices such as NDVI, but can be used to show a comprehensive and visually simple view of the spatial and temporal variations in all S2 data bands across a site, highlighted here by B5 differences indicating vegetation stress due to a heatwave.

The same Self-Organising Maps approach was applied to intra-peatland variation of radiometric signal. This resulted in a multi-variate, quantitative means of linking areas of similar radiometric signal with the main advantage over traditional Horizontal Gradient Magnitude being the means to visualise variations in four bands of radiometric data simultaneously. Variation in radiometric signal on this site was most likely due to soil moisture.

The combination of these two data sources within the MCASD method produced a comprehensive, integrated interpretation of intra-peatland variation of ecological and hydrological factors, without the need for an extensive ground data collection campaign. An S2 data source from 2017 provided a proxy for surface vegetation and soil moisture levels across the study site, while radiometric data

acted as a proxy for subsurface soil moisture to ~ 60 cm. The combination of these two data sources within an MCASD analysis resulted in the division of this peatlands site into three distinct zones of differing surface and subsurface conditions (Figure 4.4.3).

This study provides the framework for monitoring peatland habitat restoration, especially when considering spatially and temporally coincident, high resolution acquisition platforms, such as drones.

# Chapter 5: **Discussion & Conclusions**

## 5.1 Discussion

This thesis demonstrates the challenges of, and the potential role that airborne geophysics surveys can play, in peatland restoration (Chapter 2), how these data can be employed to identify peat soils, update peatland boundaries (Chapter 3) and how these data can be combined with satellite remote sensing to visualise intra-peatland variation of several key peatland rehabilitation indicators (Chapter 4). From the identification of statistical differences in radiometric data, to the development of a semi-automatic, data driven approach to clustering, this work augments our understanding of using Big Data concepts within the geosciences.

The need for advances in peatland mapping techniques is evident in the non-standard approach to identification or peatlands globally (Minasny et al., 2019; Xu et al., 2018). Advances in mapping techniques are also needed to fulfil peatlands habitat and rehabilitation reporting obligations as outlined by Article 6 Habitats Directive (EC, 2022). Although not yet available globally, airborne radiometric data may become a popular and relatively simple method to update national inventories of peatland extent via consistent spatial delineation of peatland boundaries and identification of previously unknown peatlands, which could have been mis-classified in traditional or satellite derived techniques.

## 5.2 Key concepts

### 5.2.1 Big Data

Throughout the methods presented in this PhD thesis, the concepts of Big Data, Data Assimilation (DA), Digital Soil Mapping (DSM) and Exploratory Data Analysis (EDA) were considered. The volume of the data used in this analysis is relatively small (gigabytes), compared to the terabytes of information that a company like Facebook may process on a daily basis (Gandomi and Haider, 2015). Satellite data record 100 x 100 km tiles of data at ~ 10 m resolution and have a return time of 3 – 5 days depending on the satellite sensor and mission (Sentinel, 2022) and airborne geophysical surveys can collect several hundred thousand individual measurements during a survey (Binley et al., 2015).

Therefore, satellite remote sensing and airborne geophysical data may be considered as “Big Data” under the Three V definitions. Data Volumes presented in this thesis are considered to be high due to the typical size of geoscience datasets (Karpatne et al., 2019). They are considered to have high Variety, or heterogeneity, as they are measuring a complex physical system of unknown variables. Finally, these data sources are considered to have high Velocity, or rate of generation.

Big Data does present some problems to geoscientists, who may not have training in data analytics. Specifically, these problems related to how to manage, interpret, and visualise such large, heterogeneous, and continuously generated spatial and temporal datasets (Carrassi et al., 2018). This thesis advances the use of numerical tools and data visualisations incorporating several geoscience Big Data sources.

### 5.2.2 Data Assimilation

Chapter 3 focused on the use of one such data source within the principles of DA (Carrassi et al., 2018), namely airborne radiometric data acquired over a large geographical region in the West of Ireland. The airborne radiometric measurements formed the “observations” within the concept of DA and supervised machine learning pattern recognition formed the “model”. Here the observations were chosen from within the full data source provided, based on the likelihood of having been acquired over a peat or a non-peat soil. This ensured that the model, here represented by supervised machine learning, would be able to determine a high order statistical difference between the two different observation types (Karpatne et al., 2019). The model could then be applied to all observations and identify each as a peat or a non-peat observation.

In order to visualise the differences between data, a separate modelling exercised was performed which highlighted a mathematical reason for the difference in observation, specifically the difference in bulk density between peat and non-peat soils. A reason for statistical differences in datasets is important when using machine learning in the geosciences (Karpatne et al., 2019; Valentine and Kalnins, 2016), as the algorithms used look purely for patterns, which may coincidentally exist in non-physically related datasets, and lead to erroneous interpretations of results.

### 5.2.3 Digital Soil Mapping and Exploratory Data Analysis

Chapter 4 focused on the concepts of DSM (McBratney et al., 2003) and EDA (Chatfield, 1986). All the principles of EDA are used in order to remove user bias and subjectivity for the analysis. Firstly, all bands of optical satellite data were used, without the calculation of specific indices (Frampton et al., 2013), which are often selected based on expert experience. This meant that no unintentional omission of an important data band could happen. Secondly the MCASD technique was developed and refined. This is a simple, effective and data driven means to determine the appropriate number of clusters needed to define or visualise any set of data, which removes the subjectivity of other methods (Delgado et al., 2017). The use of neural networks, which relies "learning" the statistical relationships (Dramsch, 2020) between data bands, also follows principles of EDA as opposed using an explicit set of rules, which traditional numerical analysis often relies on (e.g., inversion, correlation, regression) (Karpatne et al., 2019). Such traditional techniques, which are useful at extracting individual physical properties, are not designed to provide comprehensive interpretations of complex earth systems (Karpatne et al., 2019). The inclusion of unsupervised machine learning allowed for the combination of optical satellite and airborne radiometric data for a comprehensive interpretation of a peatland from surface to sub-surface and a visualisation of this interpretation using concepts from DSM.

### 5.2.4 Implications outside thesis scope

With the ever-increasing availability of large geospatial datasets, new tools are needed to simplify and visualise such data. By incorporating the key concepts from Big Data, Data Assimilation, Exploratory Data Analysis and Digital Soil Mapping in this thesis, large geoscience data sources have been used to achieve this in a peatland focused study. However, the incorporation of these concepts is important in all areas of geoscience where "Big Data" may be used. With an increase in public interest in climate sciences, and the requirement for governments to report key climatic indicators and meeting Sustainable Development Goals (SDG)(UN, 2022), the use of big data sets will become more prevalent. Their use will allow for an increased ability in fulfilling policy obligations, but also as a means to drive policy and policy reporting into the future. The methods developed within this thesis follow these concepts and are not restricted to peatlands studies but could be

incorporated into many disciplines such as urban planning, precision agriculture and renewable energy development.

## 5.3 Final remarks

In this thesis supervised and unsupervised machine learning and MCASD analysis incorporated the concepts of Big Data, DA, DSM, and EDA to create innovative maps using several geoscience data sources. These maps demonstrate the ability of such data sources, acquired over large geographic areas, to help solve problems at scales that are useful to individual sites. This incorporates the final key concept outlined in this thesis, namely the use of Big Data for Local Problems.

## 5.4 Conclusions

The objective of this PhD thesis was to advance Digital Soil Mapping for identifying peat soils, updating peatland boundaries, and visualisation of intra-peatland property variation using remote sensed “big” data sources using concepts of Data Assimilation and Exploratory Data Analysis. Several aims were outlined in order achieve this objective.

Firstly, the methods used in this thesis attempted to remove user bias where possible. This was achieved through the use of neural networks and machine learning, which required little parameterisation. The data sources used in this thesis on had minimal processing applied. This allowed for the data sources to remain free from bias or shifts introduced by, often subjective, choice of filters and other noise removal techniques.

The concept of EDA requires a data driven approach, especially when clustering data. The MCASD method was developed as part of this PhD thesis in order to further remove any subjectivity from clustering analysis and allow for a true EDA to be performed on individual and combined data sources.

The prediction of peat soils in the landscape was achieved through the use of supervised machine learning and airborne radiometric data and achieved a predictability of ~ 95 % in the study region in the West of Ireland. The presented methodology is considered unique and robust and could be expanded to national or international scale peatland extent maps.

Optical satellite data were included in the analysis of intra-peatland variation of landcover type within the MCASD analysis. In this thesis all 13 spectral bands of optical satellite data were used. The inclusion of all acquired data within this

analysis allowed for objective visualisations of how these data vary in space, without the use of calculated indices, or mathematical combinations of bands.

The inclusion of airborne radiometric data within machine learning, combined with optical satellite data, allowed for an additional subsurface dimension to any interpretation of intra-peatland variation of physical properties. This combination in an MCASD analysis provided a means to link surface landcover changes with subsurface property changes, namely soil moisture content.

When reporting peatland extent and particularly intra-peatland variations of relevant physical properties, resolution is an important consideration. Here the resolution of the results is limited by the airborne radiometric data to a resolution of 50 x 50 m. However, the MCASD analysis is not restricted to just these data sources. The use of drone-based platforms may provide sub metre resolution of similar data and so the framework developed in this thesis has implications well beyond the scope of work outlined here. Indeed, MCASD can be applied to any spatial, or in fact non spatial, data and provide the same objective analysis. Taking drone-based data as an example, MCASD may have applications in soil science, precision agriculture, hazard, and habitat monitoring.

## 5.5 Future work

Based on the findings in this PhD thesis the following future work are recommended as future research topics.

- Expanded the methodology developed in Chapter 3 to all Tellus Blocks which are currently available and produce an updated national peatland extent map. This map can be compared/combined with other peatland databases such as the Derived Irish Peatland Map v2 (Connolly and Holden, 2009).
- Based on the success of the radiometric method of peatland detection, the use of airborne radiometric surveys could be expanded and encouraged in other national jurisdictions, particularly in areas with poor ground access and remote areas. Such surveys could become a standard peatland mapping tool, providing an internationally consistent peatland map, relevant for updating and reporting peatland extent globally.

- The MCASD method, developed in Chapter 4 has implications for clustering large complex datasets outside the discipline of earth sciences. This method should be tested, firstly on other geo-spatial data sources, such as ground geophysical data. Further research into the potential for this method to reduce noise, or highlight anomalies, in such datasets should be performed. Also, the potential to "simplify" large geospatial datasets and reduce computational load in traditional geophysical techniques such as inversion should be explored. The method can then be applied to non-geoscience data sources and published in machine learning focused journals to validate and promote its use.
- The framework developed in Chapter 4 related to peatland rehabilitation monitoring should be downscaled to drone-based platforms. Current reporting of, for example, Special Areas of Conservation (SAC), require appropriate assessment based on European Commission Article 6 of the habitats directive (EC, 2022) and these assessments must be based on best scientific knowledge in the field. Research into the application of MCASD on combined drone based remote sensing and their ability to identify ecotopes within a peatland, and their development over time, could significantly improve habitat reporting on SAC, and other sites, at the European level. This would help Ireland, and other European countries meet their obligations under the habitat's directive.

# List of References


Abdalla, M., Hastings, A., Truu, J., Espenberg, M., Mander, Ü., Smith, P., 2016. Emissions of methane from northern peatlands: a review of management impacts and implications for future management options, pp. 7080-7102. https://doi.org/10.1002/ece3.2469

Airo, M.-L., Hyvönen, E., Lerssi, J., Leväniemi, H., Ruotsalainen, A., 2014. Tips and tools for the application of GTK's airborne geophysical data, Geological Survey of Finland, https://tupa.gtk.fi/julkaisu/tutkimusraportti/tr_215.pdf, (accessed 09/05/2022)

Aitkenhead, M.J., 2017. Mapping peat in Scotland with remote sensing and site characteristics. Eur J Soil Sci 68(1), 28-38. https://doi.org/10.1111/ejss.12393

Altdorff, D., Bechtold, M., van der Kruk, J., Vereecken, H., Huisman, J.A., 2016. Mapping peat layer properties with multi-coil offset electromagnetic induction and laser scanning elevation data. Geoderma 261, 178-189. https://doi.org/10.1016/j.geoderma.2015.07.015

Ameglio, L., 2018. Review of developments in airborne geophysics and geomatics to map variability of soil properties. 14th International Conference on Precision Agriculture, https://www.ispag.org/proceedings/?action=download&item=5024, (accessed 14/04/2022)

Anderson, K., Bennie, J., Milton, E., Hughes, P., Lindsay, R., Meade, R., 2010. Combining LiDAR and IKONOS data for eco-hydrological classification of an ombrotrophic peatland. Journal of environmental quality 39(1), 260-273. https://doi.org/10.2134/jeq2009.0093

Arekhi, M., Goksel, C., Sanli, F.B., Senel, G., 2019. Comparative Evaluation of the Spectral and Spatial Consistency of Sentinel-2 and Landsat-8 OLI Data for Igneada Longos Forest. Isprs Int J Geo-Inf 8(2). https://doi.org/10.3390/ijgi8020056

Aune-Lundberg, L., Strand, G.H., 2021. The content and accuracy of the CORINE Land Cover dataset for Norway. International Journal of Applied Earth Observation and Geoinformation 96. https://doi.org/10.1016/j.jag.2020.102266

Barchiesi, S., Davies, P.E., Kulindwa, K.A.A., Lei, G., Martinez Ríos del Río, L., 2018. Implementing environmental flows with benefits for society and different wetland ecosystems in river systems. Ramsar Policy Brief No. 4. Gland, Switzerland: Ramsar Convention Secretariat. https://doi.org/10.3389/fenvs.2020.00106

Bauer-Marschallinger, B., Freeman, V., Cao, S., Paulik, C., Schaufler, S., Stachl, T., Modanesi, S., Massario, C., Ciabatta, L., Brocca, L., Wagner, W., 2019. Toward Global Soil Moisture Monitoring With Sentinel-1: Harnessing Assets and Overcoming Obstacles. Ieee T Geosci Remote 57(1), 520-539. https://doi.org/10.1109/TGRS.2018.2858004

Beamish, D., 2013. Gamma ray attenuation in the soils of Northern Ireland, with special reference to peat. J Environ Radioactiv 115, 13-27. https://doi.org/10.1016/j.jenvrad.2012.05.031

Beamish, D., 2014. Peat Mapping Associations of Airborne Radiometric Survey Data. Remote Sens-Basel 6(1), 521-539. https://doi.org/10.3390/rs6010521

Beamish, D., 2015. Relationships between gamma-ray attenuation and soils in SW England. Geoderma 259, 174-186. http://dx.doi.org/10.1016%2Fj.geoderma.2015.05.018

Beamish, D., 2016. Enhancing the resolution of airborne gamma-ray data using horizontal gradients. Journal of Applied Geophysics 132, 75-86. https://doi.org/10.1016/j.jappgeo.2016.07.006

Beamish, D., Young, M., 2009. Geophysics of Northern Ireland - the Tellus Effect. First Break 27(8). https://doi.org/10.3997/1365-2397.27.1302.32176

Bechtold, M., Schlaffer, S., Tiemeyer, B., De Lannoy, G., 2018. Inferring Water Table Depth Dynamics from ENVISAT-ASAR C-Band Backscatter over a Range of Peatlands from Deeply-Drained to Natural Conditions. Remote Sens-Basel 10(4). https://doi.org/10.3390/rs10040536

Beltman, B., Ven, P., Verhoeven, J., Sarneel, J., 2014. Phosphate Release Upon Long- and Short -Term Flooding of Fen Meadows Depends on Land Use History and Soil pH. Wetlands 34(5), 989-1001. https://doi.org/10.1007/s13157-014-0563-9

Benabdellah, A.C., Benghabrit, A., Bouhaddou, I., 2019. A survey of clustering algorithms for an industrial context. Procedia Computer Science 148, 291-302. https://doi.org/10.1016/j.procs.2019.01.022

Berglund, O., Berglund, K., 2010. Distribution and cultivation intensity of agricultural peat and gyttja soils in Sweden and estimation of greenhouse gas emissions from cultivated peat soils. Geoderma 154(3-4), 173-180. https://doi.org/10.1016/j.geoderma.2008.11.035

Bhatnagar, S., Gill, L., Regan, S., Naughton, O., Johnston, P., Waldren, S., Ghosh, B., 2020. Mapping vegetation communities inside Wetlands using Sentinel-2 imagery in Ireland. International Journal of Applied Earth Observation and Geoinformation 88, 102083. https://doi.org/10.1016/j.jag.2020.102083

Binley, A., Hubbard, S., Huisman, J., Revil, A., Robinson, D., Singha, K., Slater, L., 2015. The emergence of hydrogeophysics for improved understanding of subsurface processes over multiple scales. Water Resources Research 51(6), 3837-3866. https://doi.org/10.1002/2015WR017016

Blackwell, M.S., Carswell, A.M., Bol, R., 2013. Variations in concentrations of N and P forms in leachates from dried soils rewetted at different rates. Biology and fertility of soils 49(1), 79-87. https://doi.org/10.1007/s00374-012-0700-7

Boaga, J., 2017. The use of FDEM in hydrogeophysics: A review. Journal of Applied Geophysics 139, 36-46. https://doi.org/10.1016/j.jappgeo.2017.02.011

Boaga, J., Viezzoli, A., Cassiani, G., Deidda, G.P., Tosi, L., Silvestri, S., 2020. Resolving the thickness of peat deposits with contact-less electromagnetic methods: A case study in the Venice coastland. Science of the Total Environment 737. https://doi.org/10.1016/j.scitotenv.2020.139361

Bord na Móna, 2021. Garryduff Decommissioning and Rehabilitation Plan 2021, https://www.bnmpcas.ie/wp-content/uploads/sites/18/2021/08/Garryduff-Rehab-Plan-V8.pdf, (accessed 17/05/2022)

Bourgeau-Chavez, L., Endres, S.L., Graham, J., Hribljan, J.A., Chimner, R., Lillieskov, E., Battaglia, M., 2018. Mapping peatlands in boreal and tropical ecoregions. In: Liang, S., ed. Comprehensive Remote Sensing, vol. 6. Oxford, UK: Elsevier: 24–44., 24-44. http://dx.doi.org/10.1016/B978-0-12-409548-9.10544-5

Brödlin, D., Kaiser, K., Hagedorn, F., 2019. Divergent Patterns of Carbon, Nitrogen, and Phosphorus Mobilization in Forest Soils. Frontiers in Forests and Global Change 2(66). https:/doi.org/10.3389/ffgc.2019.00066

Brogi, C., Huisman, J.A., Patzold, S., von Hebel, C., Weihermuller, L., Kaufmann, M.S., van der Kruk, J., Vereecken, H., 2019. Large-scale soil mapping using multi-configuration EMI and supervised image classification. Geoderma 335, 133-148. 10.1016/j.geoderma.2018.08.001

Buschmann, C., Röder, N., Berglund, K., Berglund, Ö., Lærke, P.E., Maddison, M., Mander, Ü., Myllys, M., Osterburg, B., van den Akker, J.J.H., 2020. Perspectives on agriculturally used drained peat soils: Comparison of the socioeconomic and ecological business environments of six European regions. Land Use Policy 90, 104181. https://doi.org/10.1016/j.landusepol.2019.104181

Caliński, T., Harabasz, J., 1974. A dendrite method for cluster analysis. Communications in Statistics 3(1), 1-27. https://doi.org/10.1080/03610927408827101

Carcione, J.M., Seriani, G., Gei, D., 2003. Acoustic and electromagnetic properties of soils saturated with salt water and NAPL. Journal of Applied Geophysics 52(4), 177-191. https://doi.org/10.1016/S0926-9851(03)00012-0

Carrassi, A., Bocquet, M., Bertino, L., Evensen, G., 2018. Data assimilation in the geosciences: An overview of methods, issues, and perspectives. Wires Clim Change 9(5). https://doi.org/10.1002/wcc.535

Charlet, L., Markelova, E., Parsons, C., Couture, R.-M., Madé, B., 2013. Redox Oscillation Impact on Natural and Engineered Biogeochemical Systems: Chemical Resilience and Implications for Contaminant Mobility. Procedia Earth and Planetary Science 7(C), 135-138. https://doi.org/10.1016/j.proeps.2013.03.048

Chatfield, C., 1986. Exploratory data analysis. European Journal of Operational Research 23(1), 5-13. https://doi.org/10.1016/0377-2217(86)90209-2

Chavez, P.S., 1996. Image-Based Atmospheric Corrections - Revisited and Improved. Photogrammetric Engineering and Remote Sensing 62, 1025-1036. https://doi.org/10.4236/acs.2016.62026

Clarke, D., Rieley, J., 2010. Strategy for responsible peatland management. International Peat Society Finland, https://peatlands.org/assets/uploads/2019/10/srpm2019finalforprint.pdf , (accessed 03/10/22)

Clément, R., Pärn, J., Maddison, M., Henine, H., Chaumont, C., Tournebize, J., Uri, V., Espenberg, M., Günther, T., Mander, Ü., 2020. Frequency-domain electromagnetic induction for upscaling greenhouse gas fluxes in two hemiboreal drained peatland forests. Journal of Applied Geophysics, 103944. http://dx.doi.org/10.1016/j.jappgeo.2020.103944

Congedo, L., 2021. Semi-Automatic Classification Plugin: A Python tool for the download and processing of remote sensing images in QGIS. Journal of Open Source Software 6(64), 3172. https://doi.org/10.21105/joss.03172

Connolly, J., 2019. Mapping land use on Irish peatlands using medium resolution satellite imagery. Irish Geography; Vol 51, No 2 (2018): Special Issue - The vulnerability of Irish landscape systems to climate change and human activity - Part 1DO - 10.2014/igj.v51i2.1371, http://www.irishgeography.ie/index.php/irishgeography/article/view/1371, (accessed

Connolly, J., Holden, N.M., 2009. Mapping peat soils in Ireland: updating the derived Irish peat map. Irish Geography 42(3), 343-352. http://dx.doi.org/10.1080/00750770903407989

Connolly, J., Holden, N.M., Ward, S.M., 2007. Mapping Peatlands in Ireland using a Rule-Based Methodology and Digital Data. Soil Science Society of America Journal 71(2), 492-499. https://doi.org/10.2136/sssaj2006.0033

CORINE, 2018. European Union, Copernicus Land Monitoring Service 2018. https://land.copernicus.eu/, (accessed 02/03/2022)

Creamer, R., 2014b. Irish SIS Final Technical Report 8: Correlation of the Irish Soil Classification System to World Reference Base 2006 system, Environmental Protection Agency Ireland, Secure Archive For Environmental Research Data, https://eparesearch.epa.ie/safer/iso19115/displayISO19115.jsp?isoID=3071, (accessed 09/05/2022)

Creamer, R., 2015b. Irish SIS Final Technical Report 11: Methodology for the Validation of predictive mapping, Environmental Protection Agency Ireland, Secure Archive For Environmental Research Data, https://eparesearch.epa.ie/safer/iso19115/displayISO19115.jsp?isoID=3064, (accessed 09/05/2022)

Creamer, R., O'Sullivan, L., 2018. The Soils of Ireland. Springer International Publishing, Cham, Cham. https://doi.org/10.1007/978-3-319-71189-8

Czapiewski, S., Szumińska, D., 2022. An Overview of Remote Sensing Data Applications in Peatland Research Based on Works from the Period 2010–2021. Land 11(1). https://doi.org/10.3390/land11010024

Dargie, G.C., Lewis, S.L., Lawson, I.T., Mitchard, E.T.A., Page, S.E., Bocko, Y.E., Ifo, S.A., 2017. Age, extent and carbon storage of the central Congo Basin peatland complex. Nature 542(7639), 86-+. https://doi.org/10.1038/nature21048

Davies, D.L., Bouldin, D.W., 1979. A Cluster Separation Measure. IEEE Transactions on Pattern Analysis and Machine Intelligence PAMI-1(2), 224-227. https://doi.org/10.1109/TPAMI.1979.4766909

Davisson, C.M., Evans, R.D., 1952. Gamma-ray absorption coefficients. Reviews of Modern Physics 24(2), 79-107. https://doi.org/10.1103/RevModPhys.24.79

Delgado, S., Higuera, C., Calle-Espinosa, J., Morán, F., Montero, F., 2017. A SOM prototype-based cluster analysis methodology. Expert Systems With Applications 88, 14-28. https://doi.org/10.1016/j.eswa.2017.06.022

Dinh, M.-V., Guhr, A., Weig, A.R., Matzner, E., 2018. Drying and rewetting of forest floors: dynamics of soluble phosphorus, microbial biomass-phosphorus, and the composition of microbial communities. Biology and Fertility of Soils 54(6), 761-768. https://doi.org/10.1007/s00374-018-1300-y

Djodjic, F., Elmquist, H., Collentine, D., 2018. Targeting critical source areas for phosphorus losses: Evaluation with soil testing, farmers' assessment and modelling. Ambio 47(1), 45-56. https://doi.org/10.1007/s13280-017-0935-5

Donlan, J., O'Dwyer, J., Byrne, K.A., 2016. Area estimations of cultivated organic soils in Ireland: reducing GHG reporting uncertainties. Mires Peat 18. http://dx.doi.org/10.19189/MaP.2016.OMB.230

Dramsch, J.S., 2020. 70 years of machine learning in geoscience in review. Advances in Geophysics, 61. https://doi.org/10.1016/bs.agph.2020.08.002

Dronova, I., Kislik, C., Dinh, Z., Kelly, M., 2021. A Review of Unoccupied Aerial Vehicle Use in Wetland Applications: Emerging Opportunities in Approach, Technology, and Data. Drones 5(2). https://doi.org/10.3390/drones5020045

EC, 2022. Article 6 of the Habitats Directive, https://ec.europa.eu/environment/nature/info/pubs/docs/others/ECJ_rulings%20Art_%206%20-%20Final%20Sept%202014-2.pdf, (accessed 16/10/2022)

EC, G., 2006. Directive 2006/118/EC of the European Parliament and of the Council of 12 December 2006 on the protection of groundwater against pollution and deterioration. Official Journal of the European Union, L 372, 19-31, https://eur-lex.europa.eu/legal-content/EN/TXT/?uri=celex%3A32006L0118, (accessed 03/10/22)

EC, W.F., 2000. Directive 2000/60/EC of the European Parliament and of the Council of 23 October 2000 establishing a framework for Community action in the field of water policy. Official journal of the European communities 22(12), 2000, https://www.eea.europa.eu/policy-documents/directive-2000-60-ec-of, (accessed 03/10/22)

Endrestøl, G.O., 1980. Principle and method for measurement of snow water equivalent by detection of natural gamma radiation / Principe et méthode pour la mesure de l'hauteur d'eau équivalente par détection du rayonnement gamma naturel. Hydrological Sciences Bulletin 25(1), 77-83. https://doi.org/10.1080/02626668009491906

Escribano, P., Schmid, T., Chabrillat, S., Rodríguez-Caballero, E., García, M., 2017. Chapter 4 - Optical Remote Sensing for Soil Mapping and Monitoring. In: P. Pereira, E.C. Brevik, M. Muñoz-Rojas, B.A. Miller (Eds.), Soil Mapping and Process Modeling for Sustainable Land Use Management. Elsevier, pp. 87-125. https://doi.org/10.1016/B978-0-12-805200-6.00004-9

EU, 2020. 2030 climate & energy framework. https://ec.europa.eu/clima/eu-action/climate-strategies-targets/2030-climate-energy-framework_en#ecl-inpage-910, (accessed 09/05/2022)

Evans, C.D., Peacock, M., Baird, A.J., Artz, R.R.E., Burden, A., Callaghan, N., Chapman, P.J., Cooper, H.M., Coyle, M., Craig, E., Cumming, A., Dixon, S., Gauci, V., Grayson, R.P., Helfter, C., Heppell, C.M., Holden, J., Jones, D.L., Kaduk, J., Levy, P., Matthews, R., McNamara, N.P., Misselbrook, T., Oakley, S., Page, S.E., Rayment, M., Ridley, L.M., Stanley, K.M., Williamson, J.L., Worrall, F., Morrison, R., 2021. Overriding water table control on managed peatland greenhouse gas emissions. Nature 593(7860), 548-552. https://doi.org/10.1038/s41586-021-03523-1

Everard, M., McInnes, R.J., 2018. Ramsar convention on Wetlands, resolution XIII. 17: Rapidly assessing wetland ecosystem services. https://uwe-repository.worktribe.com/OutputFile/858230, (accessed 03/10/22)

Fahmi, A., Nurzakiah, S., Susilawati, A., 2019. The interaction of peat and sulphidic material as substratum in wetland: ash content and electrical conductivity dynamic, IOP Conference Series: Earth and Environmental Science. IOP Publishing, pp. 012045. https://doi.org/10.1088/1755-1315/393/1/012045

Faulwetter, J.L., Gagnon, V., Sundberg, C., Chazarenc, F., Burr, M.D., Brisson, J., Camper, A.K., Stein, O.R., 2009. Microbial processes influencing performance of treatment wetlands: A review. Ecological Engineering 35(6), 987-1004. https://doi.org/10.1016/j.ecoleng.2008.12.030

Fenner, N., Williams, R., Toberman, H., Hughes, S., Reynolds, B., Freeman, C., 2011. Decomposition 'hotspots' in a rewetted peatland: implications for water quality and carbon cycling. Hydrobiologia 674(1), 51-66. https://doi.org/10.1007/s10750-011-0733-1

Filella, I., Penuelas, J., 1994. The red edge position and shape as indicators of plant chlorophyll content, biomass and hydric status. International Journal of Remote Sensing 15(7), 1459-1470. https://doi.org/10.1080/01431169408954177

Foulon, E., Scarpari Spolidorio Junior, E., Rousseau, A.N., 2019. High Resolution Data for Semi-Distributed Hydrological Modeling: Is it Worth the Trouble?, AGU Fall Meeting Abstracts, pp. H22A-07, https://ui.adsabs.harvard.edu/abs/2019AGUFM.H22A..07F, (accessed

Frampton, W.J., Dash, J., Watmough, G., Milton, E.J., 2013. Evaluating the capabilities of Sentinel-2 for quantitative estimation of biophysical variables in vegetation. ISPRS Journal of Photogrammetry and Remote Sensing 82, 83-92. https://doi.org/10.1016/j.isprsjprs.2013.04.007

Galvin, L.F., 1976. Physical-Properties of Irish Peats. Irish J Agr Res 15(2), 207-&, http://www.jstor.org/stable/25555820 . (accessed 09/05/2022)

Gandomi, A., Haider, M., 2015. Beyond the hype: Big data concepts, methods, and analytics. International Journal of Information Management 35(2), 137-144. https://doi.org/10.1016/j.ijinfomgt.2014.10.007

Gao, X., Huete, A.R., Ni, W., Miura, T., 2000. Optical–Biophysical Relationships of Vegetation Spectra without Background Contamination. Remote Sens Environ 74(3), 609-620. https://doi.org/10.1016/S0034-4257(00)00150-4

Gatis, N., Luscombe, D.J., Carless, D., Parry, L.E., Fyfe, R.M., Harrod, T.R., Brazier, R.E., Anderson, K., 2019. Mapping upland peat depth using airborne radiometric and lidar survey data. Geoderma 335, 78-87. https://doi.org/10.1016/j.geoderma.2018.07.041

Gaudig, G., Tanneberger, F., 2019. Peatland Science and Conservation: Contributions of the Greifswald Mire Centre, Germany, Current Trends in Landscape Research. Springer, pp. 611-629. https://doi.org/10.1007/978-3-030-30069-2_28

Gersho, A., 1982. On the structure of vector quantizers. IEEE Transactions on Information Theory 28(2), 157-166. https://doi.org/10.1109/TIT.1982.1056457

Ghebremichael, L.T., Veith, T.L., Hamlett, J.M., 2013. Integrated watershed-and farm-scale modeling framework for targeting critical source areas while maintaining farm economic viability. Journal of environmental management 114, 381-394. https://doi.org/10.1016/j.jenvman.2012.10.034

Giarola, V., 2018. Advanced LiDAR Systems. Design of a LiDAR Platform, https://core.ac.uk/download/pdf/189852747.pdf, (accessed 03/10/22)

Giri, S., Qiu, Z., Prato, T., Luo, B., 2016. An Integrated Approach for Targeting Critical Source Areas to Control Nonpoint Source Pollution in Watersheds. Water Resources Management 30(14), 5087-5100. https://doi.org/10.1007/s11269-016-1470-z

Goyal, M.K., Panchariya, V.K., Sharma, A., Singh, V., 2018. Comparative Assessment of SWAT Model Performance in two Distinct Catchments under Various DEM Scenarios of Varying Resolution, Sources and Resampling Methods. Water Resources Management 32(2), 805-825. https://doi.org/10.1007/s11269-017-1840-1

GPI, 2016. Global Peatlands Initiative. https://www.globalpeatlands.org/, (accessed 05/04/2022)

Graf, M.D., Rochefort, L., 2016. A conceptual framework for ecosystem restoration applied to industrial peatlands. Peatland restoration and ecosystem services: science, policy and practice. Edited by SA Bonn, T. Allott, M. Evans, H. Joosten, and R. Stoneman. Cambridge University Press, Cambridge, UK, 192-212. http://dx.doi.org/10.1017/CBO9781139177788.012

Grand-Clement, E., Anderson, K., Smith, D., Luscombe, D., Gatis, N., Ross, M., Brazier, R.E., 2013. Evaluating ecosystem goods and services after restoration of marginal upland peatlands in South-West England. J Appl Ecol 50(2), 324-334. https://doi.org/10.1111/1365-2664.12039

Griffiths, N.A., Sebestyen, S.D., Oleheiser, K.C., 2019. Variation in peatland porewater chemistry over time and space along a bog to fen gradient. Science of The Total Environment 697, 134152. https://doi.org/10.1016/j.scitotenv.2019.134152

GSI, 2022a. National Bedrock Map 1:100K. https://www.gsi.ie/en-ie/data-and-maps/Pages/Bedrock.aspx#100k, (accessed 01/05/2022)

GSI, 2022b. National Quaternary Sedement Map 1:50K. https://www.gsi.ie/en-ie/data-and-maps/Pages/Quaternary.aspx#Sed, (accessed 02/05/2022)

GSI, 2022c. Quaternary Field Mapping. https://www.gsi.ie/en-ie/programmes-and-projects/geological-mapping/activities/Pages/Quaternary-Field-Mapping.aspx, (accessed 02/05/2022)

GSI, 2022d. Tellus Survey. https://www.gsi.ie/en-ie/programmes-and-projects/tellus/Pages/default.aspx, (accessed 01/05/2022)

Gu, S., Gruau, G., Dupas, R., Rumpel, C., Crème, A., Fovet, O., Gascuel-Odoux, C., Jeanneau, L., Humbert, G., Petitjean, P., 2017. Release of dissolved phosphorus from riparian wetlands: Evidence for complex interactions among hydroclimate variability, topography and soil properties. Science of The Total Environment 598, 421-431. https://doi.org/10.1016/j.scitotenv.2017.04.028

Harris, A., Bryant, R.G., 2009. A multi-scale remote sensing approach for monitoring northern peatland hydrology: Present possibilities and future challenges. Journal of Environmental Management 90(7), 2178-2188. https://doi.org/10.1016/j.jenvman.2007.06.025

Heger, T., Jeschke, J.M., Febria, C., Kollmann, J., Murphy, S., Rochefort, L., Shackelford, N., Temperton, V.M., Higgs, E., 2022. Mapping and assessing the knowledge base of ecological restoration. Restoration Ecology n/a(n/a), e13676. https://doi.org/10.1111/rec.13676

Heiri, O., Lotter, A.F., Lemcke, G., 2001. Loss on ignition as a method for estimating organic and carbonate content in sediments: reproducibility and comparability of results. J Paleolimnol 25(1), 101-110. https://doi.org/10.1023/A:1008119611481

Hepp, G., Zoboli, O., Strenge, E., Zessner, M., 2022. Particulate PhozzyLogic Index for policy makers—an index for a more accurate and transparent identification of critical source areas. Journal of Environmental Management 307, 114514. https://doi.org/10.1016/j.jenvman.2022.114514

Hill, B.H., Jicha, T.M., Lehto, L.L.P., Elonen, C.M., Sebestyen, S.D., Kolka, R.K., 2016. Comparisons of soil nitrogen mass balances for an ombrotrophic bog and a minerotrophic fen in northern Minnesota. Science of The Total

Environment 550, 880-892. https://doi.org/10.1016/j.scitotenv.2016.01.178

Hinckley, B.R., Etheridge, J.R., Peralta, A.L., 2019. Wetland Conditions Differentially Influence Nitrogen Processing within Waterfowl Impoundments. Wetlands. https://doi.org/10.1007/s13157-019-01246-8

Hird, J.N., DeLancey, E.R., McDermid, G.J., Kariyeva, J., 2017. Google Earth Engine, Open-Access Satellite Data, and Machine Learning in Support of Large-Area Probabilistic Wetland Mapping. Remote Sens-Basel 9(12). https://doi.org/10.3390/rs9121315

Holden, J., 2004. Hydrological connectivity of soil pipes determined by ground-penetrating radar tracer detection. Earth Surf Proc Land 29(4), 437-442, (accessed

Hua, L., Li, W., Zhai, L., Yen, H., Lei, Q., Liu, H., Ren, T., Xia, Y., Zhang, F., Fan, X., 2019. An innovative approach to identifying agricultural pollution sources and loads by using nutrient export coefficients in watershed modeling. J Hydrol 571, 322-331. https://doi.org/10.1016/j.jhydrol.2019.01.043

Huete, A.R., 2004. Remote Sensing for Environmental Monitoring. In: J.F. Artiola, I.L. Pepper, M.L. Brusseau (Eds.), Environmental Monitoring and Characterization. Academic Press, Burlington, pp. 183-206. https://doi.org/10.1016/B978-012064477-3/50013-8

Husen, E., Salma, S., Agus, F., 2014. Peat emission control by groundwater management and soil amendments: evidence from laboratory experiments. Mitigation and Adaptation Strategies for Global Change 19(6), 821-829. https://doi.org/10.1007/s11027-013-9526-3

Huth, V., Günther, A., Bartel, A., Gutekunst, C., Heinze, S., Hofer, B., Jacobs, O., Koebsch, F., Rosinski, E., Tonn, C., Ullrich, K., Jurasinski, G., 2022. The climate benefits of topsoil removal and Sphagnum introduction in raised bog restoration. Restoration Ecology 30(1), e13490. https://doi.org/10.1111/rec.13490

IAEA, 2003. Guidelines for Radioelement Mapping Using Gamma Ray Spectrometry Data. INTERNATIONAL ATOMIC ENERGY AGENCY, Vienna, https://www.iaea.org/publications/6746/guidelines-for-radioelement-mapping-using-gamma-ray-spectrometry-data, (accessed 16/04/2022)

IPCC, 2021. AR6 Climate change 2021: the physical science basis. https://www.ipcc.ch/report/ar6/wg1/#FullReport, (accessed 03/10/22)

Jeanneau, L., Jaffrézic, A., Pierson-Wickmann, A.-C., Gruau, G., Lambert, T., Petitjean, P., 2014. Constraints on the sources and production mechanisms of dissolved organic matter in soils from molecular biomarkers. Vadose Zone J 13(7). https://doi.org/10.2136/vzj2014.02.0015

Jiang, X., Hou, X., Zhou, X., Xin, X., Wright, A., Jia, Z., 2015. pH regulates key players of nitrification in paddy soils. Soil Biology and Biochemistry 81, 9-16. https://doi.org/10.1016/j.soilbio.2014.10.025

Joosten, H., Clarke, D., 2002. Wise use of mires and peatlands. International Mire Conservation Group and International Peat Society 304, http://www.imcg.net/media/download_gallery/books/wump_wise_use_of_mires_and_peatlands_book.pdf, (accessed 03/10/22)

Kalacska, M., Arroyo-Mora, J.P., Soffer, R.J., Roulet, N.T., Moore, T.R., Humphreys, E., Leblanc, G., Lucanus, O., Inamdar, D., 2018. Estimating Peatland water table depth and net ecosystem exchange: A comparison between satellite and airborne imagery. Remote Sens-Basel 10(5), 687. https://doi.org/10.3390/rs10050687

Kamal, S., Grodzińska-Jurczak, M., Brown, G., 2015. Conservation on private land: a review of global strategies with a proposed classification system. Journal of Environmental Planning and Management 58(4), 576-597. https://doi.org/10.1080/09640568.2013.875463

Kareksela, S., Haapalehto, T., Juutinen, R., Matilainen, R., Tahvanainen, T., Kotiaho, J.S., 2015. Fighting carbon loss of degraded peatlands by jump-starting ecosystem functioning with ecological restoration. Science of The Total Environment 537, 268-276. https://doi.org/10.1016/j.scitotenv.2015.07.094

Karjalainen, S.M., Heikkinen, K., Ihme, R., Kløve, B., 2016. Long-term purification efficiency of a wetland constructed to treat runoff from peat extraction. Journal of Environmental Science and Health, Part A 51(5), 393-402. https://doi.org/10.1080/10934529.2015.1120519

Karpatne, A., Ebert-Uphoff, I., Ravela, S., Babaie, H.A., Kumar, V., 2019. Machine Learning for the Geosciences: Challenges and Opportunities. Ieee T Knowl Data En 31(8), 1544-1554. https://doi.org/10.1109/TKDE.2018.2861006

Kasak, K., Espenberg, M., Anthony, T.L., Tringe, S.G., Valach, A.C., Hemes, K.S., Silver, W.L., Mander, Ü., Kill, K., McNicol, G., Szutu, D., Verfaillie, J., Baldocchi, D.D., 2021. Restoring wetlands on intensive agricultural lands modifies nitrogen cycling microbial communities and reduces N2O production potential. Journal of Environmental Management 299, 113562. https://doi.org/10.1016/j.jenvman.2021.113562

Kasischke, E.S., Bourgeau-Chavez, L.L., Rober, A.R., Wyatt, K.H., Waddington, J.M., Turetsky, M.R., 2009. Effects of soil moisture and water depth on ERS SAR backscatter measurements from an Alaskan wetland complex. Remote Sens Environ 113(9), 1868-1873. https://doi.org/10.1016/j.rse.2009.04.006

Kaufman, L., 2005. Finding groups in data an introduction to cluster analysis. Hoboken, N.J. : Wiley-Interscience, Hoboken, N.J. https://doi.org/10.1002/9780470316801

Keaney, A., McKinley, J., Graham, C., Robinson, M., Ruffell, A., 2013. Spatial statistics to estimate peat thickness using airborne radiometric data. Spat Stat-Neth 5, 3-24. https://doi.org/10.1016/j.spasta.2013.05.003

Keaney, A., McKinley, J., Ruffell, A., Robinson, M., Graham, C., Hodgson, J., Ture, M., 2012. Ground-truthing Airborne Geophysical Data for Carbon Stock Monitoring. EAGE/GRSG Remote Sensing Workshop. https://doi.org/10.3997/2214-4609.20143284

Kiang, M.Y., 2001. Extending the Kohonen self-organizing map networks for clustering analysis. Comput Stat Data An 38(2), 161-180. https://doi.org/10.1016/S0167-9473(01)00040-8

Kiely, G., Carton, O., 2010. SoilC - Measurement and Modelling of Soil Carbon Stocks and Stock Changes in Irish Soils, https://www.epa.ie/publications/research/land-use-soils-and-transport/soilc---measurement-and-modelling-of-soil-carbon-stocks-and-stock-changes-in-irish-soils.php, (accessed 09/05/2022)

Kim, H., Ogram, A., Bae, H.-S., 2017. Nitrification, anammox and denitrification along a nutrient gradient in the Florida Everglades. Wetlands 37(2), 391-399. https://doi.org/10.1007/s13157-016-0857-1

Kohonen, T., 2013. Essentials of the self-organizing map. Neural Networks 37, 52-65. https://doi.org/10.1016/j.neunet.2012.09.018

Komorowski, M., Marshall, D.C., Salciccioli, J.D., Crutain, Y., 2016. Exploratory Data Analysis. In: M.I.T.C. Data (Ed.), Secondary Analysis of Electronic Health Records. Springer International Publishing, Cham, pp. 185-203. https://doi.org/10.1007/978-3-319-43742-2_15

Koskinen, M., Tahvanainen, T., Sarkkola, S., Menberu, M.W., Laurén, A., Sallantaus, T., Marttila, H., Ronkanen, A.-K., Parviainen, M., Tolvanen, A., Koivusalo, H., Nieminen, M., 2017. Restoration of nutrient-rich forestry-drained peatlands poses a risk for high exports of dissolved organic carbon, nitrogen, and phosphorus. Science of The Total Environment 586, 858-869. https://doi.org/10.1016/j.scitotenv.2017.02.065

Kosztra, B., Büttner, G., Hazeu, G., Arnold, S., 2017. Updated CLC illustrated nomenclature guidelines, European Topic Centre on Urban, land and soil systems (ETC/ULS). https://land.copernicus.eu/user-corner/technical-library/corine-land-cover-nomenclature-guidelines/docs/pdf/CLC2018_Nomenclature_illustrated_guide_20190510.pdf, (accessed 09/05/2022)

Kreyling, J., Tanneberger, F., Jansen, F., van der Linden, S., Aggenbach, C., Bluml, V., Couwenberg, J., Emsens, W.J., Joosten, H., Klimkowska, A., Kotowski, W., Kozub, L., Lennartz, B., Liczner, Y., Liu, H., Michaelis, D., Oehmke, C., Parakenings, K., Pleyl, E., Poyda, A., Raabe, S., Rohl, M., Rucker, K., Schneider, A., Schrautzer, J., Schroder, C., Schug, F., Seeber, E., Thiel, F., Thiele, S., Tiemeyer, B., Timmermann, T., Urich, T., van Diggelen, R., Vegelin, K., Verbruggen, E., Wilmking, M., Wrage-Monnig, N., Wolejko, L., Zak, D., Jurasinski, G., 2021. Rewetting does not return drained fen peatlands to their old selves. Nat Commun 12(1). https://doi.org/10.1038/s41467-021-25619-y

Kumar, R., McInnes, R., Everard, M., Gardner, R., Kulindwa, K., Wittmer, H., Infante Mata, D., 2017. Integrating multiple wetland values into decision-making, Ramsar Convention Secretariat, Gland, https://capitalscoalition.org/integrating-multiple-wetland-values-into-decision-making/, (accessed 03/10/22)

Lee, S., Yeo, I.Y., Lang, M.W., McCarty, G.W., Sadeghi, A.M., Sharifi, A., Jin, H., Liu, Y., 2019. Improving the catchment scale wetland modeling using remotely sensed data. Environmental Modelling & Software 122, 104069. https://doi.org/10.1016/j.envsoft.2017.11.001

Lees, K.J., Quaife, T., Artz, R.R.E., Khomik, M., Clark, J.M., 2018. Potential for using remote sensing to estimate carbon fluxes across northern peatlands – A review. Science of The Total Environment 615, 857-874. https://doi.org/10.1016/j.scitotenv.2017.09.103

Lele, S., 2017. Sustainable Development Goal 6: watering down justice concerns. Wiley Interdisciplinary Reviews: Water 4(4), n/a-n/a. 10.1002/wat2.1224

Liu, H., Rezanezhad, F., Lennartz, B., 2022. Impact of land management on available water capacity and water storage of peatlands. Geoderma 406, 115521. https://doi.org/10.1016/j.geoderma.2021.115521

Liu, H.Q., Huete, A., 1995. A feedback based modification of the NDVI to minimize canopy background and atmospheric noise. Ieee T Geosci Remote 33(2), 457-465. https://doi.org/10.1109/TGRS.1995.8746027

Lourenco, M., Fitchett, J.M., Woodborne, S., 2022. Peat definitions: A critical review. Progress in Physical Geography: Earth and Environment, 03091333221118353. https://doi.org/10.1177/03091333221118353

Lundin, L., Nilsson, T., Jordan, S., Lode, E., Strömgren, M., 2017. Impacts of rewetting on peat, hydrology and water chemical composition over 15 years in two finished peat extraction areas in Sweden. Wetlands Ecology and Management 25(4), 405-419. https://doi.org/10.1007/s11273-016-9524-9

Luo, L., Ye, H., Zhang, D., Gu, J.-D., Deng, O., 2021. The dynamics of phosphorus fractions and the factors driving phosphorus cycle in Zoige Plateau peatland soil. Chemosphere 278, 130501. https://doi.org/10.1016/j.chemosphere.2021.130501

Macek, C.L., Hale, R.L., Baxter, C.V., 2020. Dry Wetlands: Nutrient Dynamics in Ephemeral Constructed Stormwater Wetlands. Environmental Management 65(1), 32-45. https://doi.org/10.1007/s00267-019-01227-x

Mackin, F., Barr, A., Rath, P., Eakin, M., Ryan, J., Jeffrey, R. & Fernandez Valverde, F., 2017. Irish Wildlife Manual No. 99: Best practice in raised bog restoration in Ireland, https://www.npws.ie/sites/default/files/publications/pdf/IWM99_RB_Restoration_Best%20Practice%20Guidance.pdf, (accessed 20/08/2022)

Macrae, M.L., Devito, K.J., Strack, M., Waddington, J.M., 2013. Effect of water table drawdown on peatland nutrient dynamics: implications for climate change. Biogeochemistry 112(1), 661-676. https://doi.org/10.1007/s10533-012-9730-3

Maduako, I.N., Ndukwu, R.I., Ifeanyichukwu, C., Igbokwe, O., 2017. Multi-Index Soil Moisture Estimation from Satellite Earth Observations: Comparative Evaluation of the Topographic Wetness Index (TWI), the Temperature Vegetation Dryness Index (TVDI) and the Improved TVDI (iTVDI). J Indian Soc Remote 45(4), 631-642. 10.1007/s12524-016-0635-9

Mandal, D., Hosseini, M., McNairn, H., Kumar, V., Bhattacharya, A., Rao, Y.S., Mitchell, S., Robertson, L.D., Davidson, A., Dabrowska-Zielinska, K., 2019. An investigation of inversion methodologies to retrieve the leaf area index of corn from C-band SAR data. International Journal of Applied Earth Observation and Geoinformation 82, 101893. https://doi.org/10.1016/j.jag.2019.06.003

Márquez Molina, J.J., Sainato, C.M., Urricariet, A.S., Losinno, B.N., Heredia, O.S., 2014. Bulk electrical conductivity as an indicator of spatial distribution of nitrogen and phosphorous at feedlots. Journal of Applied Geophysics 111, 156-172. https://doi.org/10.1016/j.jappgeo.2014.10.002

Marsh, I., Brown, C., 2009. Neural network classification of multibeam backscatter and bathymetry data from Stanton Bank (Area IV). Appl Acoust 70(10), 1269-1276. https://doi.org/10.1016/j.apacoust.2008.07.012

Martelet, G., Truffert, C., Tourliere, B., Ledru, P., Perrin, J., 2006. Classifying airborne radiometry data with Agglomerative Hierarchical Clustering: A tool for geological mapping in context of rainforest (French Guiana). International Journal of Applied Earth Observation and Geoinformation 8(3), 208-223. https://doi.org/10.1016/j.jag.2005.09.003

McBratney, A.B., Santos, M.L.M., Minasny, B., 2003. On digital soil mapping. Geoderma 117(1-2), 3-52. https://doi.org/10.1016/S0016-7061(03)00223-4

McLachlan, P., Chambers, J.E., Uhlemann, S.S., Binley, A., 2017. Geophysical characterisation of the groundwater–surface water interface. Advances in water resources 109, 302-319. https://doi.org/10.1016/j.advwatres.2017.09.016

Menberu, M.W., Marttila, H., Tahvanainen, T., Kotiaho, J.S., Hokkanen, R., Kløve, B., Ronkanen, A.K., 2017. Changes in Pore Water Quality After Peatland Restoration: Assessment of a Large-Scale, Replicated Before-After-Control-Impact Study in Finland. Water Resources Research 53(10), 8327-8343. https://doi.org/10.1002/2017WR020630

Menberu, M.W., Tahvanainen, T., Marttila, H., Irannezhad, M., Ronkanen, A.K., Penttinen, J., Kløve, B., 2016. Water-table-dependent hydrological changes following peatland forestry drainage and restoration: Analysis of restoration success. Water Resources Research 52(5), 3742-3760. https://doi.org/10.1002/2015WR018578

Merchant, M.A., Adams, J.R., Berg, A.A., Baltzer, J.L., Quinton, W.L., Chasmer, L.E., 2017. Contributions of C-Band SAR Data and Polarimetric Decompositions to Subarctic Boreal Peatland Mapping. Ieee Journal of Selected Topics in Applied Earth Observations and Remote Sensing 10(4), 1467-1482. https://doi.org/10.1109/JSTARS.2016.2621043

Met Eireann, 2018. Summer 2018 Analysis. https://www.met.ie/summer-2018-analysis, (accessed 19/09/2022)

Millard, K., Richardson, M., 2018. Quantifying the relative contributions of vegetation and soil moisture conditions to polarimetric C-Band SAR response in a temperate peatland. Remote Sens Environ 206, 123-138. https://doi.org/10.1016/j.rse.2017.12.011

Minasny, B., Berglund, O., Connolly, J., Hedley, C., de Vries, F., Gimona, A., Kempen, B., Kidd, D., Lilja, H., Malone, B., McBratney, A., Roudier, P., O'Rourke, S., Rudiyanto, Padarian, J., Poggio, L., ten Caten, A., Thompson, D., Tuve, C., Widyatmanti, W., 2019. Digital mapping of peatlands - A critical review. Earth-Sci Rev 196. https://doi.org/10.1016/j.earscirev.2019.05.014

Minty, B.R.S., 1997. Fundamentals of airborne gamma-ray spectrometry. AGSO Journal of Australian Geology and Geophysics 17(2), 39-50, http://inis.iaea.org/search/search.aspx?orig_q=RN:28049082, (accessed 09/05/2022)

Mockler, E., M. , Deakin, J., Archbold, M., Daly, D., Bruen, M., 2016. Nutrient load apportionment to support the identification of appropriate water framework directive measures. Biology and Environment: Proceedings of the Royal Irish Academy 116B(3), 245-263. https://doi.org/10.3318/bioe.2016.22

Møller, M.F., 1993. A scaled conjugate gradient algorithm for fast supervised learning. Neural Networks 6(4), 525-533. https://doi.org/10.1016/S0893-6080(05)80056-5

Monteverde, S., Healy, M.G., O'Leary, D., Daly, E., Callery, O., 2022. Management and rehabilitation of peatlands: The role of water chemistry, hydrology, policy, and emerging monitoring methods to ensure informed decision making. Ecological Informatics 69, 101638. https://doi.org/10.1016/j.ecoinf.2022.101638

Moomaw, W.R., Chmura, G.L., Davies, G.T., Finlayson, C.M., Middleton, B.A., Natali, S.M., Perry, J.E., Roulet, N., Sutton-Grier, A.E., 2018. Wetlands In a Changing Climate: Science, Policy and Management. Wetlands 38(2), 183-205. https://doi.org/10.1007/s13157-018-1023-8

Moore, P.A., Pypker, T.G., Waddington, J.M., 2013. Effect of long-term water table manipulation on peatland evapotranspiration. Agricultural and Forest Meteorology 178-179(C), 106-119. https://doi.org/10.1016/j.agrformet.2013.04.013

Morison, M.Q., Macrae, M.L., Petrone, R.M., Fishback, L., 2018. Climate-induced changes in nutrient transformations across landscape units in a thermokarst subarctic peatland. Arctic, Antarctic, and Alpine Research 50(1). https://doi.org/10.1080/15230430.2018.1519366

Munir, T.M., Khadka, B., Xu, B., Strack, M., 2017. Mineral nitrogen and phosphorus pools affected by water table lowering and warming in a boreal forested peatland. Ecohydrology 10(8), e1893. https://doi.org/10.1002/eco.1893

Mustaffa, A.A., Mukhtar, A.N., Rasib, A.W., Suhandri, H.F., Bukari, S.M., 2020. Mapping of Peat Soil Physical Properties by Using Drone- Based Multispectral Vegetation Imagery. IOP Conference Series: Earth and Environmental Science 498(1), 012021. http://dx.doi.org/10.1088/1755-1315/498/1/012021

Negassa, W., Baum, C., Schlichting, A., Müller, J., Leinweber, P., Rezanezhad, F., Moore, T., Zak, D., 2019. Small-Scale Spatial Variability of Soil Chemical and Biochemical Properties in a Rewetted Degraded Peatland. Frontiers in Environmental Science 7, 116. https://doi.org/10.3389/fenvs.2019.00116

Niculescu, S., Lardeux, C., Grigoras, I., Hanganu, J., David, L., 2016. Synergy between LiDAR, RADARSAT-2, and Spot-5 images for the detection and mapping of wetland vegetation in the Danube Delta. IEEE Journal of Selected Topics in Applied Earth Observations and Remote Sensing 9(8), 3651-3666. http://dx.doi.org/10.1109/JSTARS.2016.2545242

Nieminen, M., Sarkkola, S., Tolvanen, A., Tervahauta, A., Saarimaa, M., Sallantaus, T., 2020. Water quality management dilemma: Increased nutrient, carbon, and heavy metal exports from forestry-drained peatlands restored for use as wetland buffer areas. Forest Ecology and Management 465, 118089. https://doi.org/10.1016/j.foreco.2020.118089

Novresiandi, D.A., Nagasawa, R., 2017. Polarimetric synthetic aperture radar application for tropical peatlands classification: a case study in Siak River Transect, Riau Province, Indonesia. J Appl Remote Sens 11. https://doi.org/10.1117/1.JRS.11.016040

O'Leary, D., Brown, C., Daly, E., 2022. Digital soil mapping of peatland using airborne radiometric data and supervised machine learning – implication for the assessment of carbon stock. Geoderma 428. https://doi.org/10.1016/j.geoderma.2022.116086

Ortigara, A.R.C., Kay, M., Uhlenbrook, S., 2018. A Review of the SDG 6 Synthesis Report 2018 from an Education, Training, and Research Perspective. Water 10(10), 1353. https://doi.org/10.3390/w10101353

Overbeek, C.C., Harpenslager, S.F., van Zuidam, J.P., van Loon, E.E., Lamers, L.P.M., Soons, M.B., Admiraal, W., Verhoeven, J.T.A., Smolders, A.J.P., Roelofs, J.G.M., van der Geest, H.G., 2019. Drivers of Vegetation Development, Biomass Production and the Initiation of Peat Formation in a Newly Constructed Wetland. Ecosystems. https://doi.org/10.1007/s10021-019-00454-x

Page, S.E., Baird, A.J., 2016. Peatlands and Global Change: Response and Resilience. Annu Rev Env Resour 41, 35-57. https://doi.org/10.1146/annurev-environ-110615-085520

Paine, J.G., 2003. Determining salinization extent, identifying salinity sources, and estimating chloride mass using surface, borehole, and airborne electromagnetic induction methods. Water Resources Research 39(3). https://doi.org/10.1029/2001wr000710

Pant, H.K., 2020. Estimation of Internal Loading of Phosphorus in Freshwater Wetlands. Current Pollution Reports 6(1), 28-35. https://doi.org/10.1007/s40726-020-00136-6

Parsekian, A.D., 2018. Inverse Methods To Improve Accuracy of Water Content Estimates from Multi-offset GprParsekian: Improved Accuracy of Water Content from Gpr. Journal of Environmental and Engineering Geophysics 23(3), 349-361. https://doi.org/10.2113/JEEG23.3.349

Price, J., Heathwaite, A., Baird, A., 2003. Hydrological processes in abandoned and restored peatlands: an overview of management approaches. Wetlands Ecology and Management 11(1-2), 65-83. https://doi.org/10.1023/A:1022046409485

Priori, S., Bianconi, N., Costantini, E.A.C., 2014. Can γ-radiometrics predict soil textural data and stoniness in different parent materials? A comparison of two machine-learning methods. Geoderma 226-227, 354-364. https://doi.org/10.1016/j.geoderma.2014.03.012

Purre, A.-H., Ilomets, M., 2018. Relationships between bryophyte production and substrate properties in restored milled peatlands. Restoration Ecology 26(5), 858-864. https://doi.org/10.1111/rec.12656

Qiu, C.J., Zhu, D., Ciais, P., Guenet, B., Peng, S.S., 2020. The role of northern peatlands in the global carbon cycle for the 21st century. Global Ecol Biogeogr 29(5), 956-973. https://doi.org/10.1111/geb.13081

Ramsar, 2002. Wetlands: water, life, and culture, Report of 8th meeting of the conference of the contracting parties to the Convention on Wetlands (Ramsar, Iran, 1971), Spain, pp. 18-26, https://wetland-tw.tcd.gov.tw/upload/file/20190528160115944.pdf, (accessed 03/10/22)

Ramsar, 2006. Resolutions VIII. 3, VIII. 17, https://www.ramsar.org/document/resolution-viii17-guidelines-for-global-action-on-peatlands, (accessed 03/10/22)

Ramsar, 2012. Resolution XI.8 Annex 2: strategic framework and guidelines for the future development of the List of Wetlands of International Importance of the Convention on Wetlands (Ramsar, Iran, 1971) – 2012 revision. Ramsar Convention, https://rsis.ramsar.org/RISapp/StatDoc/strategic_framework_en.pdf, (accessed 03/10/22)

Ramsar, 2015a. Call to action to ensure and protect the water requirements of wetlands for the present and the future. in Resolution XII.12 12th Meeting of the Conference of the Parties to the Convention on Wetlands (Ramsar), https://www.informea.org/en/decision/resolution-xii12-call-action-ensure-and-protect-water-requirements-wetlands-present-and, (accessed 03/10/22)

Ramsar, 2015b. Resolution XII. 2 The 4th Strategic Plan 2016-2024. Punta del Este (Uruguay): IUCN, https://www.informea.org/en/decision/resolution-xii2-ramsar-strategic-plan-2016-2024, (accessed 03/10/22)

Ramsar, 2018. Resolution XIII.13, Restoration of degraded peatlands to mitigate and adapt to climate change and enhance biodiversity and disaster risk. "Wetlands for a Sustainable Urban Future" Dubai, United Arab Emirates, 21-29 October 2018 13th Meeting of the Conference of the Contracting Parties to the Ramsar Convention on Wetlands https://redd.unfccc.int/uploads/2_230_xiii.13_peatland_restoration_e.pdf, (accessed 03/10/22)

Räsänen, A., Tolvanen, A., Kareksela, S., 2022. Monitoring peatland water table depth with optical and radar satellite imagery. International Journal of Applied Earth Observation and Geoinformation 112, 102866. https://doi.org/10.1016/j.jag.2022.102866

Ratcliffe, J., Payne, R.J., Sloan, T., Smith, B., Waldron, S., Mauquoy, D., Newton, A., Anderson, A., Henderson, A., Andersen, R., 2018. Holocene carbon accumulation in the peatlands of northern Scotland. http://dx.doi.org/10.19189/MaP.2018.OMB.347

Rawlins, B.G., Lark, R.M., Webster, R., 2007. Understanding airborne radiometric survey signals across part of eastern England. Earth Surf Proc Land 32(10), 1503-1515. https://doi.org/10.1002/esp.1468

Reaney, S.M., Mackay, E.B., Haygarth, P.M., Fisher, M., Molineux, A., Potts, M., Benskin, C.M.H., 2019. Identifying critical source areas using multiple methods for effective diffuse pollution mitigation. Journal of Environmental Management 250, 109366. https://doi.org/10.1016/j.jenvman.2019.109366

Rebelo, L.-M., Finlayson, M., Nagabhatla, N., 2008. Remote Sensing and GIS for Wetland Inventory, Mapping and Change Analysis. Journal of environmental management 90, 2144-2153. https://doi.org/10.1016/j.jenvman.2007.06.027

Reed, M., Bonn, A., Evans, C., Glenk, K., Hansjürgens, B., 2014. Assessing and valuing peatland ecosystem services for sustainable management. Ecosystem Services 9. https://doi.org/10.1016/j.ecoser.2014.04.007

Reinhardt, N., Herrmann, L., 2019. Gamma-ray spectrometry as versatile tool in soil science: A critical review. J Plant Nutr Soil Sc 182(1), 9-27. https://doi.org/10.1002/jpln.201700447

Renou-Wilson, F., Ireland. Environmental Protection, A., University College, D., Programme, E.S., 2011. BOGLAND: sustainable management of peatlands in Ireland. 1840954000;9781840954005;, Environmental Protection Agency, Johnstown Castle, Co. Wexford, https://www.epa.ie/publications/research/land-use-soils-and-transport/bogland-sustainable-management-of-peatlands-in-ireland-final-report.php, (accessed 03/10/22)

Renou-Wilson, F., Moser, G., Fallon, D., Farrell, C.A., Müller, C., Wilson, D., 2019. Rewetting degraded peatlands for climate and biodiversity benefits: Results from two raised bogs. Ecological Engineering 127, 547-560. https://doi.org/10.1016/j.ecoleng.2018.02.014

Renou-Wilson, F., Farrell, E.P., 2007. Phosphorus in surface runoff and soil water following fertilization of afforested cutaway peatlands. Boreal Environment Research 12, 693-709, https://helda.helsinki.fi/bitstream/handle/10138/235559/ber12-6-693.pdf?isAllowed=y&sequence=1, (accessed 03/10/22)

Reverey, F., Grossart, H.-P., Premke, K., Lischeid, G., 2016. Carbon and nutrient cycling in kettle hole sediments depending on hydrological dynamics: a review. Hydrobiologia 775(1), 1-20. https://doi.org/10.1007/s10750-016-2715-9

Rixen, T., Baum, A., Wit, F., Samiaji, J., 2016. Carbon Leaching from Tropical Peat Soils and Consequences for Carbon Balances. Frontiers in Earth Science 4(74). https://doi.org/10.3389/feart.2016.00074

Saarimaa, M., Aapala, K., Tuominen, S., Karhu, J., Parkkari, M., Tolvanen, A., 2019. Predicting hotspots for threatened plant species in boreal peatlands.

Biodiversity and Conservation 28(5), 1173-1204. https://doi.org/10.1007/s10531-019-01717-8

Salomaa, A., Paloniemi, R., Ekroos, A., 2018. The case of conflicting Finnish peatland management–Skewed representation of nature, participation and policy instruments. Journal of environmental management 223, 694-702. https://doi.org/10.1016/j.jenvman.2018.06.048

Sapek, A., Sapek, B., Chrzanowski, S., Urbaniak, M., 2009. Nutrient mobilisation and losses related to the groundwater level in low peat soils. International Journal of Environment and Pollution 37(4), 398-408. https://doi.org/10.1504/IJEP.2009.026057

Scheltinga, D., Heydon, L., 2005. Report on the Condition of Estuarine, Coastal and Marine Resources of the Burdekin Dry Tropics Region. https://www.researchgate.net/publication/236771393_Report_on_the_Condition_of_Estuarine_Coastal_and_Marine_Resources_of_the_Burdekin_Dry_Tropics_Region, (accessed 03/10/22)

Schouten, M.G.C., Netherlands, S., Geological Survey of, I., Ireland. Heritage, S., 2002. Conservation and restoration of raised bogs: geological, hydrological and ecological studies. 9780755715596;0755715594;, Dúchas -The Heritage Service of the Department of the Environment and Local Government, Dublin;Netherlands;, https://research.wur.nl/en/publications/conservation-and-restoration-of-raised-bogs-geological-hydrologic, (accessed 03/10/22)

Schulte, M.L., McLaughlin, D.L., Wurster, F.C., Balentine, K., Speiran, G.K., Aust, W.M., Stewart, R.D., Varner, J.M., Jones, C.N., 2019. Linking ecosystem function and hydrologic regime to inform restoration of a forested peatland. Journal of Environmental Management 233, 342-351. https://doi.org/10.1016/j.jenvman.2018.12.042

Searchinger, T., James, O., Dumas, P., 2022. Europe's Land Future? Opportunities to use Europes land to fight climate change and improve biodiversity;and why proposed policies could undermine both, https://scholar.princeton.edu/tsearchi/publications/europes-land-future, (accessed 09/05/2022)

Sentinel-2, Sentinel-2. https://sentinel.esa.int/web/sentinel/missions/sentinel-2, (accessed 18/08/2022)

Sentinel, 2022. Sentinel Overview. https://sentinel.esa.int/web/sentinel/missions, (accessed 18/08/2022)

SGL, 2017. Fixed-Wing High-Resolution Aeromagnetic, Gamma-ray Spectrometric and Frequency-Domain Electromagnetic Survey. In: G.S.o. Ireland (Ed.), https://secure.dccae.gov.ie/GSI_DOWNLOAD/Tellus/SGL_Tech_Report_831A2_000.pdf, (accessed 09/05/2022)

Shen, C.P., 2018. A Transdisciplinary Review of Deep Learning Research and Its Relevance for Water Resources Scientists. Water Resources Research 54(11), 8558-8593. https://doi.org/10.1029/2018WR022643

Shore, M., Jordan, P., Mellander, P.E., Kelly-Quinn, M., Wall, D.P., Murphy, P.N.C., Melland, A.R., 2014. Evaluating the critical source area concept of phosphorus loss from soils to water-bodies in agricultural catchments. Science of The Total Environment 490, 405-415. https://doi.org/10.1016/j.scitotenv.2014.04.122

Siemon, B., Ibs-von Seht, M., Frank, S., 2020. Airborne Electromagnetic and Radiometric Peat Thickness Mapping of a Bog in Northwest Germany

(Ahlen-Falkenberger Moor). Remote Sens-Basel 12(2). https://doi.org/10.3390/rs12020203

Silvestri, S., Christensen, C.W., Lysdahl, A.O.K., Anschütz, H., Pfaffhuber, A.A., Viezzoli, A., 2019a. Peatland Volume Mapping Over Resistive Substrates With Airborne Electromagnetic Technology. Geophysical Research Letters 46(12), 6459-6468. https://doi.org/10.1029/2019GL083025

Silvestri, S., Knight, R., Viezzoli, A., Richardson, C.J., Anshari, G.Z., Dewar, N., Flanagan, N., Comas, X., 2019b. Quantification of Peat Thickness and Stored Carbon at the Landscape Scale in Tropical Peatlands: A Comparison of Airborne Geophysics and an Empirical Topographic Method. Journal of Geophysical Research: Earth Surface 124(12), 3107-3123. https://doi.org/10.1029/2019JF005273

Sola, A.D., Marazzi, L., Flores, M.M., Kominoski, J.S., Gaiser, E.E., 2018. Short-term effects of drying-rewetting and long-term effects of nutrient loading on Periphyton N: P stoichiometry. Water 10(2), 105. https://doi.org/10.3390/w10020105

Stimson, A.G., Allott, T.E.H., Boult, S., Evans, M.G., Pilkington, M., Holland, N., 2017. Water quality impacts of bare peat revegetation with lime and fertiliser application. Applied Geochemistry 85, 97-105. https://doi.org/10.1016/j.apgeochem.2017.09.003

Taghizadeh-Toosi, A., Clough, T., Petersen, S.O., Elsgaard, L., 2020. Nitrous Oxide Dynamics in Agricultural Peat Soil in Response to Availability of Nitrate, Nitrite, and Iron Sulfides. Geomicrobiology Journal 37(1), 76-85, (accessed

Tampuu, T., Praks, J., Uiboupin, R., Kull, A., 2020. Long Term Interferometric Temporal Coherence and DInSAR Phase in Northern Peatlands. Remote Sens-Basel 12(10), 1566, https://www.mdpi.com/2072-4292/12/10/1566, (accessed

Tan, Z.D., Lupascu, M., Wijedasa, L.S., 2021. Paludiculture as a sustainable land use alternative for tropical peatlands: A review. Science of The Total Environment 753, 142111. https://doi.org/10.1016/j.scitotenv.2020.142111

Tanneberger, F., Tegetmeyer, C., Busse, S., Barthelmes, A., Shumka, S., Marine, A.M., Jenderedjian, K., Steiner, G.M., Essl, F., Etzold, J., Mendes, C., Kozulin, A., Frankard, P., Milanovic, D., Ganeva, A., Apostolova, I., Alegro, A., Delipetrou, P., Navratilova, J., Risager, M., Leivits, A., Fosaa, A.M., Tuominen, S., Muller, F., Bakuradze, T., Sommer, M., Christanis, K., Szurdoki, E., Oskarsson, H., Brink, S.H., Connolly, J., Bragazza, L., Martinelli, G., Aleksans, O., Priede, A., Sungaila, D., Melovski, L., Belous, T., Saveljic, D., de Vries, F., Moen, A., Dembek, W., Mateus, J., Hanganu, J., Sirin, A., Markina, A., Napreenko, M., Lazarevic, P., Stanova, V.S., Skoberne, P., Perez, P.H., Pontevedra-Pombal, X., Lonnstad, J., Kuchler, M., Wust-Galley, C., Kirca, S., Mykytiuk, O., Lindsay, R., Joosten, H., 2017. The peatland map of Europe. Mires Peat 19. https://doi.org/10.1111/rec.12865

Tfaily, M.M., Cooper, W.T., Kostka, J.E., Chanton, P.R., Schadt, C.W., Hanson, P.J., Iversen, C.M., Chanton, J.P., 2014. Organic matter transformation in the peat column at Marcell Experimental Forest: Humification and vertical stratification. Journal of Geophysical Research: Biogeosciences 119(4), 661-675. https://doi.org/10.1002/2013jg002492

Tfaily, M.M., Wilson, R.M., Cooper, W.T., Kostka, J.E., Hanson, P., Chanton, J.P., 2018. Vertical Stratification of Peat Pore Water Dissolved Organic Matter Composition in a Peat Bog in Northern Minnesota. Journal of Geophysical

Research: Biogeosciences 123(2), 479-494. https://doi.org/10.1002/2017jg004007

Tian, J., Philpot, W.D., 2015. Relationship between surface soil water content, evaporation rate, and water absorption band depths in SWIR reflectance spectra. Remote Sens Environ 169, 280-289. https://doi.org/10.1016/j.rse.2015.08.007

Tiéga, A., 2011. Ramsar Convention on Wetlands: 40 Years of Biodiversity Conservation and Wise Use. Journal of International Wildlife Law & Policy: The Fortieth Anniversary of the Ramsar Convention on Wetlands 14(3-4), 173-175. https://doi.org/10.1080/13880292.2011.626686

Ting, K.M., 2010. Confusion Matrix. In: C. Sammut, G.I. Webb (Eds.), Encyclopedia of Machine Learning. Springer US, Boston, MA, pp. 209-209. https://doi.org/10.1007/978-0-387-30164-8_157

Treat, C.C., Kleinen, T., Broothaerts, N., Dalton, A.S., Dommain, R., Douglas, T.A., Drexler, J.Z., Finkelstein, S.A., Grosse, G., Hope, G., 2019. Widespread global peatland establishment and persistence over the last 130,000 y. Proceedings of the National Academy of Sciences 116(11), 4822-4827. https://doi.org/10.1073/pnas.1813305116

Tuukkanen, T., Marttila, H., Kløve, B., 2017. Predicting organic matter, nitrogen, and phosphorus concentrations in runoff from peat extraction sites using partial least squares regression. Water Resources Research 53(7), 5860-5876. https://doi.org/10.1002/2017WR020557

UN, 2022. Do you know all 17 SDGs? https://sdgs.un.org/goals, (accessed 24/10/2022)

UNEP, 2019. Resolution adopted by the United Nations Environment Asssembly on 15 March 2019 UNEP/EA.4/Res.16 United Nations Environment Assembly of the United Nations Environment Programme Fourth session, Nairobi, https://wedocs.unep.org/bitstream/handle/20.500.11822/30675/UNEPEA4RES16E.pdf?sequence=1&isAllowed=y, (accessed 03/10/22)

UNEP, 2022. Global Peatlands Assessment – The State of the World's Peatlands: Evidence for action toward the conservation, restoration, and sustainable management of peatlands. Main Report., United Nations Environment Programme, Nairobi, https://wedocs.unep.org/bitstream/handle/20.500.11822/41222/peatland_assessment.pdf?sequence=1&isAllowed=y, (accessed 05/01/2023)

UNFCCC, 2011. Consideration of further commitments for Annex I Parties under the Kyoto Protocol. https://unfccc.int/documents/7085, (accessed 16/08/2022)

Valentine, A., Kalnins, L., 2016. An introduction to learning algorithms and potential applications in geomorphometry and Earth surface dynamics. Earth Surf Dynam 4(2), 445-460. https://doi.org/10.5194/esurf-4-445-2016

van de Riet, B.P., Hefting, M.M., Verhoeven, J.T.A., 2013. Rewetting Drained Peat Meadows: Risks and Benefits in Terms of Nutrient Release and Greenhouse Gas Exchange. Water, Air, & Soil Pollution 224(4), 1440. https://doi.org/10.1007/s11270-013-1440-5

Vitt, D.H., Halsey, L.A., Bauer, I.E., Campbell, C., 2000. Spatial and temporal trends in carbon storage of peatlands of continental western Canada through the Holocene. Canadian Journal of Earth Sciences 37(5), 683-693. https://doi.org/10.1139/e99-097

Vodyanitskii, Y.N., Grebenkin, N.A., Manakhov, D.V., Sashchenko, A.V., Tiuleneva, V.M., 2019. Positive Uranium Anomalies in the Peatlands of Humid Zone: A

Review. Eurasian Soil Sci+ 52(12), 1533-1541. https://doi.org/10.1134/S1064229319120135

Vogel, H.-J., Wollschläger, U., Helming, K., Heinrich, U., Willms, M., Wiesmeier, M., Russell, D., Franko, U., 2019. Assessment of Soil Functions Affected by Soil Management. In: M. Schröter, A. Bonn, S. Klotz, R. Seppelt, C. Baessler (Eds.), Atlas of Ecosystem Services: Drivers, Risks, and Societal Responses. Springer International Publishing, Cham, pp. 77-82. https://doi.org/10.1007/978-3-319-96229-0_13

von Hebel, C., Reynaert, S., Pauly, K., Janssens, P., Piccard, I., Vanderborght, J., van der Kruk, J., Vereecken, H., Garre, S., 2021. Toward high-resolution agronomic soil information and management zones delineated by ground-based electromagnetic induction and aerial drone data. Vadose Zone J 20(4), <Go to ISI>://WOS:000674053400011, (accessed

Wang, H., Richardson, C.J., Ho, M., Flanagan, N., 2016. Drained coastal peatlands: A potential nitrogen source to marine ecosystems under prolonged drought and heavy storm events—A microcosm experiment. Science of The Total Environment 566-567, 621-626. https://doi.org/10.1016/j.scitotenv.2016.04.211

Wang, L., Qu, J.J., 2009. Satellite remote sensing applications for surface soil moisture monitoring: A review. Frontiers of Earth Science in China 3(2), 237-247. https://doi.org/10.1007/s11707-009-0023-7

Watson, S.J., Luck, G.W., Spooner, P.G., Watson, D.M., 2014. Land-use change: incorporating the frequency, sequence, time span, and magnitude of changes into ecological research. Frontiers in Ecology and the Environment 12(4), 241-249. https://doi.org/10.1890/130097

Webster, R., 2007. Digital Soil Mapping: An Introductory Perspective - Edited by P. Lagacherie, A. B. McBratney & M. Voltz. Eur J Soil Sci 58(5), 1217-1218. https://doi.org/10.1111/j.1365-2389.2007.00943_6.x

Wijedasa, L.S., Sloan, S., Michelakis, D.G., Clements, G.R., 2012. Overcoming Limitations with Landsat Imagery for Mapping of Peat Swamp Forests in Sundaland. Remote Sens-Basel 4(9), 2595-2618. https://doi.org/10.3390/rs4092595

Wilson, D., Blain, D., Couwenberg, J., Evans, C.D., Murdiyarso, D., Page, S.E., Renou-Wilson, F., Rieley, J.O., Sirin, A., Strack, M., Tuittila, E.S., 2016. Greenhouse gas emission factors associated with rewetting of organic soils. Mires Peat 17. https://doi.org/10.19189/MaP.2016.OMB.222

Wilson, D., Mackin, F., Tuovinen, J.-P., Moser, G., Farrell, C., Renou-Wilson, F., 2022. Carbon and climate implications of rewetting a raised bog in Ireland. Global Change Biology n/a(n/a). https://doi.org/10.1111/gcb.16359

Wood, M.E., Macrae, M.L., Strack, M., Price, J.S., Osko, T.J., Petrone, R.M., 2016. Spatial variation in nutrient dynamics among five different peatland types in the Alberta oil sands region. Ecohydrology 9(4), 688-699. https://doi.org/10.1002/eco.1667

Worsfold, R.D., Parashar, S.K., Perrott, T., 1986. Depth profiling of peat deposits with impulse radar. Canadian Geotechnical Journal 23(2), 142-154. https://doi.org/10.1139/t86-024

Xing, G., Wang, X., Zhang, Y., Lu, C., Pless, R., Gill, C., 2005. Integrated coverage and connectivity configuration for energy conservation in sensor networks. ACM Trans. Sen. Netw. 1(1), 36–72. https://doi.org/10.1145/1077391.1077394

Xu, J.R., Morris, P.J., Liu, J.G., Holden, J., 2018. PEATMAP: Refining estimates of global peatland distribution based on a meta-analysis. Catena 160, 134-140. https://doi.org/10.1016/j.catena.2017.09.010

Yang, L., Jiang, M., Zou, Y., Qin, L., Chen, Y., 2021. Geographical Distribution of Iron Redox Cycling Bacterial Community in Peatlands: Distinct Assemble Mechanism Across Environmental Gradient. Frontiers in Microbiology 12. https://doi.org/10.3389/fmicb.2021.674411

Yu, Z., Beilman, D.W., Frolking, S., Macdonald, G.M., Roulet, N.T., Camill, P., Charman, D.J., 2011. Peatlands and Their Role in the Global Carbon Cycle. Eos, Transactions American Geophysical Union 92(12), 97-98. https://doi.org/10.1029/2011EO120001

Yu, Z.C., Loisel, J., Brosseau, D.P., Beilman, D.W., Hunt, S.J., 2010. Global peatland dynamics since the Last Glacial Maximum. Geophysical Research Letters 37. https://doi.org/10.1029/2010GL043584

Zajícová, K., Chuman, T., 2019. Application of ground penetrating radar methods in soil studies: A review. Geoderma 343, 116-129. https://doi.org/10.1016/j.geoderma.2019.02.024

Zhang, G.L., Liu, F., Song, X.D., 2017. Recent progress and future prospect of digital soil mapping: A review. J Integr Agr 16(12), 2871-2885. https://doi.org/10.1016/S2095-3119(17)61762-3

Zhao, C., Liu, S., Jiang, Z., Wu, Y., Cui, L., Huang, X., Macreadie, P.I., 2019. Nitrogen purification potential limited by nitrite reduction process in coastal eutrophic wetlands. Science of the total environment 694, 133702. https://doi.org/10.1016/j.scitotenv.2019.133702

Zhu, X., Song, C., Chen, W., Zhang, X., Tao, B., 2018. Effects of Water Regimes on Methane Emissions in Peatland and Gley Marsh. Vadose Zone J 17(1), 180017. https://doi.org/10.2136/vzj2018.01.0017

Živković, T., Disney, K., Moore, T.R., 2017. Variations in nitrogen, phosphorus, and δ 15 N in Sphagnum mosses along a climatic and atmospheric deposition gradient in eastern Canada. Botany 95(8), 829-839. https://doi.org/10.1139/cjb-2016-0314

# Appendix 1 : Quaternary Geology Map for ANN training

The correct selection of training areas, where the presence of peatlands is well known, is vital for a machine learning methodology to be successful. Given three national databases which describe peatland in the study area, the challenge is to select one to use for training of the neural network. As noted, (section 2.3.3), all three databases matched with LOI analysis. The application of a 200m buffer zone is also considered necessary to account for the airborne radiometric footprint to reduce misclassification (section 2.3.4). The final analysis was to determine which database, after the application of a 200m buffer (Figure A 1), had the most overlap with the other databases (Table A 1).

Table A 1: Percentage overlap between databases with 200m buffer and each database without a buffer

| | **Full QGM % Overlap** | **Full CLC18 % Overlap** | **Full ISIS % Overlap** |
|---|---|---|---|
| **QGM (200m buffer)** | 100 | 70.2 | 99.4 |
| **CLC18 (200m buffer)** | 64.7 | 100 | 76.0 |
| **ISIS (200m buffer)** | 83.1 | 67.2 | 100 |

The QGM (with buffer zone) was chosen as it firstly matched with LOI data. Secondly it had the largest overlap with the other peatland extent databases available (Table A 1) meaning that it was limited to areas where all three databases reported peat to be present. Finally, it was also the most conservative in terms of peatland extent (Figure A 1-B), which would focus training to localised areas where peat was likely to be present.

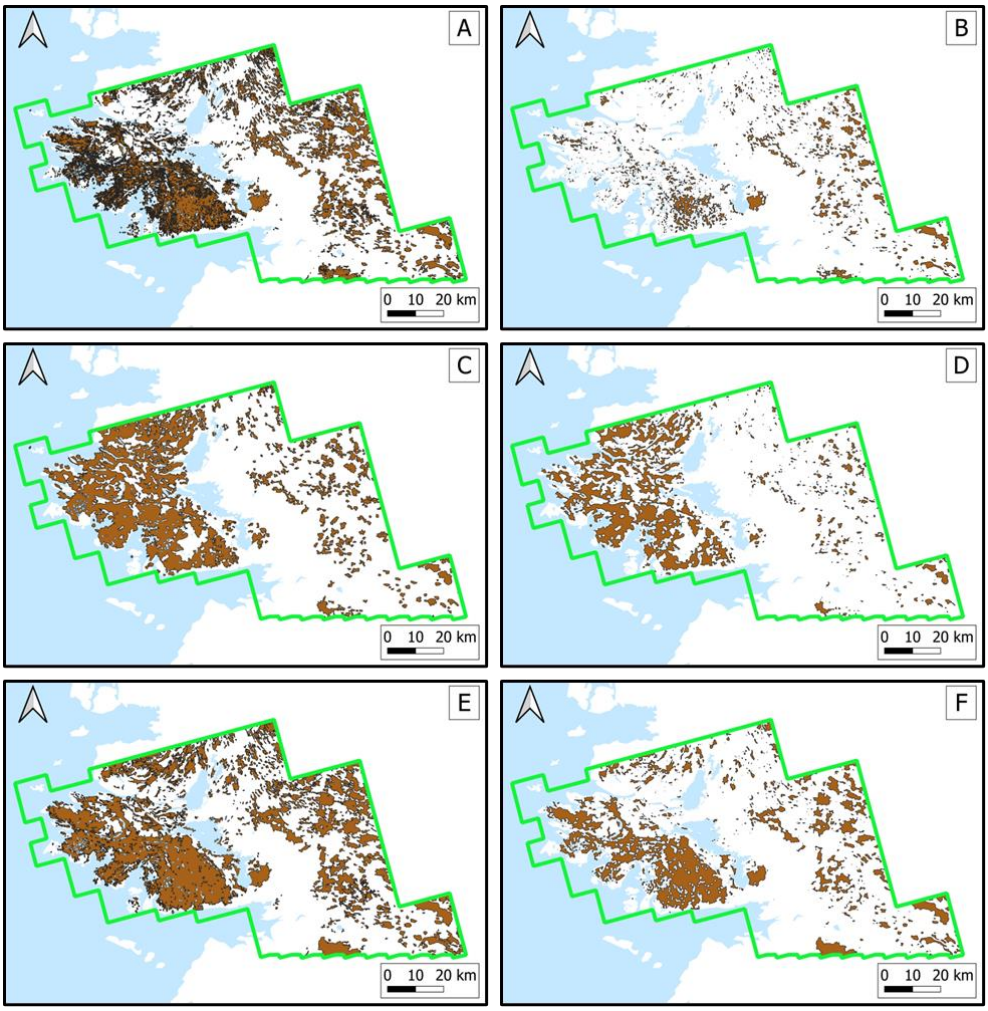


Figure A 1: Existing peatland extent maps within Tellus Block A2 A) QGM, B) QGM with 200m buffer, C) CLC18, D) CLC18 with 200m buffer, E) ISIS, F) ISIS with 200m buffer.

# Appendix 2 : Validation of ANN classification

Validation of local re-classification was performed via aerial imagery within the Garryduff study site with Aerial imagery were taken from Bing Imagery (https://www.bing.com/maps/aerial). Aerial images were used to verify if two highlighted local sites were correctly re-classified as peat, including an updated boundary classification (Figure A 2) and identification of a new peatland site (Figure A 3). Peat was identified on aerial imagery from bare exposure, colour changes and differences to surrounding areas, similar to the main Garryduff peatland.

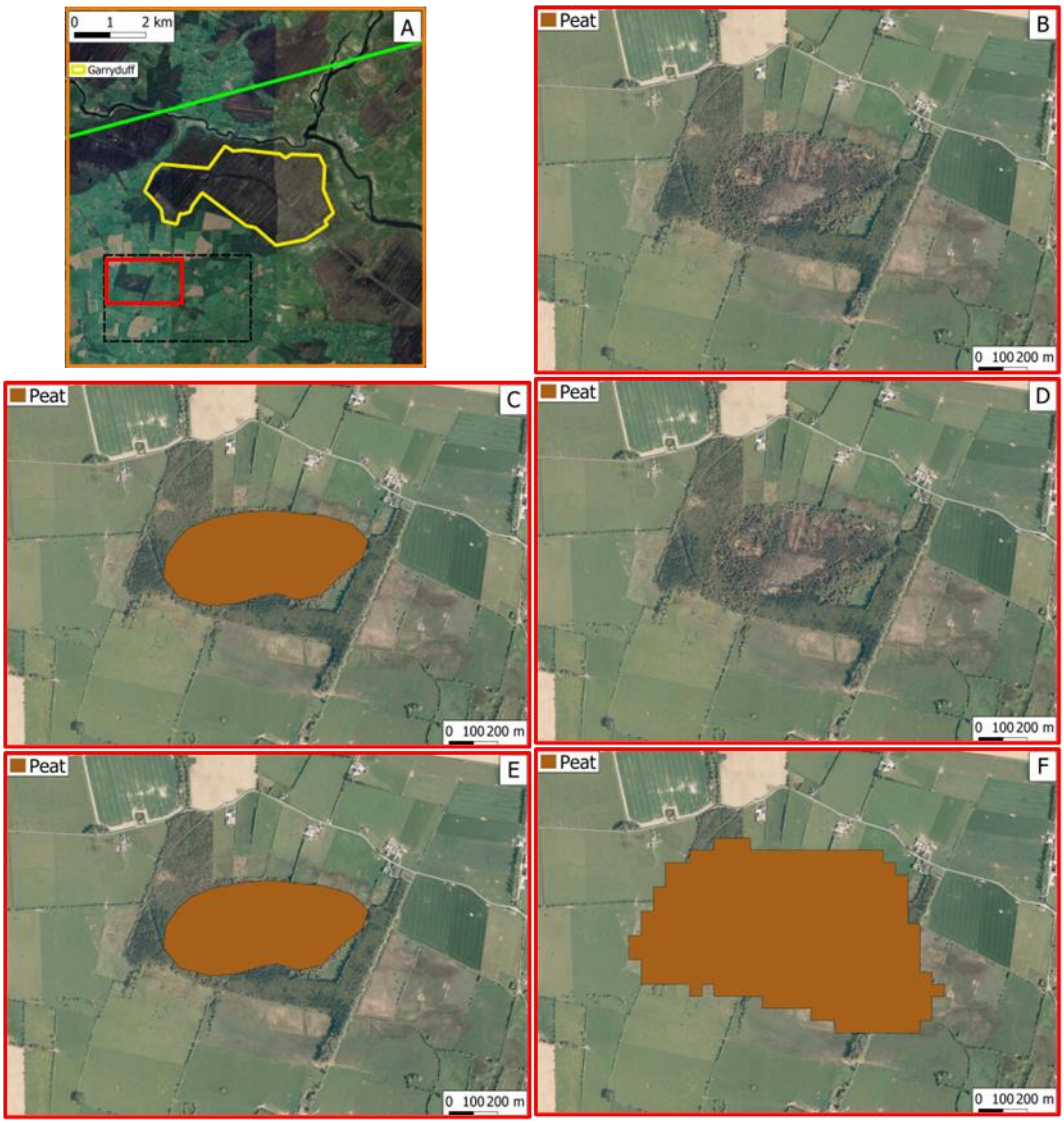


Figure A 2: A) Google image of study area. Yellow boundary defined from commercial surveys on site. Black Dashed area highlighting two sites identified as peat by ANN classification. Red Box shows zoomed area in B, C, D and E. B) Aerial image of zoomed area. C) QGM definition of peat in zoomed area, surrounded by “Till derived from limestone”. D) CLC18 definition of peat in zoomed area. CLC18 misclassifies this area as “Mixed forest” surrounded by “pasture” and “Non-irrigated arable land”. E) ISIS definition of peat in zoomed area. F) ANN classification of peat in zoomed area

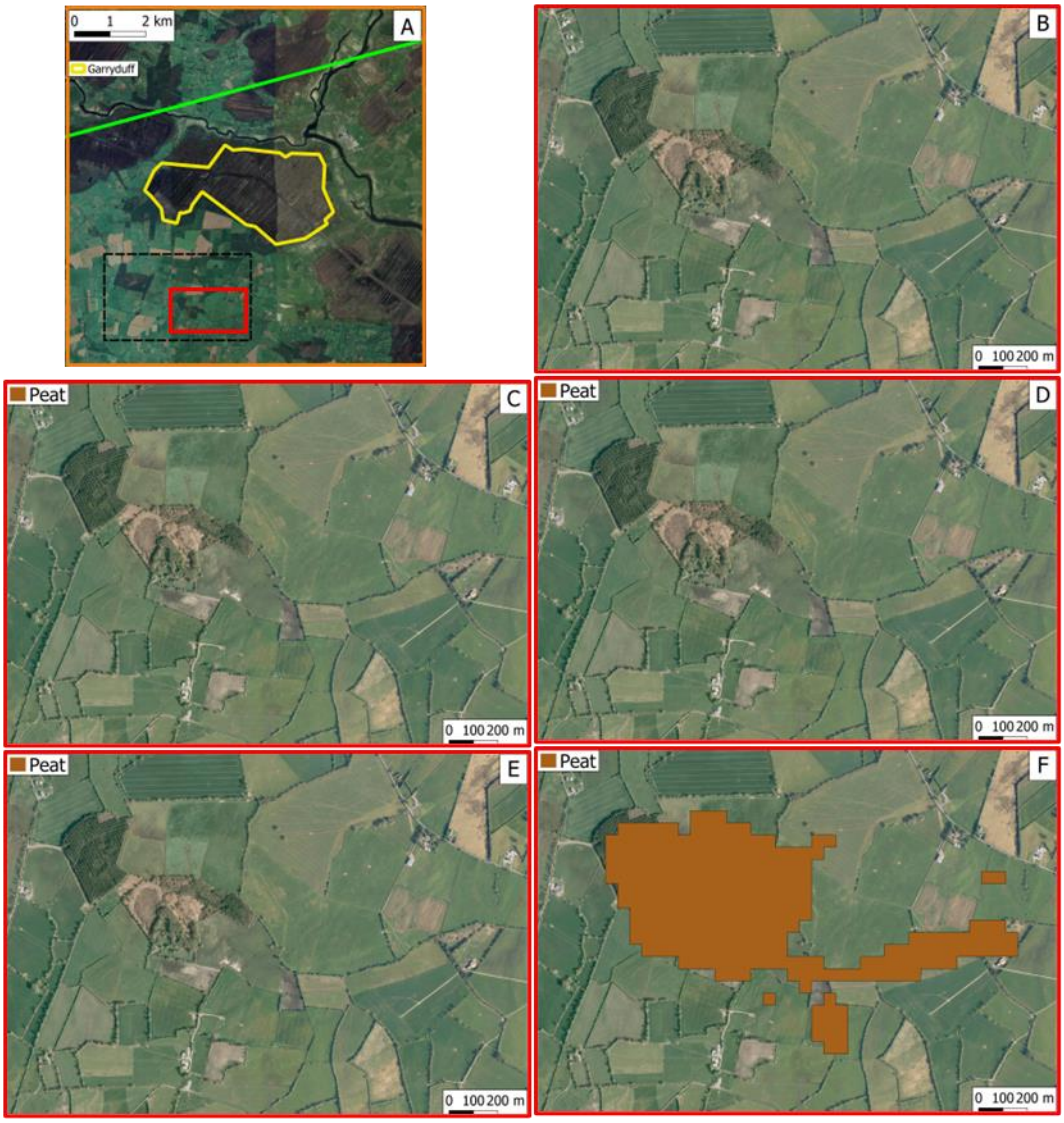


Figure A 3: A) Google image of study area. Yellow boundary defined from commercial surveys on site. Black Dashed area highlighting two sites identified as peat by ANN classification. Red Box shows zoomed area in B, C, D and E. B) Aerial image of zoomed area. C) QGM does not define any peat in zoomed area, classed as “Till derived from limestone”. D CLC18 does not define any peat in zoomed area, classed as “pasture”. E) ISIS does not define any peat in zoomed area, classed as non-peat soils. F) ANN definition of peat in zoomed area.

# Appendix 3 : Peat depth on Garryduff

Ground penetrating radar was provided by Bord na Móna as part of their rehabilitation work on Garryduff site (Bord na Móna, 2021) This was combined with high resolution LiDAR (Light Detection and Ranging) data and was used to derive peat thickness information.

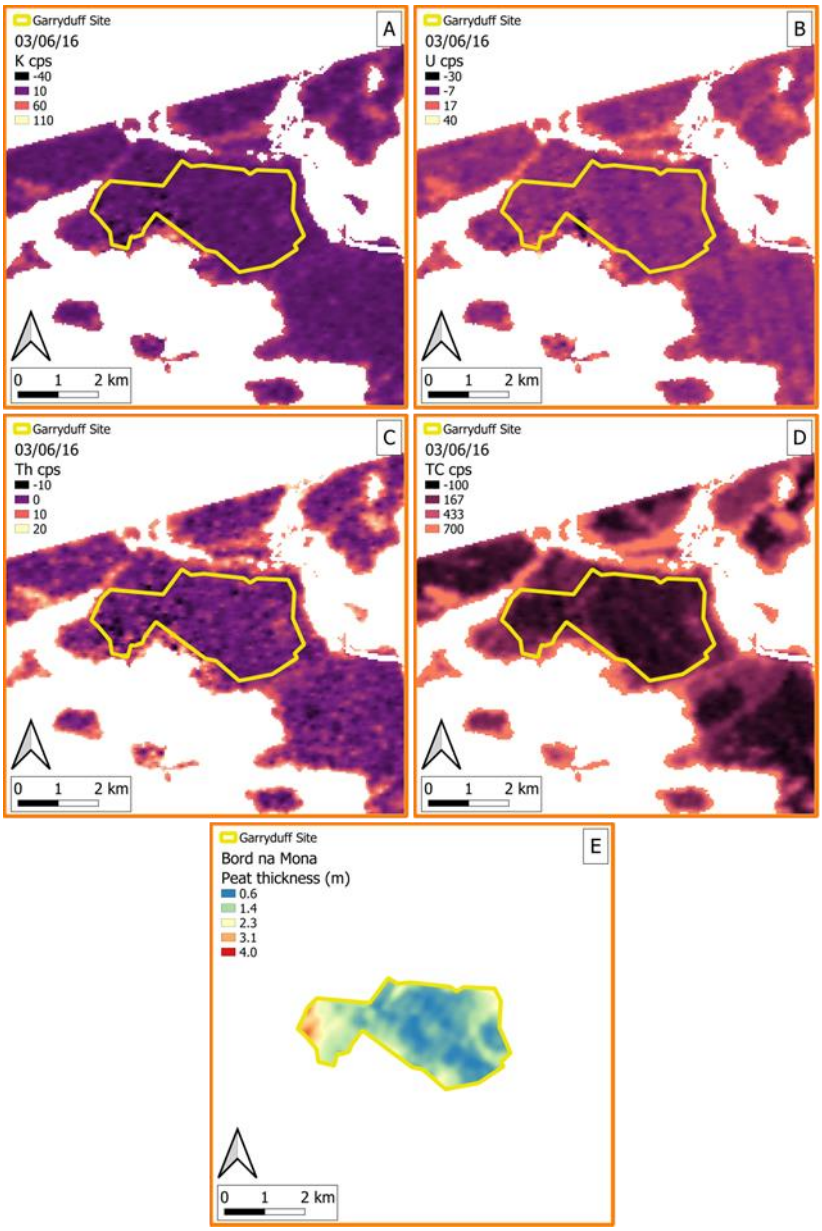


Figure A 4: A) Tellus Radiometric K cps. B) Tellus Radiometric U cps. C) Tellus Radiometric Th cps. D) Tellus Radiometric TC cps E) Peat thickness data (Derived from Ground Penetrating Radar)

# Appendix 4 : Comparison of 2017 and 2018 S2 MCASD results

MCASD analysis was performed twice, once on airborne radiometric data source combined with Sentinel 2 data sources from June 2017 and then also combined with Sentinel 2 data source from 2018. The purpose of this was to assess the validity of using 2017 data, which was the temporally closest to the acquisition date of the radiometric data source. Comparison between the radiometric combined with 2017 Sentinel 2 (Figure A 5) and radiometric combined with 2018 Sentinel 2 (Figure A 6) show that the number of clusters, the spatial distribution and the cluster signatures are all very similar, with the only noted differences discussed already in the main text (section 4.5.1)

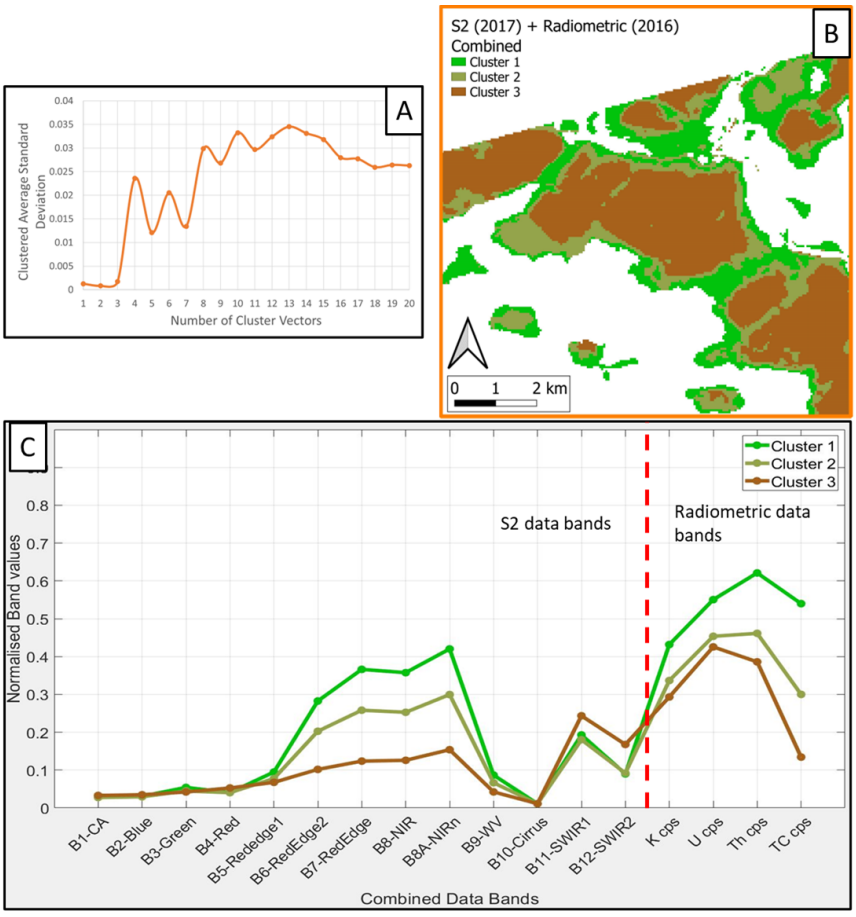


Figure A 5: MCASD results for 2017 S2 data source

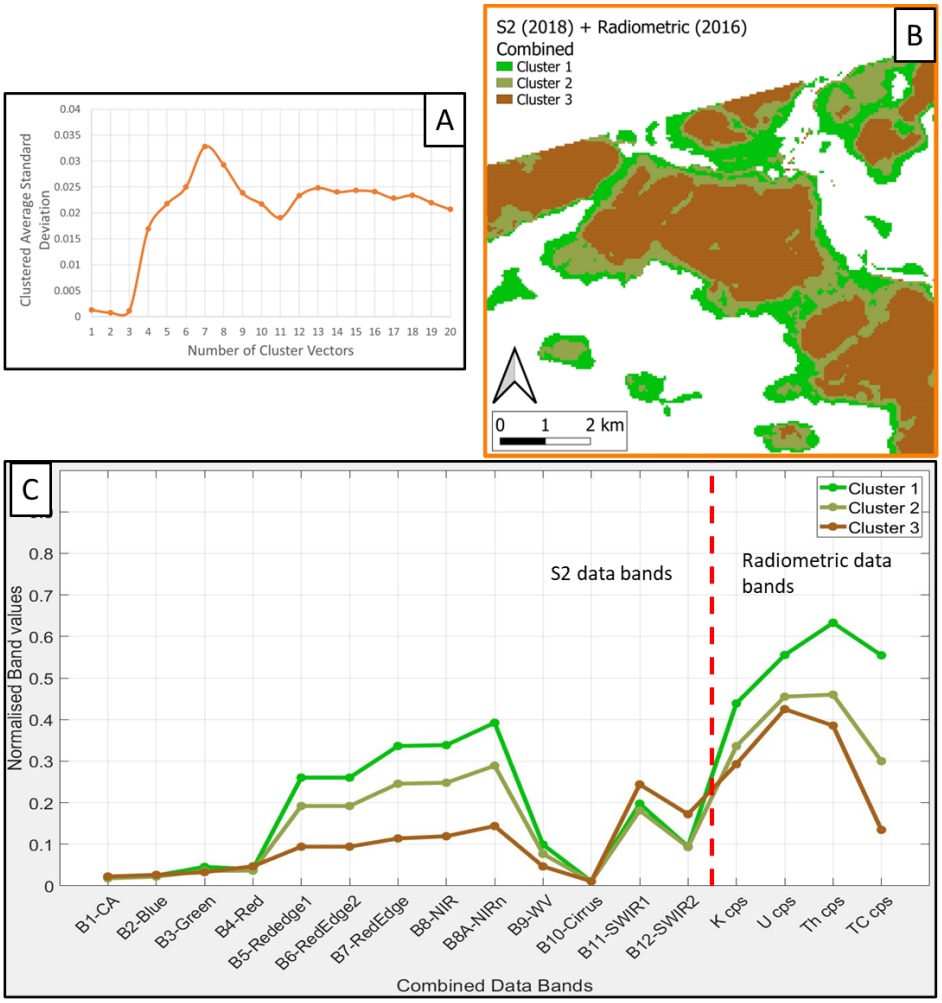


Figure A 6: MCASD results for 2018 S2 data source

# Summary of research outputs

**Chapters**:

The work presented in this thesis forms three papers currently either published, accepted or in prep:

- Chapter 2 forms a paper published in Ecological Informatics (IF 4.5). As co-author, I was responsible for conducting the literature review, specifically for the remote sensing section of the article. I was also responsible for writing initial drafts and review and editing of final draft.
- Chapter 3 forms a paper published in Geoderma (IF 7.4). As lead author, I was responsible for analysis of the airborne radiometric data, development of computer code to model radiometric attenuation, development of methodology for supervised classification using neural networks, interpretation of the results, initial writing, reviewing, and editing of the final manuscript.
- Chapter 4 forms a paper published in Geoderma (IF 7.4). As lead author, I was responsible for analysis of the airborne radiometric and satellite remote sensing data, development of the MCASD analysis methodology, interpretation of the results, initial writing, reviewing, and editing of the final manuscript.

**Articles:**

**O'Leary, D.,** Brown, C., Healy, M.G., Regan, S., Daly, E., Observations of intra-peatland variability using multiple spatially coincident remotely sensed data sources and machine learning. Geoderma, Volume 430, 2023, ISSN 0016-7061, https://doi.org/10.1016/j.geoderma.2023.116348

Healy, M.G., Siggins, A., Molloy, K., Potito, A., **O'Leary, D.,** Daly, E., Callery, O., The impact of alternating drainage and inundation cycles on geochemistry and microbiology of intact peat cores. Science of the Total Environment, 2022, 159664, ISSN 0048-9697, https://doi.org/10.1016/j.scitotenv.2022.159664

**O'Leary, D.,** Brown, C., Daly, E., Digital soil mapping of peatland using airborne radiometric data and supervised machine learning – Implication for the assessment of carbon stock. Geoderma, Volume 428, 2022, 116086, ISSN 0016-7061, https://doi.org/10.1016/j.geoderma.2022.116086

Monteverde, S., Healy, M.G., **O'Leary, D.,** Daly, E., Callery, O., Management and rehabilitation of peatlands: The role of water chemistry, hydrology, policy, and emerging monitoring methods to ensure informed decision making. Ecological Informatics, Volume 69, 2022, 101638, ISSN 1574-9541, https://doi.org/10.1016/j.ecoinf.2022.101638

**O'Leary, D.,** Mapping peat using radiometrics. Nat Rev Earth Environ 2, 523 (2021). https://doi.org/10.1038/s43017-021-00200-9

Dolan, MJ., McCabe, BA., Molloy, K., Murray, J., Henry, T., Daly, E., **O'Leary, D.,** A Pleistocene deposit preserved in deep karst at Coolough, County Galway, western Ireland. Geological Journal. 2021; 56: 1897– 1910. https://doi.org/10.1002/gj.4029

**Conference oral presentations:**

**O'Leary, D.,** Tuohy, P., Mellender, P., Fenton, O., Brown, C., Daly, E., Potential of machine learning in linking national airborne radiometric data to soil class mapping. Irish Geoscience Regional Meeting 2020. Athlone, Ireland.

**O'Leary, D.,** Monteverde, S., Callery, O., Healy, M., Brown, C., Daly, E., Defining peatland zones using self-organising map clustering on airborne radiometric data and OS digital elevation model. Irish Quaternary Association Autumn Symposium 2020 – Carbon Sequestration. Online.

**O'Leary, D.,** Monteverde, S., Callery, O., Healy, M., Brown, C., Daly, E., The potential of Self-Organising maps clustering to characterise a harvested peatland using airborne radiometric data and a digital elevation model. Irish Geoscience Regional Meeting 2021. Online

**O'Leary, D.,** Mapping Peatland Boundaries and Intra-Peat variation using Radiometric Data and Machine Learning. International Association of Hydrogeologists – Technical Discussion Meeting 2021. Online.

**O'Leary, D.,** Mapping Peatland Boundaries and Intra-Peat variation using Radiometric Data and Machine Learning. 8th Annual Irish Geomorphology Scientific Workshop 2021. Online.

**O'Leary, D.,** Daly, E., Brown, C., Method to obtain optimum number of clusters in geo-spatial data using stability analysis of cluster centres. European Geosciences Union General Assembly 2021. Online

Daly, E., **O'Leary, D.,** Monteverde, S., Callery, O., Healy, M., Brown, C., The potential of Self-Organising maps clustering to characterise a harvested peatland using airborne radiometric data and OS digital elevation model. European Geoscience Union General Assembly 2021. Online

**O'Leary, D.,** Daly, E., Large Scale EMI Survey linking Electrical Conductivity to Soil Type Properties using Machine Learning Classification Methods. AgriGeo2022 – Agriculture and Geophysics: an Electrical Meeting! Brussels Belgium.

**O'Leary, D.,** Brown, C., Daly, E., Digital Soil Mapping of Peatlands using Airborne Radiometric Data and Supervised Machine Learning. Irish Quaternary Association Spring Symposium 2022. Queens University Belfast, UK.

**O'Leary, D.,** Brown, C., Daly, E., Digital Soil Mapping of Peatlands using Airborne Radiometric Data and Supervised Machine Learning. European Geoscience Union General Assembly 2022. Vienna Austria.

**O'Leary, D.,** Daly, E., Brown, C., Regional Mapping of Peatland Boundaries using Airborne Radiometric Data and Supervised Machine Learning. Irish Earth Observation Symposium 2022, TU Dublin, Dublin.

**O'Leary, D.,** Daly, E., Brown, C., Data Driven Method for Selection of Optimum Number of Clusters in Earth Science Data using Centroid based Self-Organising Maps Clustering. American Geophysical Union 2022. Chicago.

**Conference poster presentations:**

**O'Leary, D.,** Thebaudeau, B., Fenton, O., Mellender, P., Green, S., Brown, C., Tuohy, P., O'Connor, S., Daly, E., Geophysical remote sensing of subsurface properties for sustainable agricultural management. Irish Geoscience Regional Meeting 2019. University College Dublin.

**O'Leary, D.,** Fenton, O., Mellender, P., Brown, C., Tuohy, P., Daly, E., Linking Hydro-Geophysics and Remote Sensing Technology for Sustainable Water and Agricultural Catchment Management. Ryan Institute Research Day 2019. National University of Ireland, Galway.

**O'Leary, D.,** Tuohy, P., Mellender, P., Fenton, O., Brown, C., Daly, E., Potential of machine learning in linking national airborne radiometric data to soil class mapping. AgriGeo 2020 Agriculture and Geophysics: the perfect match? Gembloux Agro-Technical Institute, Belgium.

**O'Leary, D.,** Healy, M., Callery, O., Brown, C., Daly, E., Defining Potential Peatland Management Zones using Unsupervised Self-Organizing Map Clustering on Airborne Radiometric Data. American Geophysical Union 2020. Online

**O'Leary, D.,** Brown, C., Daly, E., Mapping Peatland Boundaries and Intra-Peat variation using Airborne Geophysical Data and Machine Learning. CARE-PEAT – Restoring carbon storage capacity of peatlands 2022. National University of Ireland, Galway.

**O'Leary, D.,** Daly, E., Brown, C., Regional Mapping of Peatland Boundaries using Airborne Radiometric Data and Supervised Machine Learning. American Geophysical Union 2022. Chicago.

# Paper Acknowledgements

**Chapter 2 Acknowledgements**

The authors would like to thank the European Commission and the Irish Environmental Protection Agency (EPA) (Project reference number 2019-W-MS-42) for funding the collaborative international consortium (WATERPEAT) financed under the Water JPI 2018 Joint Call of the WaterWorks2017 ERA-NET Cofund. This project is funded under the EPA Research Programme 2014-2020. The EPA Research Programme is a Government of Ireland initiative funded by the Department of Communications, Climate Action and Environment. It is administered by the Environmental Protection Agency, which has the statutory function of co-ordinating and promoting environmental research.

**Chapter 3 Acknowledgements**

The research conducted in this publication was funded by the Irish Research Council under grant number GOIPG-2018-233. Contains Irish Public Sector Data (Geological Survey Ireland) licensed under a Creative Commons Attribution 4.0 International (CC BY 4.0) licence. The authors wish to acknowledge Prof. Mark Healy (NUIG), Prof. Owen Fenton (NUIG/Teagasc) and Dr Pat Tuohy (Teagasc) for their constructive comments during the production of this paper. Many thanks to the two anonymous reviewers for providing insightful feedback leading to a much-improved article.

**Chapter 4 Acknowledgements**

The research conducted in this publication was funded by the Irish Research Council under grant number GOIPG-2018-233. Contains Irish Public Sector Data (Geological Survey Ireland) licensed under a Creative Commons Attribution 4.0 International (CC BY 4.0) licence. Peat thickness data was provided to the authors by Bord na Móna.